UNIVERSIDADE ESTADUAL DE CAMPINAS

INSTITUTO DE BIOLOGIA

CLEITON BREDER ELLER

THE EFFECTS OF ENVIRONMENTAL CHANGES ON WATER AND CARBON RELATIONS OF CLOUD FOREST TREES

EFEITOS DE MUDANÇAS AMBIENTAIS NAS RELAÇÕES HÍDRICAS E DE CARBONO DE ÁRVORES DE FLORESTAS NEBULARES

CAMPINAS

2016

CLEITON BREDER ELLER

THE EFFECTS OF ENVIRONMENTAL CHANGES ON WATER AND CARBON RELATIONS OF CLOUD FOREST TREES

EFEITOS DE MUDANÇAS AMBIENTAIS NAS RELAÇÕES HÍDRICAS E DE CARBONO DE ÁRVORES DE FLORESTAS NEBULARES

Thesis presented to the Institute of Biology of the University of Campinas in partial fulfillment of the requirements for the Doctoral degree in Ecology.

Tese apresentada ao Instituto de Biologia da Universidade Estadual de Campinas como parte dos requisitos exigidos para a obtenção do Título de Doutor em Ecologia.

ESTE ARQUIVO DIGITAL CORRESPONDE À VERSÃO FINAL DA TESE DEFENDIDA PELO ALUNO CLEITON BREDER ELLER E ORIENTADA PELO PROF. DR. RAFAEL SILVA OLIVEIRA.

Orientador: PROF. DR. RAFAEL SILVA OLIVEIRA.

CAMPINAS

2016

Agência(s) de fomento e nº(s) de processo(s): FAPESP, 2010/17204-0; FAPESP, 2011/52072-0; FAPESP, 2013/19555-2; CAPES; CNPq

Ficha catalográfica
Universidade Estadual de Campinas
Biblioteca do Instituto de Biologia
Mara Janaina de Oliveira - CRB 8/6972

EL54e

Eller, Cleiton Breder, 1986-
The effects of environmental changes on water and carbon relations of cloud forest trees / Cleiton Breder Eller. - Campinas, SP: [s.n.], 2016.

Orientador: Rafael Silva Oliveira.
Tese (doutorado) – Universidade Estadual de Campinas, Instituto de Biologia.

1. Seca. 2. Neblina. 3. Floresta nebular. 4. Mudanças climáticas. 5. Árvores - Crescimento. I. Oliveira, Silva Rafael,1974-. II. Universidade Estadual de Campinas. Instituto de Biologia. III. Título.

Informações para Biblioteca Digital

Título em outro idioma: Efeitos de mudanças ambientais nas relações hídricas e de carbono de árvores de florestas nebulares
Palavras-chave em Inglês:
Drought
Fog
Cloud forests
Climate changes
Trees – Growth
Área de concentração: Ecologia
Titulação: Doutor em Ecologia
Banca examinadora:
Rafael Silva Oliveira [Orientador]
Luiz Eduardo Oliveira e Cruz Aragão
Lucia Rebello Dillenburg
Simone Aparecida Vieira
Laszlo Karoly Nagy
Data da defesa: 22-09-2016
Programa de Pós Graduação: Ecologia

Campinas, 22 de Setembro de 2016.

COMISSÃO EXAMINADORA

Prof. Dr. Rafael Silva Oliveira

Prof. Dr. Laszlo Karoly Nagy

Prof. Dr. Luiz Eduardo Oliveira e Cruz de Aragão

Profa. Dra. Lucia Rebello Dillenburg

Profa. Dra. Simone Aparecida Vieira

Os membros da Comissão Examinadora acima assinaram a Ata de defesa, que se encontra no processo de vida acadêmica do aluno.

ACKNOWLEDGEMENTS

I gratefully acknowledge the support of my advisor Prof. Dr. Rafael Silva Oliveira, which was essential for the completion of this thesis. I am also grateful for the support of Prof. Dr. Maurizio Mencuccini that made invaluable contributions to the data analysis section of chapter 2. I must also thank Aline Lima and Fernanda Barros for contributing for the data collection on chapters 1 and 2, respectively, and Oliver Binks for helping me to improve the writing of chapter 1.

I am very grateful to Prof. Dr. Simone Aparecida Vieira, Prof. Dr. Laszlo Karoly Nagy, Prof. Dr. Luiz Eduardo Oliveira e Cruz de Aragão, Prof. Dr. Lucia Rebello Dillenburg, Prof. Dr. Leonardo Dias Meirelles, Prof. Dr. Ricardo Augusto Gorne Viani, Dr. Grazielle Sales Teodoro and Dr. Vinícius de Lima Dantas for agreeing in being part of the examination board of this thesis. I am also grateful to Prof. Dr. Roman Zweifel, Prof. Dr. Patrick Meir and Prof. Dr. Peter Groenendijk for reviewing and providing important suggestions that helped me to improve this thesis. I also acknowledge the support of the postgraduate program in Ecology at UNICAMP, and fazenda Lavrinhas.

This thesis was funded by São Paulo Research Foundation (FAPESP; Grant no. 10/17204-0), FAPESP/Microsoft research (Grant no. 11/52072-0); and National Counsel of Technological and Scientific Development (CNPq), Higher Education Co-ordination Agency (CAPES) and FAPESP (Grant no. 13/19555-2) scholarships.

RESUMO

Florestas tropicais nebulares (FTN) são um dos ecossistemas tropicais mais vulneráveis a mudanças climáticas. Esses ecossistemas possuem um grande número de espécies endêmicas que só podem sobreviver nas condições microclimáticas encontradas em FTN. Mudanças climáticas ameaçam a diversidade e funcionamento desses ecossistemas. Nessa tese eu investigo como mudanças em condições ambientais afetam as relações hídricas e o crescimento de árvores de FTN. No capítulo 1, eu investigo como absorção foliar de água (AFA) contribui para a manutenção do turgor foliar em árvores de TFN durante períodos de seca. Eu conduzi experimentos para avaliar diferenças na capacidade de AFA entre três espécies de árvores comuns em FTN. Eu também medi o efeito de exposição regular a neblina no potencial hídrico foliar de plantas expostas a seca, e usamos esses dados para modelar a resposta das espécies a secas de maior duração. Todas as espécies estudadas foram capazes de absorver água através de suas cutículas foliares e/ou tricomas, mas a taxa de AFA variou entre espécies. Durante o experimento de seca, as espécies com maior AFA mantiveram o turgor foliar por maior tempo quando expostas a neblina, enquanto espécies com menor AFA exerceram um maior controle estomático para manter o turgor foliar. Resultados do modelo ajustado aos dados do experimento de seca sugerem que, sem neblina, as espécies com maior AFA tem uma maior probabilidade de perder o turgor foliar durante secas sazonais. No capítulo 2, eu usei dois métodos de análise de dados dendrométricos distintos para medir o crescimento diário de árvores de FTN, e investigar como o crescimento de árvores com diferentes características funcionais responde a mudanças ambientais. Eu estimei o crescimento das árvores (c) diretamente de dados de mudanças de diâmetro da casca (dD_b), e também com uma combinação de dD_b e dados de velocidade de seiva no xilema para excluir o efeito da capacitância hidráulica da casca de dD_b. Ambos os métodos usados para estimar c produziram resultados razoavelmente semelhantes em árvores de crescimento rápido (R^2=0.46-0.81), mas produziram resultados bastante distintos em árvores de crescimento lento. Árvores de crescimento rápido foram capazes de crescer em um intervalo maior de condições de temperatura, radiação solar, disponibilidade de água no solo e tempo com folhas molhadas, do que espécies de crescimento lento. Entretanto, árvores de crescimento rápido também tiveram margens de segurança hidráulica menores e madeira menos densa. A maior parte das árvores aumentou seu c durante as condições mais quentes e nubladas da estação chuvosa. Nossos resultados mostram que as condições ambientais de FTN frequentemente limitam o crescimento das árvores e podem promover a perda de turgor foliar. Algumas árvores adotam estratégias hidraulicamente mais arriscadas para lidar com essas restrições ambientais, mantendo a transpiração e crescimento mesmo em condições ambientais desfavoráveis. Outras árvores adotam estratégias mais conservadoras e favorecem a manutenção de sua integridade hidráulica. Mudanças climáticas podem ameaçar particularmente árvores com alto AFA, que dependem de eventos de neblina para manutenção do turgor e crescimento durante secas.

PALAVRAS-CHAVE: Seca; neblina; floresta nebular; mudanças climáticas; crescimento de árvores.

ABSTRACT

Tropical Montane Cloud Forests (TMCF) are considered one of the most vulnerable tropical ecosystems to climate change. These ecosystems possess a high number of endemic species that can only thrive on the particular environmental conditions found in TMCF. Increases in temperature and changes in the frequency of cloud immersion events might threaten the diversity and functioning of these ecosystems. In this thesis, I investigate how environmental conditions affect carbon and water relations of TMCF trees. In chapter 1, I investigated how foliar water uptake (FWU) helps TMCF trees to maintain leaf turgor during soil drought. I conducted several experiments using apoplastic tracers, deuterium labeling and leaf immersion in water to evaluate differences in FWU among three common TMCF tree species. I also measured the effect of regular fog exposure on the leaf water potential of plants subjected to soil drought and used these data to model species' response to long-term drought. All the studied species were able to absorb water through their leaf cuticles and/or trichomes, although the capacity to do so differed between species. During the drought experiment, the species with higher FWU capacity maintained leaf turgor for a longer period when exposed to fog, whereas the species with lower FWU exerted tighter stomatal regulation to maintain leaf turgor. The model fitted to the experimental data suggest that without fog, species with high FWU are more likely to lose turgor during seasonal droughts. In chapter 2, I used two different dendrometer techniques to measure daily growth of TMCF trees, and investigate how the growth of trees with different functional traits responds to changes in environmental conditions. I estimated tree growth (g) directly from bark diameter changes (dD_b), and also using a combination of dD_b and sap velocity measurements to exclude the bark capacitance effect from dD_b. I measured tree functional traits such as xylem hydraulic safety margins, stomatal regulation strategies and wood density. Both methods to estimate g showed a medium to high agreement (R^2=0.46-0.81) in fast-growing trees, but poor agreement in slow growing trees. Fast growing trees were able to grow in a wider range of temperature, irradiance, soil water availability and leaf-wetting conditions than slow growing trees. However, fast growing trees had narrower xylem safety margins and less dense wood. Most trees increased g during hotter and cloudy wet season conditions. These results show that environmental conditions in TMCF often limit tree growth and promote leaf turgor loss. The TMCF trees developed different strategies to deal with these environmental restrictions. Some trees adopt hydraulically riskier strategies favoring carbon uptake even during unfavorable periods; while others are more conservative and favor hydraulic safety. Climatic changes that alter fog events might threaten particularly trees with high FWU, which depend on leaf-wetting events for the maintenance of leaf turgor and growth during droughts.

KEYWORDS: Drought; fog; cloud forest; climate change; tree growth.

INDEX

GENERAL INTRODUCTION

Tropical Montane Cloud Forests (TMCF) are unique, valuable and vulnerable tropical ecosystems (Bruijnzeel, 2004; Bubb *et al.*, 2004; Foster, 2001). The main climatic characteristic of TMCF is the persistence of cloud-immersion events (i.e. fog; Scholl *et al.*, 2010; Bruijnzeel *et al.*, 2011). These events create an environment with very peculiar hydroclimatic conditions that hosts a large diversity of species, many of these endemic to these sites (Gentry, 1992; Foster, 2001). The biological and climatic uniqueness of TMCF makes many processes from these ecosystems, including carbon and water fluxes, to be significantly different from lowland tropical forests (Bruijnzeel & Veneklaas, 1998; Girardin *et al.*, 2010; Bruijnzeel *et al.*, 2011; Oliveira *et al.*, 2014; Hu & Riveros-Iregui, 2016). Despite comprising only about 2.5% of the world tropical forests (Fig. 1), TMCF are known to provide valuable ecosystem services in mountainous tropical regions (Bruijnzeel, 2004; Bubb *et al.*, 2004). The generally smaller leaf area of TMCF vegetation (both leaf size and leaf area index; LAI) and its lower transpiratory rates, associated with the significant hydrological input from fog events (Fig. 2) makes TMCF very important to the regional hydrological cycle. These ecosystems contribute to the maintenance of streamflow and groundwater recharge, especially during dry seasons, which makes TMCF essential for the water supply of many mountainous tropical regions (Bruijnzeel, 2004; Bubb *et al.*, 2004). In addition, TMCF are known to decrease soil erosion, which improves water quality and decrease landslide risks (LaBastille & Pool, 1978; Bubb *et al.*, 2004).

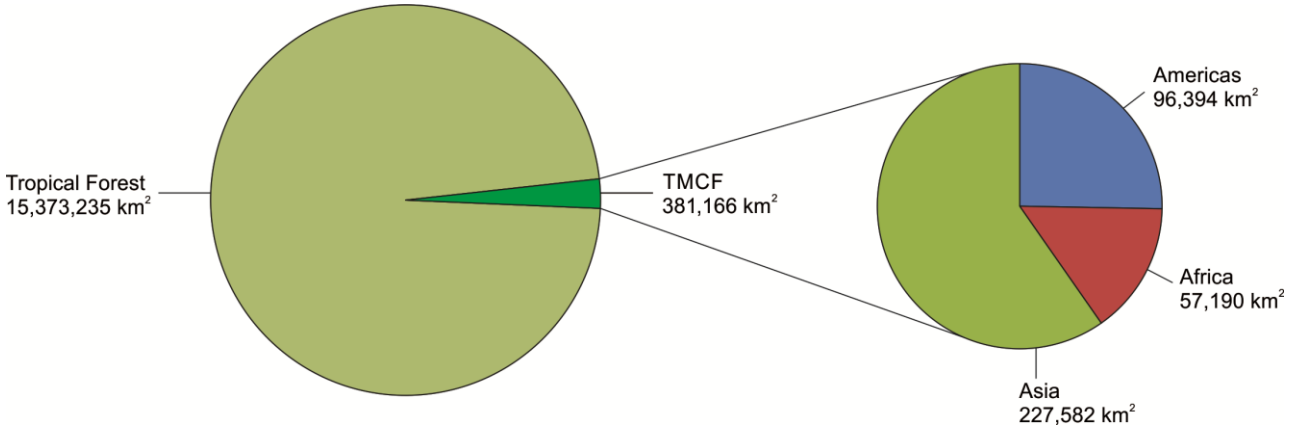

Figure 1. Distribution of Tropical Montane Cloud Forests (TMCF) across the world. On the left chart, the potential TMCF area in relation to the total tropical forest area. On the right chart, the potential TMCF area by region. Data from Bubb *et al.*, (2004).

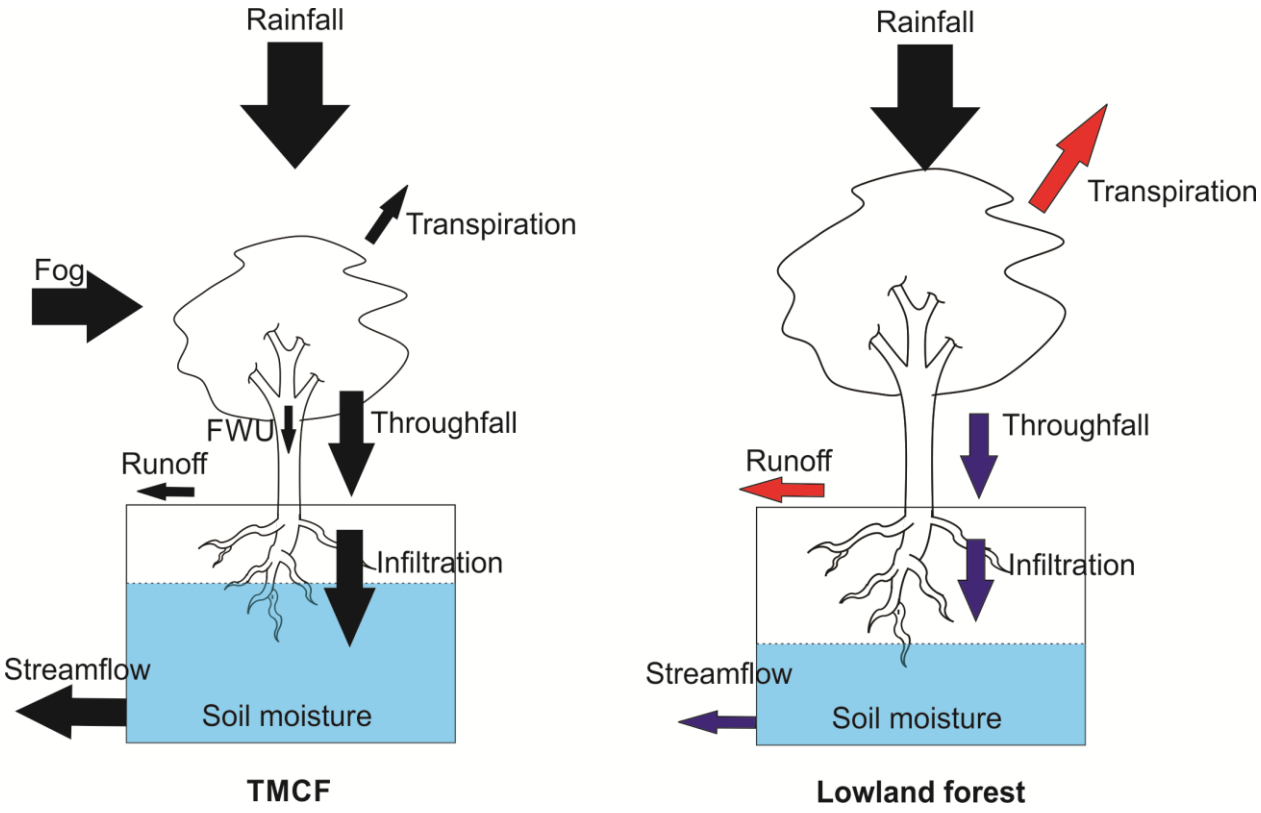

Figure 2. Representation of the hydrological importance of Tropical Montane Cloud Forests (TMCF) in comparison with a typical lowland tropical forest. Different arrow sizes indicates the relative magnitude of the flux. Different arrow colors in the lowland forest indicates changes in the flux magnitude in comparison with the TMCF flux (red indicates bigger flux and blue indicates smaller flux). On the TMCF, the additional fog hydrological input in addition to the rain, which promotes sap flow reversals caused by foliar water uptake (FWU; see Eller *et al.*, 2013) and enhances Throughfall with fog dripping. This additional water input coupled with the lower TMCF transpiration enables TMCF to contribute more to the regional streamflow and groundwater recharge than lowland forests. This illustration was based on Foster (2001).

Climate change is one of the most serious threats to the structure and function of TMCF around the globe (Foster, 2001; Bubb *et al*., 2004). Many TMCF species are highly adapted to the specific environmental conditions found only in TMCF, and changes on these conditions, including changes in temperature and fog frequency, might induce the mortality of native TMCF species and promote the invasion of TMCF by lowland species (Pound *et al.*, 1999; Foster, 2001). Observations around the globe indicate that earth temperature is increasing (Folland *et al.*, 2001), and model simulations indicate that this trend will continue in the future (Solomon *et al.*, 2009). Therefore, most ecosystems on earth will be subject to temperature increments in the future, including TMCF (Still *et al.*, 1999; Karmalkar *et al.*, 2008). Increases in the earth surface temperature might also increase the elevation of cloud formation in tropical

mountains (Still *et al.*, 1999; Lawton *et al.*, 2001; Karmalkar *et al.*, 2008), which would decrease the frequency of cloud immersion events in TMCF. It is essential to understand how environmental conditions affects the functioning of TMCF species to make accurate predictions on how TMCF will respond to a hotter and less foggy climate.

Fog events have two main impacts on the water relations of TMCF trees. The first impact is to suppress tree transpiration, due to the atmospheric vapor pressure being close to saturation during fog events, and because of the formation of a water film on the leaf surface (Smith & McClean, 1989; Letts & Mulligan, 2005). The second impact is to provide an additional hydrological input for TMCF trees, which might be indirect, through the interception of fog particles and subsequent dripping to the soil (Cavelier *et al.*, 1996; Holder, 2004; Liu *et al.*, 2004) or direct, through foliar water uptake (FWU; Eller *et al.*, 2013; 2015; Goldsmith *et al.*, 2013; Gotsch *et al.*, 2014). Despite TMCF being widely considered mesic environments, they can occur at sites with annual rainfall as low as 600 mm (Jarvis & Mulligan, 2011) and with significant rainfall seasonality (Jarvis & Mulligan, 2011; Goldsmith *et al.*, 2013; Eller *et al.*, 2015). Therefore, the fog water input might be very ecologically important for some TMCF species.

The water acquired by FWU is a particularly useful mechanism for some species to maintain physiological activities and growth during drought (Simonin *et al.*, 2009; Eller *et al.*, 2013). Other studies also have shown that different species within a community may possess different FWU capabilities (Goldsmith *et al.*, 2013; Limm *et al.*, 2009), which implies that some TMCF species could be more vulnerable to the reduction in leaf-wetting events than others, as they would be more reliant on FWU water. I investigate this possibility in chapter 1 of this thesis. I used anatomical data to visualize the different FWU pathways, and deuterium labelling and leaf immersion experiments to quantify differences in FWU capabilities among three abundant TMCF tree species. Then, I measured the effect of soil drought and FWU on the leaf water potential of each species in a glasshouse drought experiment. I coupled the experimental data with 32-years of TMCF meteorological data to understand the ecological importance of leaf-wetting events for these three species with different FWU capacity.

Carbon relations of TMCF are also an understudied topic, if compared with lowland forests (Bruijnzeel & Veneklaas, 1998). Tree growth in TMCF is frequently lower than in lowland tropical forests (Bruijnzeel & Veneklaas, 1998; Wilcke *et al.*, 2008; Moser *et al.*, 2008; Girardin *et al.*, 2010). Low irradiance and wet leaves caused by the frequent fog events have

been proposed as possible causes for the low productivity of TMCF (Bruijnzeel & Veneklaas, 1998; Letts & Mulligan, 2005). Other studies suggest that the low availability of soil nutrients, particularly nitrogen, also might limit tree growth in TMCF (Wilcke *et al.*, 2008; Moser *et al.*, 2010; Fisher *et al.*, 2013). There are limited data to support either of these views, and understanding what controls TMCF tree growth is of utmost importance to predict how these important ecosystems might respond to climate change.

One of the main challenges of studying interactions between tree growth and climate is the difficulty of having accurate measurements of growth in short temporal scales. This difficulty exists because much of the changes in tree stem diameter are caused by radial water fluxes between bark and xylem, instead of actually cambium cells multiplication and expansion (Steppe *et al.*, 2015; Zweifel, 2016). Recently some methods have been proposed to separate the cambial growth singal contained in dendrometer data from radial changes induced by radial water fluxes (Mencuccini *et al.*, 2013; Zweifel *et al.*, 2016). In chapter 2, I use these techniques to measure the growth of TMCF trees at a daily time scale, and investigate how the growth of trees with different functional traits responds to changes in environmental conditions. I monitored bark diameter changes, sap velocity and measured several functional traits in nine trees, which belonged to some of the more abundant species in a TMCF fragment located in southeastern Brazil (Fig. 3). I measured functional traits related to stomatal regulation, xylem hydraulic safety, size-related traits and growth rates (that were derived from dendrometer growth data). I also compare the two methods used to estimate growth (Mencuccini *et al.*, 2013 and Zweifel *et al.*, 2016) for the different TMCF tree species.

The overall goal for this thesis was to investigate the mechanisms subjacent to the interactions between TMCF trees and climate. Many aspects of the ecophysiology of TMCF species are currently not elucidated, and this thesis intend to fill the gaps on the knowledge about how carbon and water relations of TMCF trees respond to environmental conditions. This knowledge is very useful to make predictions on how climate change might affect the structure and function of TMCF, and consequently the important services provided by this ecosystem. In addition, understanding the response of TMCF trees to climate change might provide a useful theoretical basis for the creation of effective TMCF management strategies.

Figure 3. *Upper left*: High-resolution point dendrometer used to measure bark diameter changes. *Upper right:* Heat-ratio method sap flow sensor used to monitor tree sap velocity. *Bottom:* Aerial view of the tropical montane cloud forest fragment studied on this thesis. The fragment is located in Campos do Jordão, SP – Brazil at approximately 2000 m above sea level. Bottom picture by Vitor Barão.

REFERENCES

Bruijnzeel LA. 2004. Hydrological functions of tropical forests: not seeing the soil for the trees? *Agriculture, ecosystems & environment* **104**:185-228.

Bruijnzeel LA, Veneklaas EJ. 1998. Climatic conditions and tropical montane forest productivity: the fog has not lifted yet. *Ecology* **79**: 3-9.

Bruijnzeel LA, Mulligan M, Scatena FN. 2011. Hydrometeorology of tropical montane cloud forests: emerging patterns. *Hydrological Processes* **25**: 465-498.

Bubb P, May IA, Miles L, Sayer J. 2004. Cloud forest agenda. *UNEP World Conservation Monitoring Centre*.

Cavelier J, Solis D, Jaramillo MA. 1996. Fog interception in montane forests across the Central Cordillera of Panama. *Journal of Tropical Ecology* **12**: 357-369.

Eller CB, Lima AL, Oliveira RS. 2013. Foliar uptake of fog water and transport belowground alleviates drought effects in the cloud forest tree species, *Drimys brasiliensis* (Winteraceae). *New Phytologist* **199**: 151-162.

Eller CB, Burgess SSO, Oliveira RS. 2015. Environmental controls in the water use patterns of a tropical cloud forest tree species, *Drimys brasiliensis* (Winteraceae). *Tree physiology* **35**: 387-399.

Fisher JB, Malhi Y, Torres IC, Metcalfe DB, van de Weg MJ, Meir P, Silva-Espejo JE, Huasco WH. 2013. Nutrient limitation in rainforests and cloud forests along a 3,000-m elevation gradient in the Peruvian Andes. *Oecologia* 172:889-902.

Folland CK, Rayner NA, Brown SJ, Smith TM, Shen SS, Parker DE, Macadam I, Jones PD, Jones RN, Nicholls N, Sexton DM. 2001. Global temperature change and its uncertainties since 1861. *Geophysical Research Letters* **28**: 2621-2624.

Foster P. 2001. The potential negative impacts of global climate change on tropical montane cloud forests. *Earth-Science Reviews* **55**: 73-106.

Gentry AH. 1992. Tropical forest biodiversity: distributional patterns and their conservational significance. *Oikos* **63**: 19–28.

Girardin CA, Malhi Y, Aragao LE, Mamani M, Huaraca Huasco W, Durand L, Feeley KJ, Rapp J, Silva-Espejo JE, Silman M, Salinas N. 2010. Net primary productivity

allocation and cycling of carbon along a tropical forest elevational transect in the Peruvian Andes. *Global Change Biology* **16**:3176-3192.

Goldsmith GR, Matzke NJ, Dawson TE. 2013. The incidence and implications of clouds for cloud forest plant water relations. *Ecology letters* **16**: 307-314.

Gotsch SG, Asbjornsen H, Holwerda F, Goldsmith GR, Weintraub AE, Dawson TE. 2014. Foggy days and dry nights determine crown-level water balance in a seasonal tropical montane cloud forest. *Plant, cell and environment* **37**: 261-272.

Holder CD. 2004. Rainfall interception and fog precipitation in a tropical montane cloud forest of Guatemala. *Forest Ecology and Management* **190**: 373-384.

Hu J, Riveros-Iregui DA. 2016. Life in the clouds: are tropical montane cloud forests responding to changes in climate? *Oecologia* **6**:1-3.

Jarvis A, Mulligan M. 2011. The climate of cloud forests. *Hydrological Processes* **25**: 327-343.

Karmalkar AV, Bradley RS, Diaz HF. 2008. Climate change scenario for Costa Rican montane forests. *Geophysical Research Letters* **35** (11).

LaBastille A, Pool DJ. 1978. On the need for a system of cloud-forest parks in Middle America and the Caribbean. *Environmental Conservation* **5**:183-90.

Lawton RO, Nair US, Pielke RA, Welch RM. 2001. Climatic impact of tropical lowland deforestation on nearby montane cloud forests. *Science* **294**: 584-587.

Letts MG, Mulligan M. 2005. The impact of light quality and leaf wetness on photosynthesis in north-west Andean tropical montane cloud forest. *Journal of Tropical Ecology* **21**: 549-557.

Limm E, Simonin K, Bothman A, Dawson T. 2009. Foliar water uptake: a common water acquisition strategy for plants of the redwood forest. *Oecologia* **161**: 449-459.

Liu W, Meng FR, Zhang Y, Liu Y, Li H. 2004. Water input from fog drip in the tropical seasonal rain forest of Xishuangbanna, South-West China. *Journal of Tropical Ecology* **20**: 517-524.

Mencuccini M, Hölttä T, Sevanto S, Nikinmaa E. 2013. Concurrent measurements of change in the bark and xylem diameters of trees reveal a phloem-generated turgor signal. *New Phytologist* **198**:1143-1154.

Moser G, Leuschner C, Hertel D, Graefe S, Soethe N, Iost S. 2011. Elevation effects on the carbon budget of tropical mountain forests (S Ecuador): the role of the belowground compartment. *Global Change Biology* **17**: 2211-2226.

Oliveira RS, Eller CB, Bittencourt PR, Mulligan M. 2014. The hydroclimatic and ecophysiological basis of cloud forest distributions under current and projected climates. *Annals of botany* **113**: 909-920.

Pounds JA, Fogden MP, Campbell JH. 1999. Biological response to climate change on a tropical mountain. *Nature* **398**: 611-615.

Scholl M, Eugster W, Burkard R. 2010. Understanding the role of fog in forest hydrology: stable isotopes as tools for determining input and partitioning of cloud water in montane forests. *Hydrological Processes* **25**: 353-366.

Simonin KA, Santiago LS, Dawson TE. 2009. Fog interception by *Sequoia sempervirens* (D. Don) crowns decouples physiology from soil water deficit. *Plant, Cell & Environment* **32**: 882–892.

Smith WK, McClean TM. 1989. Adaptive relationship between leaf water repellency, stomatal distribution, and gas exchange. *American Journal of Botany* **76**: 465-469.

Solomon S, Plattner GK, Knutti R, Friedlingstein P. 2009. Irreversible climate change due to carbon dioxide emissions. *Proceedings of the national academy of sciences* **28**: pnas-0812721106.

Steppe K, Sterck F, Deslauriers A. 2015. Diel growth dynamics in tree stems: linking anatomy and ecophysiology. *Trends in plant science* **20**: 335-343.

Still CJ, Foster PN, Schneider SH. 1999. Simulating the effects of climate change on tropical montane cloud forests. *Nature* **398**: 608-610.

Wilcke W, Oelmann Y, Schmitt A, Valarezo C, Zech W, Homeier J. 2008. Soil properties and tree growth along an altitudinal transect in Ecuadorian tropical montane forest. *Journal of plant nutrition and soil science* **171**: 220-230.

Zweifel R. 2015. Radial stem variations – a source of tree physiological information not fully exploited yet. *Plant, Cell and Environment* 10.1111/pce.12613.

Zweifel R, Haeni M, Buchmann N, Eugster W. 2016. Are trees able to grow in periods of stem shrinkage? *New Phytologist* 10.1111/nph.13995.

CHAPTER 1

Cloud forest trees with higher foliar water uptake capacity and anisohydric behavior are more vulnerable to drought and climate change

(Eller CB, Lima AL, Oliveira RS. 2016. *New Phytologist* 211:489-501)

Cloud forest trees with higher foliar water uptake capacity and anisohydric behavior are more vulnerable to drought and climate change

Summary

- Many tropical montane cloud forests (TMCF) trees are capable of foliar water uptake (FWU) during leaf-wetting events. In this study, we tested the hypothesis that maintenance of leaf turgor during periods of fog exposure and soil drought is related to species' FWU capacity.

- We conducted several experiments using apoplastic tracers, deuterium labeling and leaf immersion in water to evaluate differences in FWU among three common TMCF tree species. We also measured the effect of regular fog exposure on the leaf water potential of plants subjected to soil drought and used these data to model species' response to long-term drought.

- All species were able to absorb water through their leaf cuticles and/or trichomes, although the capacity to do so differed between species. During the drought experiment, the species with higher FWU capacity maintained leaf turgor for a longer period when exposed to fog, whereas the species with lower FWU exerted tighter stomatal regulation to maintain leaf turgor. Model results suggest that without fog, species with high FWU are more likely to lose turgor during seasonal droughts.

- We show that leaf wetting events are essential for trees with high FWU, which tend to be more anisohydric, maintain leaf turgor during seasonal droughts.

Key words: Foliar water uptake; stomatal regulation; drought; fog; tropical montane cloud forest; climate change; turgor loss point; apoplastic tracers.

Introduction

Recent tree mortality events associated with drought (Breshears *et al.*, 2005; 2009; Gitlin *et al.*, 2006; Allen *et al.*, 2010; Rowland *et al.*, 2015), and predictions that extreme drought events are likely to increase worldwide (Sheffield & Wood, 2008), have led to recognition of the importance of the physiological mechanisms associated with drought induced tree mortality (McDowell *et al.*, 2008; 2011). While there is still not a complete picture of these physiological mechanisms, some traits, such as stomatal behavior (McDowell *et al.*, 2008; 2011), are widely considered useful predictors of plant response to drought. Most plants fall somewhere in a continuum between two modes of stomatal regulation during drought: isohydric plants avoid reaching low leaf water potential (Ψ_l) by closing stomata during drought, while anisohydric tend to keep their stomata open and endure lower Ψ_l (Klein, 2014; Martínez-Vilalta *et al.*, 2014; Skelton *et al.*, 2015). In many species, stomatal regulation is related to another physiological trait of major relevance to plant drought tolerance, the turgor loss point (π_{TLP}). This value is classically used as a threshold indicator of plant water stress, as it is often correlated with the hydration status when growth ceases, gas exchange declines sharply and leaves desiccate irreversibly (Brodribb *et al.*, 2003; Blackman *et al.*, 2010); which makes π_{TLP} a useful trait for predicting plant drought tolerance (Bartlett *et al.*, 2012).

Despite considerable advances that have been made on the subject, it is still unclear how certain physiological traits influence plant survival during drought, especially in tropical ecosystems. A physiological trait that has been shown to favor plant performance during drought is foliar water uptake (FWU). The water absorbance of leaves during FWU might be facilitated by specialized structures, such as trichomes (Benzig *et al*., 1978; Fernández *et al*., 2014) and hydathodes (Martin & Von Willert, 2000), but even leaves without specialized structures can be permeable to water either directly through the cuticle (Kerstiens, 1996, 2006; Riederer and Schreiber, 2001) or through the stomatal aperture (Burkhardt, 2010; Burkhardt *et al.*, 2012). As there are multiple possible pathways for water entry in leaves, FWU seems to be a widespread water acquisition strategy and has been observed in plants from a variety of ecosystems (Martin & Von Willert, 2000; Gouvra & Gramatikopoulos, 2003; Oliveira *et al*., 2005, Limm *et al*., 2008; Breshears *et al*., 2008; Eller *et al*., 2013; Goldsmith *et al*., 2013; Berry *et al*., 2014; Gotsch *et al*., 2014; Cassana *et al.*, 2015). The water acquired by FWU is considered of particular ecological relevance in dry or seasonally dry environments in which leaf-wetting events occur frequently (Oliveira *et al*., 2014a), as it may facilitate physiological

activity and growth in plants during drought conditions (Simonin *et al*., 2009; Eller *et al*., 2013).

The FWU capacity of plants from tropical montane cloud forests (TMCF) has been verified in recent studies (Eller *et al*., 2013; Goldsmith *et al*., 2013; Gotsch *et al*., 2014). These environments are characterized by frequent cloud immersion events (Bruijnzeel *et al*., 2011; Jarvis & Mulligan, 2011; Oliveira *et al*., 2014a), and despite being widely considered mesic environments, they can occur at sites with rainfall as low as 600 mm (Jarvis & Mulligan, 2011) and significant rainfall seasonality (Jarvis & Mulligan, 2011; Goldsmith *et al*., 2013; Eller *et al*., 2015). The FWU of fog water might be ecologically important for some TMCF species during seasonal droughts (Eller *et al*., 2013), and reductions in cloud-immersion events, which are predicted by some climate change models (Still *et al*., 1999; Williams *et al*., 2007), could threaten these species. However, it is known that different species within a community may possess different FWU capabilities (Goldsmith *et al*., 2013; Limm *et al*., 2008), raising the possibility that certain TMCF species could be more vulnerable to the reduction in leaf-wetting events than others, as they would be more reliant on FWU water.

Our objectives in this study were: 1 - identify FWU pathways and quantify FWU capabilities of three common TMCF trees, 2 - investigate relationships between FWU and stomatal behavior and 3 - quantify FWU contribution for the maintenance of leaf turgor during soil drought in these species, and use this information to predict how these species would perform in a climate with less fog. We used anatomical data to visualize the different FWU pathways, and deuterium labelling and leaf immersion experiments to quantify differences in FWU capabilities among the species. The fog effect on drought tolerance for each species was assessed with a glasshouse drought experiment, and to understand the ecological relevance of our experiment, we coupled the glasshouse experiment results with 32-years of TMCF meteorological data.

Material and Methods

Study site and species

The saplings used in the glasshouse experiment and samples used for the foliar water uptake experiments were collected in a TMCF close to Campos do Jordão State Park (CJSP; 22°69′ S, 45° 52′ W), located in the Mantiqueira mountain range, SP, Brazil. The climate at the site often presents a distinct dry (<50 mm monthly rainfall) and cold period (mean of 10.3°C in the coldest month) during the middle of the year (June-September) but fog events are

common at the site during the entire year. More details about vegetation structure and climate at the site can be found in Safford (1999) and Eller *et al* (2013; 2015).

The species chosen for this study were *Drimys brasiliensis* Miers (Winteraceae), *Myrsine umbellata* Mart. (Primulaceae) and *Eremanthus erythropappus* (DC.) MacLeish (Asteraceae). *Drimys brasiliensis* is a characteristic cloud forest tree species and its distribution is strongly associated with the occurrence of cloud forest sites in South and Southeast Brazil (Bertoncello *et al.,* 2011). *Myrsine umbellata* and *E. erythropappus* are more widely distributed, and while they can be very abundant tree species in some montane forests (Ledru *et al.,* 2007; Ávilla *et al.,* 2014; Meireles *et al.,* 2014; Freitas & Kinoshita, 2015), they are also found in lowland sites (Cândido, 1991; Ruggiero *et al.,* 2002; Dantas & Batalha, 2011; Freitas & Kinoshita, 2015). We collected *E. erythropappus* and *M. umbellata* samples in altitudes of *c.* 1700 m (where these species were more common at the site), while the *D. brasiliensis* samples were collected closer to the top of the site (*c.* 2000 m).

Foliar water uptake

Anatomical assays

To evaluate differences in FWU pathways among the three species we exposed fresh, mature leaves of saplings to a fluorescent apoplastic tracer solution (1% Lucifer Yellow carbohydrazide dilithium salt aqueous solution; LY; Sigma-Aldrich, St Louis, MO, USA) for 24 h. Then, leaves were washed in distilled water, dried with filter paper, hand sectioned and prepared for microscopic observation in a 90% glycerol-phosphate buffer (Mastroberti and Mariath, 2008). Sections were observed using epifluorescence (Leica DFC500MR; Wetzlar, Germany), under intense blue excitation of 450 – 490 nm with a 515-nm barrier filter (Oparka & Read, 1994). We also conducted classical anatomical assays to identify hydrophilic compounds on leaf tissues. Mature leaves were fixed in 50% ethyl alcohol-formaldehyde-acetic acid (FAA) (Johansen, 1940), embedded in plastic resin (Historesin®, Leica Biosystems), and then sectioned. These sections were then stained with Periodic Acid Schiff reaction (PAS) to identify hydrophilic polysaccharide compounds such as mucilage, glycogen, glycolipids and glycoproteins (McManus, 1948). Scanning microscopy images of mature leaves were provided by Laboratory of Electron Microscopy – University of Campinas (Campinas, Brazil).

Deuterium labelling experiment

To quantify the contribution of water derived from FWU on the leaf water content of each species, we exposed the shoots of 5-9 saplings of each species to deuterium-enriched fog during one night. These saplings were collected in CJSP and allowed to acclimate for one month in a glasshouse at University of Campinas (Campinas, SP, Brazil). The artificial fog was created using an ultrasonic device (model Waterclear Premium; Soniclear, São Paulo, Brazil) inside a fog chamber made with PVC and plastic (1.5 X 1.0 X 0.8 m).

Before the fog treatment the irrigation was suspended for one week. Then we collected leaves, washed with tap water, dried with paper towels and kept sealed in vials with parafilm. The same procedure was performed the following day, after the plants had been exposed to fog for 12 h during the night. Using the standard delta notation (δD‰) to express the deuterium ratio of each source, we estimated the FWU contribution (f_{FWU}; %) to leaf water content as a linear mixing model (Dawson *et al.,* 2002) :

$$f_{FWU} = \left(\frac{\delta D_a - \delta D_b}{\delta D_f - \delta D_b}\right) 100 \qquad \text{(Eqn 1)}$$

, where δD_a is the observed leaf δD after the fog session, δD_f is the fog δD (668‰) and δD_b is the leaf water δD before the fog session. We used plastic bags and parafilm to prevent fog water from reaching the soil and roots of the plants and, because any enrichment in ^2H of leaf water induced by transpiration inside the fog chamber was negligible, we expect that any increment in leaf δD originates from water derived from FWU. The Ψ_l of each species before the fog treatment was -0.54 MPa (SE±0.08) for *D. brasiliensis*, -0.97 MPa (SE±0.33) for *M. umbellata* and -0.9 MPa (SE±0.33) for *E. erythropappus*.

Leaf immersion experiment

We measured FWU contribution to leaf rehydration in a laboratory experiment in which fresh, mature, detached leaves of excised branches were immersed in distilled water for 3 hours and we measured the Ψ_l increment after the immersion (similar to Goldsmith *et al.,* 2013). The branches were collected at CJSP one day prior to the experiment and were kept hydrated until they were used. We sealed the petioles with parafilm and kept them out of water to avoid water entry. We used a Scholander pressure chamber (Model 1000; PMS, Corvallis, OR, USA) to measure Ψ_l immediately before and after the immersion, after drying the leaf thoroughly with paper towel. We immersed the leaves in water for 3 hours. We used this time interval because leaf-wetting events in their natural environment rarely last less than 3 hours. The immersion of 3 hours also allows for an increase in Ψ_l large enough to be easily detectable with the

Scholander pressure chamber. Leaving the leaves in the water for too much time, would allow all species to completely rehydrate and we would not be able to make meaningful FWU rates comparisons. We conducted these measurements along a range of initial Ψ_l as we expect the increase in Ψ_l after immersion ($\Delta\Psi_l$) to be related with the pre-immersion Ψ_l. To reach more negative initial Ψ_l, we allowed some of the leaves to bench dry before water immersion until they reached a Ψ_l close to -3 MPa.

Glasshouse experiment

We investigated how FWU would affect each species tolerance to soil drought by conducting an experiment with a total of 27-36 saplings (height of 20-60 cm) of each species in a glasshouse at the University of Campinas. After a one-month acclimation period, we exposed the saplings to a drought treatment (no soil irrigation) for 60 days, but 15-23 saplings of each species were exposed regularly to a fog treatment (artificial fog applied on sapling shoots three times per week for 12 hours during the night using the same protocol described above for the deuterium labeling experiment). The plants used in this experiment were in 34-l pots that contained a 2:1 (v/v) mixture of sand and commercial organic soil. The pots were irrigated until saturation before the beginning of the experiment.

We measured predawn (PD) and midday (MD) Ψ_l and stomatal conductance (g_s) eight times during the experiment. The destructive Ψ_l measurements were conducted in a different group of plants than the plants we used for g_s measurements. The midday Ψ_l measurements were made with a Scholander pressure chamber in 3-8 random individuals of each species per treatment. The g_s was measured in mature fully expanded leaves of 4-8 individuals of each species per treatment with an infrared gas analyzer (ADC BioScientific LCpro+; Analytical Development Company, Hoddesdon, Hertfordshire, UK) during the periods of maximum gas exchange activity (8-9:30 h for *D. brasiliensis* and 10-12 h for *E. erythropappus* and *M. umbellata*), which were assessed before the beginning of the experiment. We also measured the leaf area of the individuals used for g_s measurements at the beginning and at the end of the experiment. To calculate the total leaf area, we used ImageJ 1.42 to measure the area of 25 leaves of each species and fitted a linear regression to the measured leaf area as a function of the product between each leaf length and width. We used the regression equation of each species to predict the area of the other leaves from length and width measurements, and obtained the total leaf area by summing the areas of every leaf in a plant. At the end of the experiment we quantified the mortality rates of each species by considering plants with

completely desiccated leaves and branches as dead. During the experiment we monitored the glasshouse air temperature and humidity (model U23-001; Onset Computer Corporation, Bourne, MA, USA) and used these data to calculate air-to-air vapor pressure deficit (VPD).

We estimated the π_{TLP} of each species with the pressure-volume technique (Tyree and Hammel, 1972). The pressure-volume curves were constructed with leaves from detached rehydrated branches using the bench-dry method described in Sack *et al* (2011). We used the π_{TLP} as a reference point to indicate significant drought stress (Bartlett *et al.,* 2012; Blackman *et al.,* 2010).

Field meteorological data

In order to understand how the studied species could respond under actual climatic conditions of a TMCF, we used a long time-series of rain and midday air temperature and humidity data collected by a meteorological station located close to the TMCF site where our research was conducted (22°45′ S, 45° 36′ W; 1642 m). This time-series contained data from 1970 to 2010, but the years of 1971-1973, 1976, 1985, 2000-2001, 2008-2009 were excluded for having data gaps during the dry season.

Data analysis

Foliar water uptake experiments

For the deuterium labelling experiment data, we used a linear generalized least squares model to compare f_{FWU} among species. In the leaf immersion experiment, we described the relationship between $\Delta\Psi_{l_i}$ of each leaf *i* and its initial Ψ_{l_i} as a linear function:

$$\Delta\Psi_{l_i} = \alpha + \beta_{\Delta\Psi_l}\Psi_{l_i} \quad \text{(Eqn 2)}$$

, where the slope ($\beta_{\Delta\Psi l}$) represents the $\Delta\Psi_l$ increment per unit of initial Ψ_l and we believe it might be a useful parameter to compare among species to evaluate differences in FWU capacity. The $\beta_{\Delta\Psi l}$ should vary between 0 and -1 with $\beta_{\Delta\Psi l}$ = -1 representing complete rehydration. Another parameter of interest derived from the function (2) is the x-intercept ($-\alpha/\beta_{\Delta\Psi l}$), as it represents the minimum Ψ_l necessary to produce a detectable $\Delta\Psi_l$, which might be related with the leaf permeability to water during FWU. Assuming that during FWU the water enters the leaf passively following a water potential gradient (Oliveira *et al.,* 2014a), a more negative x-intercept value suggests that a bigger gradient is necessary to overcome the

leaf resistance to water entry. We used ordinary least squares regressions to estimate these parameters for each species.

Glasshouse experiment

To measure the effects of drought length, VPD and fog treatment on each species $MD\Psi_l$ we used linear mixed effects models. We used a linear generalized least squares model to compare leaf area change among species (details on supporting information notes S1).

We used the logistic function described in Klein (2014) and Guyot *et al* (2011) to describe the relationship between g_s and Ψ_l and estimate parameters of interest, such as g_{smax}, the maximum g_s reached by the species, Ψ_{g50} the Ψ_l value when g_s drops to half of g_{smax}, and s which is related with the slope of the linear portion of the model (details on supporting information notes S1).

We also used the approach described by Martinez-Vilalta *et al* (2014) to assess the plant conductivity loss during soil drought based on the linear relationship between $MD\Psi_l$ and $PD\Psi_l$:

$$MD\Psi_{l_i} = \Lambda + (\sigma + \sigma_i) PD\Psi_{l_i} \quad \text{(Eqn 3)}$$

In this approach, the slope of the relationship (σ) represents the sensitivity of the plant hydraulic conductivity to soil drought, and the intercept (Λ) represents the maximum transpiration rate per unit of hydraulic conductivity (Martinez-Vilalta *et al.*, 2014). We used linear mixed effects models to estimate these parameters for each species, with $MD\Psi_{l_i}$ as the response of each plant *i*, $PD\Psi_l$ as the fixed effect and a random slope structure (σ_i) that allowed each plant to have a different slope parameter (Zuur *et al.*, 2009).

Field meteorological data

We used the mixed effects models fitted to the glasshouse data and the field meteorological data to predict how many days it would take for each species to reach π_{TLP} under field conditions. We also calculated the probabilities of dry periods long enough to make the plants lose turgor occurring under three different scenarios: *fog*, *no fog* and *no fog and high VPD*. For a detailed explanation of each scenario and our analysis procedure see supporting information notes S1.

All analyses were conducted using the software R v.3.2.0 (R Core Team, 2015), and the packages "nlme" (Pinheiro *et al.*, 2015), "lsmeans" (Lenth, 2015) and "MASS" (Venables

and Ripley, 2002). We used Efron's pseudo-R_2 (Efron, 1978) as a measurement of the explained variance by the mixed-effects and non-linear models used on this study.

Results

Foliar water uptake

Anatomical assays

Adaxial and abaxial leaf surfaces of all species showed fluorescence due to the presence of salt apoplastic tracer paths (Fig. 1, see Eller *et al*. 2013 for *D. brasiliensis* figures). In *E. erythropappus*, after permeating the cuticle, the tracer solution moved via apoplastic pathways through the epidermis and parenchyma and into the xylem (Fig. 1a, b). Tector trichomes are very abundant in the abaxial epidermis and may be an important pathway for FWU in this species (Fig. 1g), as a high concentration of solution with apoplastic tracers was observed in their cell walls (Fig. 1b-d). There was also a high concentration of salts in the apical cell walls and the contact regions between apical and basal cells of tector trichomes (Fig. 1c), in addition to its occurrence in the shallow depressions in the adaxial cuticle formed after the senescence of glandular trichomes (Fig. 1e, f). Despite the Lucifer yellow (LY) impregnation in *E. erythropappus* leaves, the abundance of hydrophilic polysaccharides on its leaves was substantially less than in the other species (Fig. 1h).

In *M. umbellata*, we observed LY accumulation in cell walls throughout the entire leaf mesophyll (Fig. 1i, j). Direct diffusion through the adaxial and abaxial cuticle seems to be an important water entry pathway in this species also (Fig. 1i-l). We found high LY concentration throughout the middle of the mesophyll where collecting cells are located, suggesting a regular distribution of absorbed solution just below the palisade parenchyma (in linear aspect in cross section) (Fig. 1j). Collecting cells (Donato & Morretes, 2011; Donatini *et al.*, 2013) are the layer of mesophyll cells that connect the palisade parenchyma and the spongy mesophyll. The cytoplasmic extensions of collecting cells can be involved on the transport of solution deposited on the adaxial surface (Fig. 1m). We also found a strong LY presence in peltate glandular trichomes in both leaf surfaces, which suggest that these structures might facilitate water entry into the leaves (Fig. 1n). Hydrophilic polysaccharides were particularly abundant in *M. umbellata* leaves (Fig. 1o).

Deuterium labeling experiment

All three species had deuterium enriched water in their leaves following exposure to deuterium enriched fog, but the magnitude of the enrichment differed between species (generalized least squares model: $F_{2, 17} = 4.92$; $p = 0.02$). The leaves of *D. brasiliensis* had higher deuterated water content (37.02 %) than *E. erythropappus* (23.25 %), while *M. umbellata* showed intermediate f_{FWU} levels (30.16 %; Fig. 2a).

Leaf immersion experiment

As we expected, $\Delta\Psi_l$ was strongly and linearly related with initial Ψ_l in all species (Fig. 2b). The $\beta_{\Delta\Psi l}$ (the slope of this linear relationship) was more negative in *D. brasiliensis* and *M. umbellata* (-0.93 and -0.87 MPa MPa^{-1}, respectively) than in *E. erythropappus* (-0.72 MPa MPa^{-1}), which indicates a higher rehydration capacity in the former species. The x-intercept of the linear relationship was also higher in *D. brasiliensis* and *M. umbellata* (-0.31 MPa in both species) than in *E. erythropappus* (-0.43 MPa), which suggests that *D. brasiliensis* and *M. umbellata* leaves are more permeable to water.

Glasshouse experiment

The fog treatment had a stronger effect in *D. brasiliensis* and *M. umbellata* saplings than in *E. erythropappus* saplings (Table 1; Fig. 3). *Drimys brasiliensis* $MD\Psi_l$ in the control treatment (no fog) reduced, on average, by 0.026 MPa per day in relation to the fog treatment, which showed a slight increase throughout the experiment. The leaves of *D. brasiliensis* in the control treatment started losing turgor after 39-45 days of drought, while the leaves from plants in the fog treatment maintained their turgor until the end of the experiment (60 days). The $PD\Psi_l$ of *D. brasiliensis* in the control treatment also remained constant throughout the experiment, never dropping below

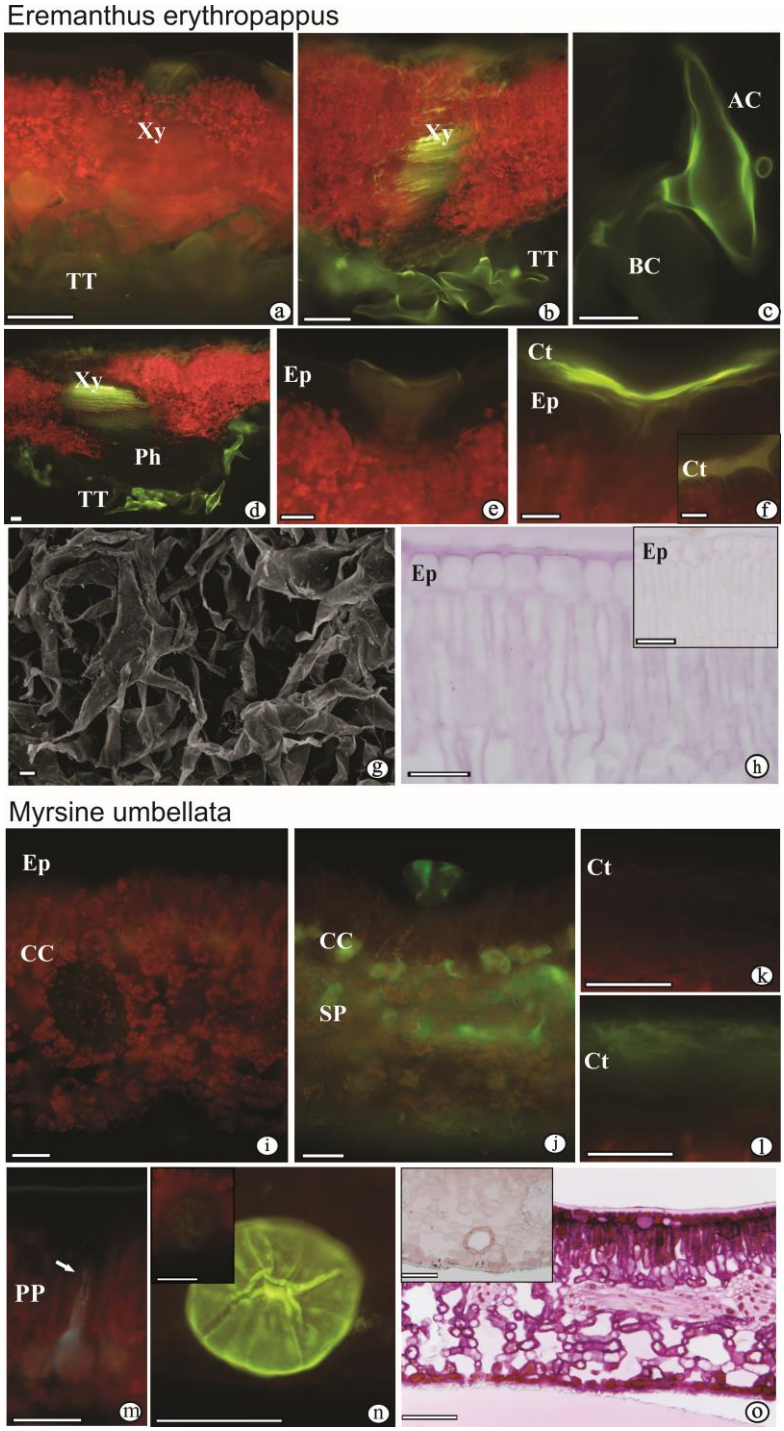

Figure 1. Evidence of foliar absorption through apoplastic pathways and leaf anatomy of *Eremanthus erythropappus* (**a-h**) and *Myrsine umbellata* (**i-o**). **a)** Autofluorescence of fresh leaf (control); **b)** Apoplastic fluorescent tracer Lucifer yellow (LY) accumulation on tector trichomes of abaxial surface, epidermis and parenchyma's apoplastic pathways and xylem; **c)** Tector trichome detail with LY accumulation on apical cell wall, note the increase in intensity in the contact region with the basal cell; **d)** Apoplastic tracer solution applied on abaxial surface moved directly to xylem, and could even reach the opposite leaf surface; **e)** Autofluorescence of fresh abaxial leaf surface with a glandular trichome before senescence (control); **f)** Presence of LY in the adaxial cuticle especially in the depressions created by glandular trichomes senescence, recesses in the epidermis with LY in detail. The bars in **a-f** represent 5 mm. **g)** Abaxial surface with ramified tector trichomes. The bar represents 25 µm; **h)** Weak presence of polysaccharide hydrophilic compounds as indicated by PAS reaction (darker pink); top left panel is the control. The bar represents 50 µm. **i)** Autofluorescence of fresh leaf (control); **j)** Presence of LY in peltate glandular trichomes, throughout all parenchyma with more concentration in collector cells (after 24 hours of LY solution application on adaxial surface). **k)** Adaxial cuticle autofluorescence (control); **l)** Apoplastic tracer presence in the adaxial cuticle; **m)** Collecting cell detail showing cytoplasmical expansion between palisade cells (indicated by arrow) reaching the contact zone between epidermal cells (obtained after two hours in contact with 0.02% HPTS solution, pyranine (8-Hydroxypyrene-1,3,6-Trisulfonic Acid, Trisodium Salt)). **n)** Presence of LY in abaxial glandular trichomes (front view); top left panel is the autofluorescence of the trichomes (control). The bars in **m-n** represent 5 µm. **o)** Strong presence of polysaccharide hydrophilic compounds as indicated by PAS reaction (darker pink); top left panel is the control. The bar represents 50 µm. BC: Basal cell of tector trichome; Ct: Cuticle; CC: Collecting cell; Ep: Uniseriate epidermis; Ph: Phloem; PP: Palisade parenchyma; SP: Spongy parenchyma; TT: Tector trichome; Xy: Xylem.

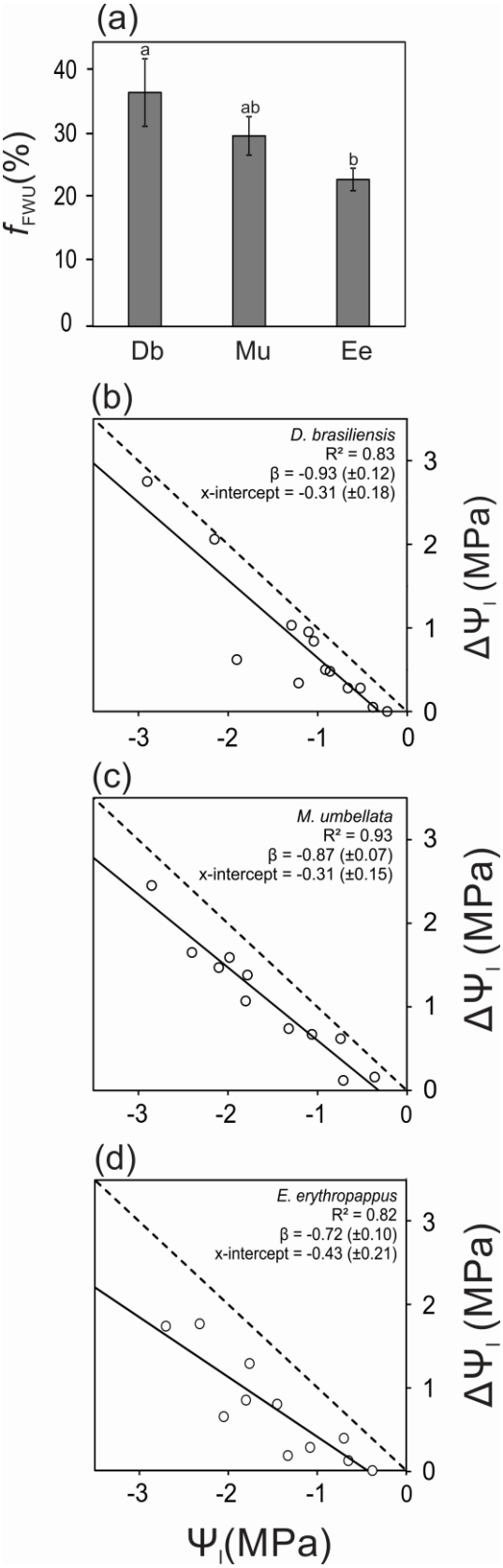

Figure 2. a) Contribution of deuterium enriched water acquired via foliar water uptake to leaf water content (f_{FWU}) after saplings being exposed to deuterium enriched fog for one night. Columns are the means of f_{FWU} contribution in each species (Db = *Drimys brasiliensis*, Mu = *Myrsine umbellata*, Ee = *Eremanthus erythropappus*) and error bars are the standard error. Different letters indicates significant difference (α=0.05) based on comparisons made using the least-squares means 95% confidence intervals estimated with a generalized least squares model. **b-d)** Relationship between leaf water potential increment ($\Delta\Psi_l$) after water immersion and initial Ψ_l for *D. brasiliensis* **(b)**, *M. umbellata* **(c)** and *E. erythropappus* **(d)**. The dashed line is a 1:1 reference line, which indicates complete rehydration.

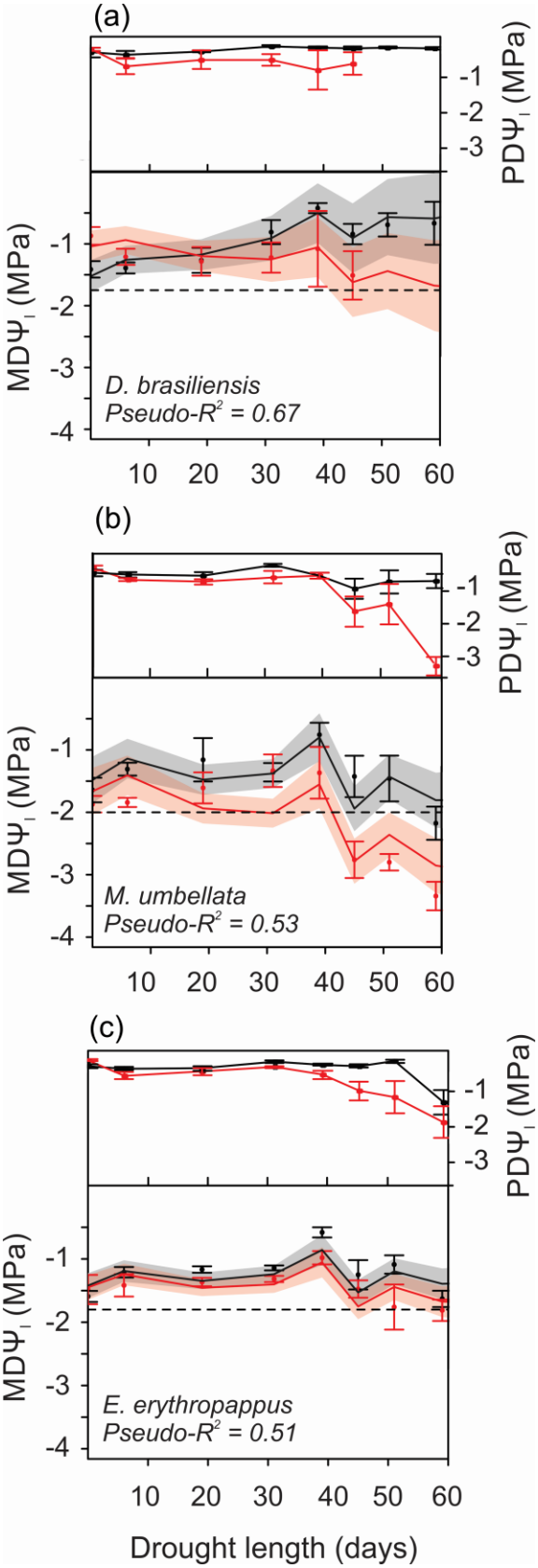

Figure 3. Predawn ($PD\Psi_l$; upper panel) and midday leaf water potential ($MD\Psi_l$; lower panel) for the fog (black) and control (red) treatments for *Drimys brasiliensis* **(a)**, *Myrsine umbellata* **(b)**, and *Eremanthus erythropappus* **(c)** during the glasshouse experiment. The dots and error bars are the observed mean and standard errors, the lines represent the predicted means by the linear mixed effects model and the colored region is the standard error x 2, as an approximation for the 95% confidence interval for the fixed effects. The two last Ψ_l measurements were not made in the control treatment for *Drimys brasiliensis* as the petioles collapsed due to the low pressure. The black dashed line represents each species' turgor loss point (π_{TLP}). Upper panel in **(a)** modified from Eller *et al.*, 2013.

Table 1. Coefficient estimates from the linear mixed effects models fitted to the glasshouse experiment data. The coefficient estimates are from the control treatment, with the *Treatment* and *Drought:Treatment* estimates indicating the difference in the *Intercept* and *Drought length* coefficient estimates between both treatments. Abbreviations used in the table are midday leaf water potential ($MD\Psi_l$) and vapor pressure deficit (VPD).

Response	Predictors	Coefficient	Std. Error	DF	t-value	p
D. brasiliensis	*(Intercept)*	- 0.682	0.156	48	-4.379	<0.01
$MD\Psi_l$	*log(VPD)*	-0.307	0.095	22	-3.223	<0.01
	Treatment	-0.481	0.018	48	-2.668	0.01
	Drought length	-0.012	0.007	48	-1.652	0.10
	Drought length:Treatment	0.026	0.009	48	2.792	<0.01
M. umbellata	*(Intercept)*	-0.846	0.201	64	-4.021	<0.01
$MD\Psi_l$	*log(VPD)*	-0.694	0.139	28	-4.980	<0.01
	Treatment	0.189	0.239	64	0.789	0.43
	Drought length	-0.023	0.005	64	-4.277	<0.01
	Drought length:Treatment	0.014	0.007	64	1.945	0.05
E. erythropappus	*(Intercept)*	-0.965	0.121	56	-7.975	<0.01
$MD\Psi_l$	*log(VPD)*	-0.413	0.087	33	-4.741	<0.01
	Treatment	0.028	0.136	56	0.206	0.84
	Drought length	-0.005	0.003	56	-1.808	0.76
	Drought length:Treatment	0.004	0.004	56	1.030	0.30

-0.5 MPa, while in the control treatment it dropped to values lower than -1 MPa (Fig. 3a). *Myrsine umbellata* $MD\Psi_l$ in the control treatment dropped 0.014 MPa per day in relation to the fog treatment, which, in contrast to *D. brasiliensis*, also dropped during the experiment, albeit slower than in the control treatment. Both treatments of *Myrsine umbellata* had leaves that reached π_{TLP}, but the turgor loss occurred earlier in the control treatment. The $PD\Psi_l$ of *M. umbellata* showed a similar pattern, dropping faster in the control treatment than in the fog treatment at the end of the experiment (Fig. 3b). The patterns of $MD\Psi_l$ and $PD\Psi_l$ in *E. erythropappus* were very similar in both treatments, the $MD\Psi_l$ dropped only 0.004 MPa per day in relation to the fog treatment throughout the experiment. Leaves of *E. erythropappus* in both treatments only started reaching π_{TLP} after more than 50 days of drought (Fig. 3c). The fog effect we observed in the experiment (i.e. the decrease in $MD\Psi_l$ per day in the control treatment relative to the fog treatment) was proportional to the species FWU capacity as measured by the deuterium labelling and leaf immersion experiment (Fig. 4).

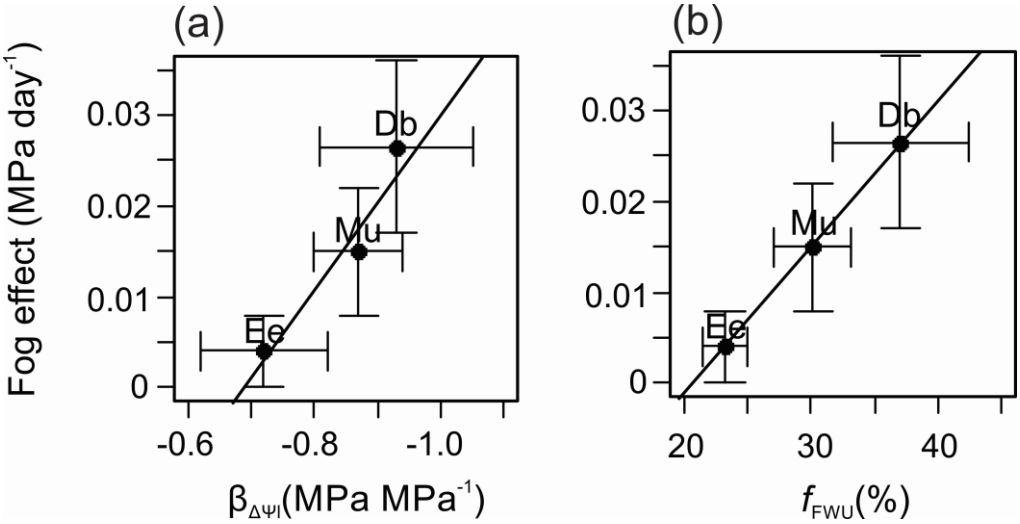

Figure 4. Relationship between the fog effect size (mean difference in water potential per day from the fog treatment to the control treatment) and foliar water uptake, represented by the slope ($\beta_{\Delta\Psi l}$) of the relationship between Ψ_l increment after water immersion ($\Delta\Psi_l$) and its initial Ψ_l **(a)**; and by the contribution of deuterium enriched water to the leaf water content (f_{FWU}) following exposure to deuterium enriched fog **(b).** The circles are the means and error bars the standard error (Db = *Drimys brasiliensis*, Mu = *Myrsine umbellata*, Ee = *Eremanthus erythropappus*). The lines were estimated using total least squares regressions.

Looking at the drought response of each species, *E. erythropappus* was the species least affected, with the $MD\Psi_l$ dropping just 0.004 MPa per day throughout the experiment, in comparison with 0.012 and 0.023 MPa day^{-1} in *D. brasiliensis* and *M. umbellata*, respectively (Table 1). In *E. erythropappus*, the small response in $MD\Psi_l$ to drought length could be related to its more isohydric stomatal regulation in comparison with the other species (Fig. 5a, c, e). We classify *E. erythropappus* as more isohydric than the other species by following the definition proposed by Klein (2014): to compare the minimum Ψ_l reached by the species while still allowing for stomatal conductance. This minimum Ψ_l value was defined by Klein (2014) as the Ψ_l value in which the plant reaches 25% of its maximum g_s (Ψ_{g25}), as it represents the minimum Ψ_l of the linear portion of the g_s (Ψ_l) function. *E. erythropappus* has a less negative Ψ_{g25} value (-1.31 MPa) than *D. brasiliensis* and *M. umbellata* (-1.48 and -1.76 Mpa, respectively). These results are consistent with the other approach we used to assess plant isohydric/anisohydric behavior: the plant conductivity loss analysis using $PD\Psi_l$ and $MD\Psi_l$ proposed by Martinez-Vilalta *et al* (2014) (Fig. 5b, d, f). The smaller slope (σ) of *E. erythropappus* (0.35 MPa MPa^{-1}) indicates that this species is closer to a strict isohydric behavior than *D. brasiliensis* and *M. umbellata*, which has a slope closer to a strict anisohydric behavior (0.85 and 0.57 MPa MPa^{-1}, respectively). Our results indicate that species with more

anisohydric behavior (*D. brasiliensis* and *M. umbellata*) generally had higher FWU capabilities than the more isohydric *E. erythropappus* (Fig. 6).

Despite *D. brasiliensis* and *M. umbellata* showing more anisohydric behavior, *D. brasiliensis* has lower g_{smax} and a lower maximum transpiration rate per unit of hydraulic conductivity (Λ from equation 2) than the other species (Fig. 5). Another important distinction between *D. brasiliensis* and *M. umbellata* are the higher leaf loss rates of *D. brasiliensis* (Fig. 7a, b). While both *D. brasiliensis* and *M. umbellata* shed more leaves in the control treatment than in fog treatment, *D. brasiliensis* also lost a considerable amount of leaf area in the fog treatment. The leaf loss on the fog treatment could have been triggered by the high VPD in the glasshouse (Fig. S1), which was higher than the values typically experienced by the plants in the field. There was no difference in leaf loss between treatments for *E. erythropappus* (Fig. 7c). Most *D. brasiliensis* and *M. umbellata* saplings in the control treatment died at the end of the experiment, while those in the fog treatment had higher survival rates (Fig. 7d, e). No individuals of *E. erythropappus* died at the end of the experiment (Fig. 7f).

Predictions based on field meteorological data

The longest periods without rain observed at our TMCF site happened almost exclusively from June-September (data not shown). The most likely drought length (i.e. period without rain) at the site is 27 days assuming the drought length data follow an approximately log-normal probability distribution (Fig. 8). In the *fog* scenario (i.e. fog and VPD set at 0.9 kPa) we predict that all the species can maintain leaf turgor for more than 70 days (the longest dry period we have in our dataset is 69 days). In this scenario, *E. erythropappus* would stay at least 0.51 MPa above its π_{TLP}, *D. brasiliensis* 0.33 MPa and *M. umbellata* 0.27 MPa. In the *no fog* scenario (i.e. no fog and VPD set at 0.9 kPa), *E. erythropappus* would still not lose turgor and would stay at least 0.18 MPa above its π_{TLP}. However the species with higher FWU, *D. brasiliensis* and *M. umbellata*, would reach their π_{TLP} at 46 and 39 days, respectively. The probability of dry periods of this size or longer occurring in our site are 0.19 and 0.29, respectively. The *no fog and high VPD* scenario (when the VPD is set at 1.94 kPa) shows how high VPD could accentuate the effects of the lack of fog by decreasing the days required for *D. brasiliensis* and *M. umbellata* to lose leaf turgor to 37 and 20 days, respectively. The probability of dry periods equal or longer than the time necessary for *D. brasiliensis* and *M. umbellata* to lose leaf turgor increases to 0.39 and 0.87, respectively. In this scenario, *E.*

erythropappus would lose leaf turgor at 60 days, which is a drought length with a probability of 0.05 of occurring (Fig. 8).

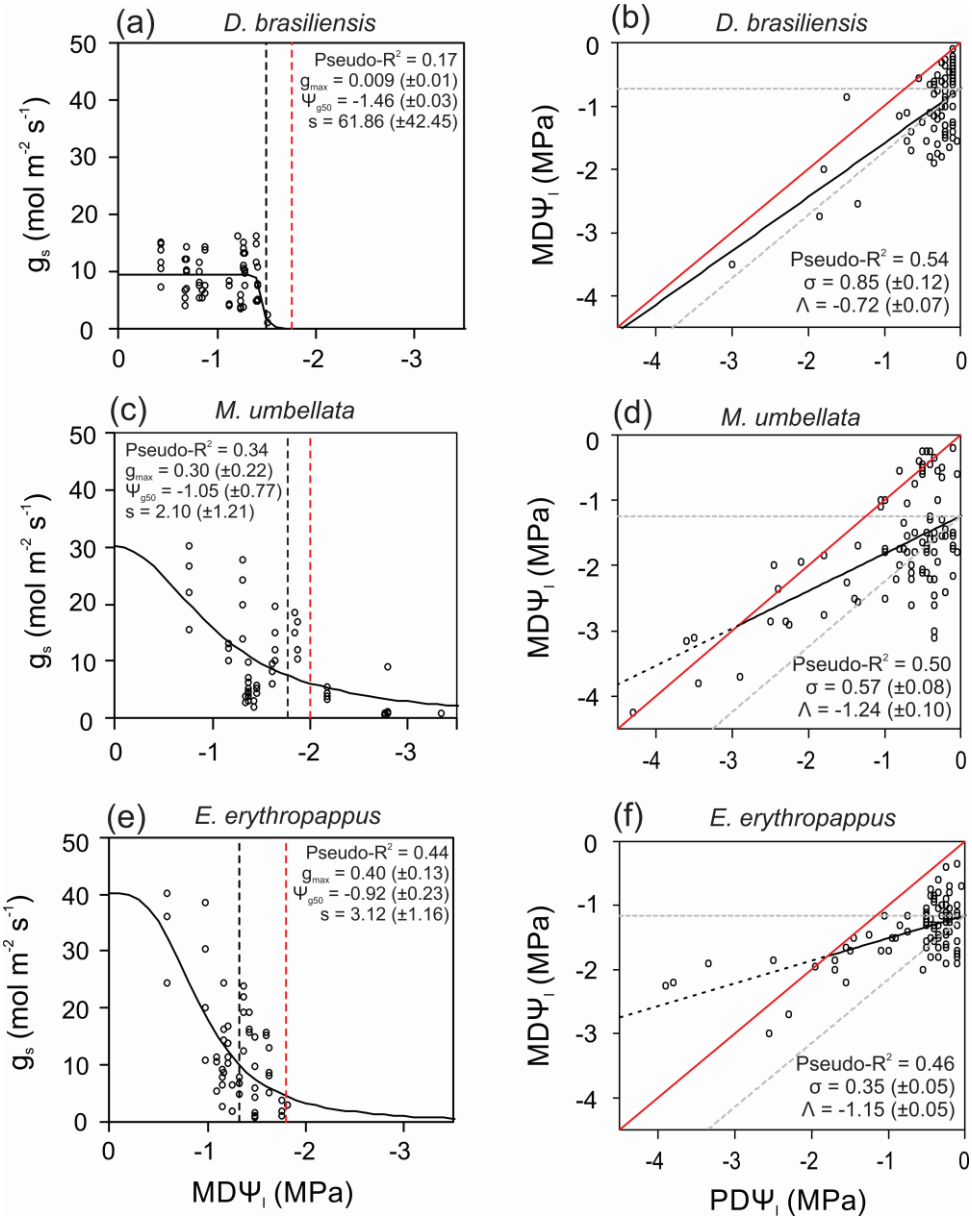

Figure 5. Relationship between stomatal conductance (g_s) and midday leaf water potential ($MD\Psi_l$) and between midday and predawn leaf water potential ($PD\Psi_l$) for *Drimys brasiliensis* (a-b), *Myrsine umbellata* (c-d) and *Eremanthus erythropappus* (e-f). The continuous black lines are the predicted means of the models fitted to the data. For the panels in the left (a,c,e), the black and the red dashed lines are the point where the g_s is reduced to 25% of its maximum value (Ψ_{g25}) and the turgor loss point (π_{TLP}), respectively. For the panels on the right (b,d,f), the gray dashed lines are, respectively, the expected strict isohydric (the flat line with $\sigma = 0$) and the strict anisohydric (the inclined line with $\sigma = 1$) behavior (Martínez-Vilalta *et al.*, 2014). The red line is the 1:1 line, which represents the point where $PD\Psi_l = MD\Psi_l$ and transpiration ceases. The regression line becomes dashed after reaching the 1:1 line to represent the transpiration cessation.

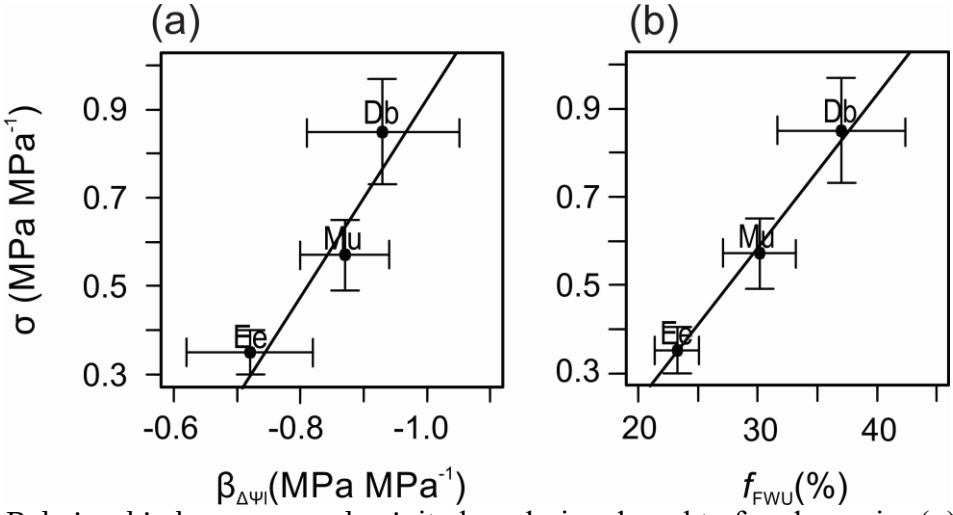

Figure 6. Relationship between conductivity loss during drought of each species (σ) and their foliar water uptake (FWU) capacity, represented by the slope ($\beta_{\Delta\Psi l}$) of the relationship between Ψ_l increment after water immersion ($\Delta\Psi_l$) and its initial Ψ_l **(a)**; and by the contribution of deuterium enriched water to the leaf water content (f_{FWU}) after the plant was exposed to deuterium enriched fog **(b).** The circles are the means and error bars the standard error (Db = *Drimys brasiliensis*, Mu = *Myrsine umbellata*, Ee = *Eremanthus erythropappus*). The lines were estimated using total least squares regressions.

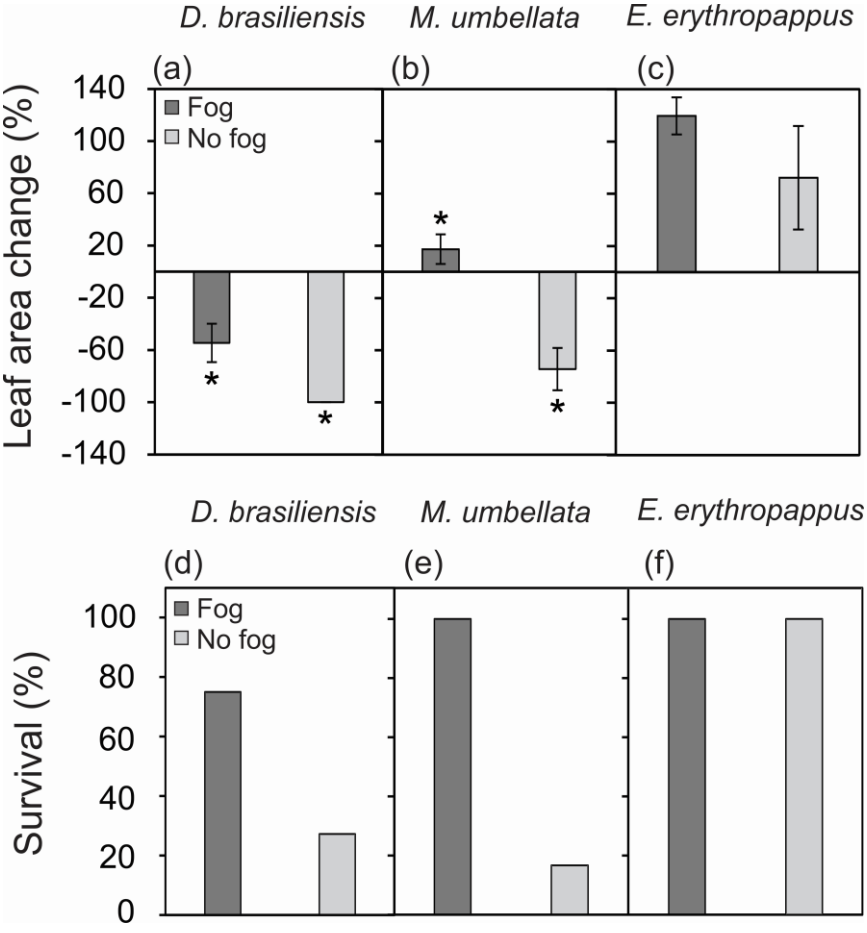

Figure 7. Leaf area change rates (a-c) and sapling survival rates at the end of experiment (d-f) for each species in the fog (dark gray) and control (lighter gray) treatment. Asterisks indicate significant difference (α=0.05) based on pairwise comparisons made using the least-squares means 95% confidence intervals estimated with a generalized least squares model.

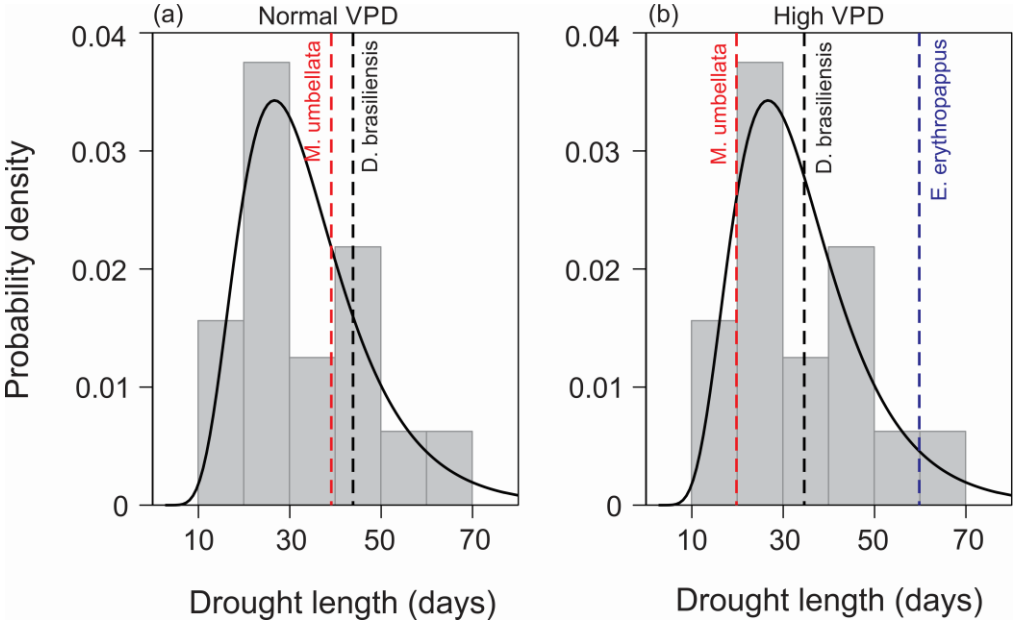

Figure 8. Log-normal probability distribution (line) of the drought length (bars) observed during 32 years in a TMCF site. The dashed lines are the predicted drought length necessary for each species to lose leaf turgor if there was no fog (black line = *Drimys brasiliensis*, red line = *Myrsine umbellata*, blue line = *Eremanthus erythropappus*). The panel (a) illustrates the predictions using the mean VPD observed at the site during the dry periods (0.9 kPa), while the panel (b) are the predictions using the mean of the VPD values above the 95-percentile in our data (1.94 kPa).

Discussion

Our results indicate that, while some TMCF species might have specialized structures that facilitate FWU (i.e. peltate and tector trichomes), the main FWU pathway for the studied species seems to be direct diffusion through the leaf cuticle. We conclude this based both on the results of the apoplastic tracers and on the constant Ψ_l increment after water immersion in all species. We also verified that, among the studied species, those with higher FWU capacity (*D. brasiliensis* and *M. umbellata*) tend to be more anisohydric and rely more on FWU to maintain their leaf turgor during soil drought than species with lower FWU capacity (*E. erythropappus*), which tend to be more isohydric.

Differences in FWU capacity and pathways

The cuticle of all species showed some degree of permeability to water, enabling the diffusion of apoplastic fluorescent tracers (Fig. 1 and Eller *et al.*, 2013). The leaves of *E. erythropappus* and *M. umbellata* also have trichomes that exhibited high concentrations of LY, which suggests they could function as preferential FWU pathways for these species. The enhanced water uptake capacity of these structures might be related to the formation of aqueous

pores at the base of trichomes when exposed to water (Schönherr, 2006). Leaves of *M. umbellata* possessed specialized collecting cells in the mesophyll that could also function as preferential pathways, leading to reduced hydraulic resistance between the cuticle and the leaf xylem vessels (Fig. 1i-j, m). Despite the role that these specialized structures might have on FWU in *E. erythropappus* and *M. umbellata*, *D. brasiliensis* leaves have no trichomes or collector cells and still have high FWU rates (Fig. 1-2). However, our results show that the leaves of the species with the highest FWU rates (*D. brasiliensis* and *M. umbellata*) both had high concentrations of hydrophilic polysaccharide compounds in the mesophyll in comparison with *E. erythropappus* (Fig. 1h-o and Eller *et al.,* 2013). As we suggested for *M. umbellata* collector cells, these hydrophilic polysaccharide compounds could create preferential pathways for water movement through the mesophyll, facilitating the transport of the water absorbed by the cuticle to the leaf xylem.

The stomata can also be a pathway for FWU (Burkhardt, 2010; Burkhardt *et al.,* 2012; Berry *et al.,* 2014). We observed patterns of fluorescent tracers on the abaxial layer of *D. brasiliensis* leaves that suggests a possible role of the stomata on FWU for this species (Eller *et al.,* 2013), but we could not find the same pattern for *M. umbellata* and *E. erythropappus* leaves (Fig. 1). Even though water could enter through stomatal pores during FWU, we believe that the bulk of water entry in the studied species happens through direct cuticle diffusion (which may be facilitated by specialized structures). The strong linear relationship between the Ψ_l increment after water immersion and pre-immersion Ψ_l in all species (Fig. 2b-d) suggests a relatively constant leaf permeability to water. If the stomata played a direct role in the amount of water acquired through FWU, we would expect lower FWU rates at more negative Ψ_l, when g_s should be lower (Fig. 5). The hypothesis that FWU is driven mostly by the gradient of water potential between the water outside the leaf and Ψ_l is supported in the whole-plant scale by observations that reversals in stem sap flow during leaf-wetting increase under drier soil conditions (Eller *et al.,* 2015; Cassana *et al.,* 2015).

Leaf turgor maintenance during drought and FWU

Our glasshouse experiment showed that leaf-wetting events might be particularly important for the leaf turgor maintenance of species with high FWU capabilities. Our fog treatment could have also affected other aspects of the plant water balance, such as suppressing nocturnal transpiration (Eller *et al.,* 2015). We assume these effects were similar among the

species and, therefore, the different effect of the fog treatment among species was mostly caused by the difference in FWU among species; this assumption is corroborated by Figure 4.

Our results suggest that TMCF species with lower FWU capacity, e.g. *E. erythropappus*, would rely on alternative strategies, such as a more isohydric stomatal regulation (Fig. 5), to maintain leaf turgor during longer droughts. Tighter stomatal regulation allows *E. erythropappus* to maintain leaf turgor for longer than the other studied species, regardless of fog occurrence (Fig. 3, 8). Isohydric, however, could limit plant carbon assimilation during these dry periods, increasing the risk of non-structural carbohydrate depletion and death by carbon starvation (McDowell *et al.,* 2008; 2011; Breshears *et al.*, 2009; Mitchell *et al.*, 2013; Oliveira *et al.*, 2013; Oliveira *et al.*, 2014b); although, in the time-scale of our experiment this strategy allowed *E. erythropappus* to have higher survival rates and leaf production during drought than the other species.

The species with a more anisohydric behavior (*D. brasiliensis* and *M. umbellata*; Fig. 5) showed higher FWU rates (Fig. 2) and benefitted more from fog during the glasshouse experiment (Fig. 3). Based on the assumption that FWU is driven by a water potential gradient (Fig. 2), it is reasonable to expect that anisohydric species would have higher FWU rates than isohydric species, as long as their leaves have similar water permeability (Fig. 6). The benefits of FWU might be particularly useful for species that are more anisohydric; the maintenance of stomatal conductance in these species may allow higher carbon assimilation during dry periods, but could pose more risks to the hydraulic integrity of the plant (McDowell *et al.,* 2008; 2011; Breshears *et al.*, 2009; Mitchell *et al.*, 2013; Oliveira *et al.*, 2013). The water provided by FWU could reduce these risks, as it can not only act as an ephemeral water source, but also have a role in the refilling of embolized vessels of leaves and branches (Laur & Hacke, 2014; Mayr *et al.*, 2014). Additionally, some species, such as *D. brasiliensis* and *Araucaria angustiolia* (Bert.) O. Kuntze, are able to redistribute FWU water towards the soil (Eller *et al.*, 2013; Cassana *et al.*, 2015). We postulate that this redistributed water would have similar effects on root physiology to the ones observed in water redistribution between soil layers, mitigating root embolism (Domec *et al.*, 2004, 2006) and prolonging root lifespan (Bauerle *et al.*, 2008).

Despite *D. brasiliensis* and *M. umbellata* sharing some similarities (high FWU and anisohydric stomatal behavior), they respond to drought differently. *D. brasiliensis* has lower hydraulic conductivity rates (Fig. 5) and higher leaf loss rates, even in the fog treatment (Fig. 7). These traits indicate that, even though *D. brasiliensis* shows some anisohydric traits, it

should use less water than the other species, and therefore would take more time to deplete its soil water supply during the experiment. This explanation is supported by the slower decrease of $PD\Psi_l$ in *D. brasiliensis* control treatment (Fig. 3). The leaf area adjustment showed by *D. brasiliensis* is a common response of plants to both atmospheric and soil drought (Mencuccini & Grace, 1994; Martínez-Vilalta *et al.*, 2009; Limousin *et al.*, 2012). While *D. brasiliensis* did not experience soil water deficit in the fog treatment (Fig. 3a), the glasshouse VPD reached values higher than those that typically occur in TMCF (Fig. 3d) and could have triggered the leaf-shedding response on this treatment. The relatively high VPD values in the glasshouse could also have been the cause of the mortality observed in some *D. brasiliensis* individuals in the fog treatment. The anisohydric behavior of *D. brasiliensis* associated with the narrow safety margin of the species (Oliveira *et al.*, 2014) could be a risky strategy under dry atmospheric conditions, regardless of soil drought. In contrast, *M. umbellata* uses more water and depletes soil water faster (Fig. 3b), which, in association with its anisohydric behavior, exposes leaves to more negative water potentials than the other species and makes them lose turgor more rapidly (Fig. 3b).

Based on our greenhouse results, high FWU/more anisohydric species (*D. brasiliensis* and *M. umbellata*) are much more likely to lose leaf turgor in field conditions if there were no fog (Fig. 8). These predictions are based on two major assumptions that should to be taken into account. The first assumption is that the π_{TLP} measured in well-hydrated branches will remain constant as drought progresses. There is evidence that many plants can show a moderate shift in their π_{TLP} during drought (Bartlett *et al.*, 2014), mostly caused by osmotic adjustment (Morgan 1984; Chen & Jiang, 2010) or developing new leaves with a more negative π_{TLP} (Wright *et al.*, 1992). However, as all the species we studied showed a sharp decline of gas exchange when close to π_{TLP} (Fig. 5) and the highest leaf loss rates were observed in the species that lost turgor during the experiment (Fig. 7), we believe the possible π_{TLP} shift experienced by the species we studied did not significantly interfere with our conclusions. Additionally, even if the species could maintain leaf turgor with an osmotic adjustment shift of the π_{TLP}, the increased demand for carbohydrates to maintain leaf turgor might be considered a physiologically demanding strategy for the plant, as stored carbohydrates are a valuable resource during drought (Mcdowell *et al.*, 2011; Mitchell *et al.*, 2013). The second assumption we made was that these species would respond to drought in the field in a similar way to that observed in the glasshouse, although we are aware of a number of factors in the field that could affect this response. In the field, plants are usually exposed to conditions that can accentuate

drought effects, such as greater wind speed (which can increase leaf water loss, Huang *et al.*, 2015), competition for water with other plants, and damage by insects and pathogens (McDowell *et al.*, 2008; 2011; Jactel *et al.*, 2011; Anderegg *et al.*, 2015). Another important point to note is that we used a fog exposure time of approximately 36 hours (3 nights) per week in our experiment and the fog occurrence in TMCF can be much higher than this (Holwerda *et al*., 2006; Jarvis & Mulligan, 2011; Nair *et al.*, 2008). This difference implies that FWU in field conditions could play an even greater role in TMCF plant water relations than that detected in our experiment.

Conclusions

We show that FWU can be an important trait for some TMCF species to maintain leaf turgor during seasonal droughts. Plants that possess lower FWU capacity, can compensate for it with other strategies, such as a more conservative stomatal regulation strategy. The consequence of this reliance on FWU during drought is that species with high FWU are more likely to lose leaf turgor under conditions in which leaf-wetting events are infrequent. Therefore, we expect that TMCF trees that are more reliant on FWU will be more affected by any decrease in the incidence of fog events and increase in evapotranspiration, both of which are predicted for these ecosystems in some climate change scenarios (Still *et al.*, 1999; Williams *et al.*, 2007).

The generality of our findings should be further tested in other species and ecosystems, but we believe that they enhance our understanding of how FWU interacts with other physiological traits in plants, and also have important implications to predict plant performance during drought and climate change. Considering how widespread FWU appears to be in TMCF (Goldsmith *et al.*, 2013; Gotsch *et al.*, 2014; Oliveira *et al.*, 2014) we conclude that a climate with less fog could pose a serious threat to the integrity and biodiversity of these ecosystems.

Acknowledgements

We thank INMET for providing the field meteorological data we used on this study; the Graduate Program in Ecology and Plant Biology from University of Campinas (UNICAMP), São Paulo Forestry Institute; staff of the CJSP; research support and facilities offered by the Plant Anatomy and Physiology Laboratories of UNICAMP (Profs. Sandra Guerreiro, Marilia Castro, Paulo Mazzafera, Carlos Joly and their students) and Federal University of Rio Grande do Sul (Prof. Jorge Mariath, Alexandra Mastroberti and Carlos Widholzer); Isotope Ecology of Center for Nuclear Energy in Agriculture (Prof. Plinio

Camargo, Marcelo Moreira, Luiz Martinelli, Geraldo Arruda and Maria Antonia Perez); Geochronological Research Center of the University of São Paulo (Alyne Barros); Márcia Duarte for the electron scanning microscopy images; Prof. Maurizio Mencuccini and Oliver Binks for reviewing this manuscript. This work was supported by the São Paulo Research Foundation (FAPESP) (Grant no. 10/17204-0), FAPESP/Microsoft Research (Grant no. 11/52072-0), both awarded to R.S.O., and the Higher Education Co-ordination Agency (CAPES/Brazil), National Counsel of Technological and Scientific Development (CNPq) and FAPESP (Grant no 13/19555-2) awarded scholarships to A.L.L. and C.B.E.

References

Allen CD, Macalady AK, Chenchouni H, Bachelet D, McDowell N, Vennetier M, Kitzberger T, Rigling A, Breshears DD, Hogg ET et al. 2010. A global overview of drought and heat-induced tree mortality reveals emerging climate change risks for forests. *Forest Ecology and Management* **259**: 660-684.

Anderegg WR, Hicke JA, Fisher RA, Allen CD, Aukema J, Bentz B, Hood S, Lichstein JW, Macalady AK, McDowell N et al. 2015. Tree mortality from drought, insects, and their interactions in a changing climate. *New Phytologist* **206**: 674-683.

Bartlett MK, Scoffoni C, Sack L. 2012. The determinants of leaf turgor loss point and prediction of drought tolerance of species and biomes: a global meta-analysis. *Ecology Letters* **15**: 393-405.

Bartlett MK, Zhang Y, Kreidler N, Sun S, Ardy R, Cao K, Sack, L. 2014. Global analysis of plasticity in turgor loss point, a key drought tolerance trait. *Ecology letters* **17**: 1580-1590.

Bauerle TL, Richard JH, Smart DR, Eissenstat DM. 2008. Importance of internal hydraulic redistribution for prolonging the lifespan of roots in dry soil. *Plant, Cell & Environment* **31**: 177-186.

Benzing DH, Seemann J, Renfrow A. 1978. Foliar epidermis in Tillandsioideae (Bromeliaceae) and its role in habitat selection. *American Journal of Botany* **65**: 359–365.

Berry ZC, White JC, Smith WK. 2014. Foliar uptake, carbon fluxes and water status are affected by the timing of daily fog in saplings from a threatened cloud forest. *Tree physiology* **34**: 459-470.

Bertoncello R, Yamamoto K, Meireles LD, Shepherd GJ. 2011. A phytogeographic analysis of cloud forests and other forest subtypes amidst the Atlantic forests in south and southeast Brazil. *Biodiversity and Conservation* **20**: 3413–3433.

Blackman CJ, Brodribb TJ, Jordan GJ. 2010. Leaf hydraulic vulnerability is related to conduit dimensions and drought resistance across a diverse range of woody angiosperms. *New Phytologist* **188**: 1113–1123.

Breshears DD, Cobb NS, Rich PM, Price KP, Allen CD, Balice RG, Romme WH, Kastens JH, Floyd ML, Belnap J et al. 2005. Regional vegetation die-off in response to global-change type drought. *Proceedings of the National Academy of Sciences* **102**: 15144–15148.

Breshears DD, McDowell NG, Goddard KL, Dayem KE, Martens SN, Meyer CW, Brown KM. 2008. Foliar absorption of intercepted rainfall improves woody plant water status most during drought. *Ecology* **89**: 41–47.

Breshears DD, Myers OB, Meyer CW, Barnes FJ, Zou CB, Allen CD, McDowell NG, Pockman WT. 2009. Tree die-off in response to global-change-type drought: mortality insights from a decade of plant water potential measurements. *Frontiers in Ecology and the Environment* **7**: 185–189.

Brodribb T, Holbrook NM, Edwards EJ, Gutierrez, MV. 2003. Relations between stomatal closure, leaf turgor and xylem vulnerability in eight tropical dry forest trees. *Plant, Cell & Environment* **26:** 443–450.

Bruijnzeel LA, Mulligan M, Scatena FN. 2011. Hydrometeorology of tropical montane cloud forests: emerging patterns. *Hydrological Processes* **25**: 465-498.

Burgess SSO, Dawson TE. 2004. The contribution of fog to the water relations of *Sequoia sempervirens* (D. Don): foliar uptake and prevention of dehydration. *Plant, Cell & Environment* **27**: 1023–1034.

Burkhardt M. 2010. Hygroscopic particles on leaves: nutrients or desiccants? *Ecological monographs* **80**: 369–399.

Burkhardt J, Basi S, Pariyar S, Hunsche M. 2012. Stomatal penetration by aqueous solutions – an update involving leaf surface particles. *New Phytologist* **196**: 774–787.

Cândido JF. 1991. Cultura da candeia (*Vanillosmopsis erythropappa Sch.Bip.*). *Boletim de*

Extensão, Viçosa: UFV.

Cassana FF, Eller CB, Oliveira RS, Dillenburg LR. 2015. Effects of soil water availability on foliar water uptake of *Araucaria angustifolia*. *Plant and Soil* **399**:147-157.

Chen H, Jiang J-G. 2010. Osmotic adjustment and plant adaptation to environmental changes related to drought and salinity. *Environmental Reviews* **18**: 309–319.

Dawson TE, Mambelli S, Plamboeck AH, Templer PH, Tu KP. 2002. Stable isotopes in plant ecology. *Annual Review of Ecology and Systematics* **33**: 507–559.

Dantas VL, Batalha MA. 2011. Vegetation structure: fine scale relationships with soil in a cerrado site. *Flora-Morphology, Distribution, Functional Ecology of Plants* **206**: 341-346.

Domec JC, Warren JM, Meinzer FC. 2004. Native root xylem embolism and stomatal closure in stands of Douglas-fir and ponderosa pine: mitigation by hydraulic redistribution. *Oecologia* **14**: 7-16.

Domec JC, Scholz FG, Bucci SJ, Meinzer FC, Goldstein G, Villalobos-Vega R. 2006. Diurnal and seasonal changes in root xylem embolism in Neotropical savanna woody species: impact on stomatal control of plant water status. *Plant, Cell & Environment* **29**: 26-35.

Donato AM, Morretes BL. 2009. Foliar anatomy of *Eugenia florida* DC. (Myrtaceae). *Brazilian Journal of Pharmacognosy* **19:** 759-770.

Donatini RS, Kato ETM, Ohara MT, Bacchi EM. 2013. Morphoanatomy and Antimicrobial Study of *Syzygium jambos* (L.) Alston (Myrtaceae) Leaves. *Latin American Journal of Pharmacy* **32**: 518-23

Efron B. 1978. Regression and ANOVA with Zero-One Data: Measures of Residual Variation, *Journal of the American Statistical Association* **73**: 113-121.

Eller CB, Lima AL, Oliveira RS. 2013. Foliar uptake of fog water and transport belowground alleviates drought effects in the cloud forest tree species, *Drimys brasiliensis* (Winteraceae*). New Phytologist* **199**: 151–162.

Eller CB, Burgess SSO, Oliveira RS. 2015. Environmental controls in the water use patterns of a tropical cloud forest tree species, *Drimys brasiliensis* (Winteraceae). *Tree physiology* **35**: 387-399.

Fernández V, Sancho-Knapik D, Guzmán P, Peguero-Pina JJ, Gil L, Karabourniotis G, Khayet M, Fasseas C, Heredia-Guerrero JA, Heredia A et al. 2014. Wettability, polarity, and water absorption of holm oak leaves: Effect of leaf side and age. *Plant physiology* **166**: 168-180.

Freitas MDF, Kinoshita LS. 2015. Myrsine (Myrsinoideae-Primulaceae) in Southeastern and Southern Brazil. *Rodriguésia* **66**: 167-189.

Gitlin AR, Sthultz CM, Bowker MA, Stumpf S, Paxton KL, Kennedy K, Munoz A, Bailey JA, Whitham TG. 2006. Mortality gradients within and among dominant plant populations as barometers of ecosystem change during extreme drought. *Conservation Biology* **20**: 1477–1486.

Goldsmith GR. 2013. Changing directions: the atmosphere–plant–soil continuum. *New Phytologist* **199**: 4-6.

Goldsmith GR, Matzke NJ, Dawson TE. 2013. The incidence and implications of clouds for cloud forest plant water relations. *Ecology Letters* **16**: 307–314.

Gotsch SG, Asbjornsen H, Holwerda F, Goldsmith GR, Weintraub AE, Dawson TE. 2013. Foggy days and dry nights determine crown-level water balance in a seasonal tropical montane cloud forest. *Plant, Cell & Environment* **37**: 261-272.

Gouvra E, Grammatikopoulos G. 2003. Beneficial effects of direct foliar water uptake on shoot water potential of five chasmophytes. *Canadian Journal of Botany* **81**:1280–1286.

Guyot G, Scoffoni C, Sack L. 2011. Combined impacts of irradiance and dehydration on leaf hydraulic conductance: insights into vulnerability and stomatal control. *Plant, Cell & Environment* **35**: 857–871.

Holwerda F, Burkard R, Eugster W, Scatena FN, Meesters AGCA, Bruijnzeel LA. 2006. Estimating fog deposition at a Puerto Rican elfin cloud forest site: comparison of the water budget and eddy covariance methods. *Hydrological Processes* **20**: 2669-2692.

Huang CW, Chu CR, Hsieh CI, Palmroth S, Katul GG. 2015. Wind-induced leaf transpiration. *Advances in Water Resources* **86**: 240-255.

Jactel H, Petit J, Desprez-Loustau ML, Delzon S, Piou D, Battisti A, Koricheva, J. 2012. Drought effects on damage by forest insects and pathogens: a meta-analysis. *Global Change Biology* **18**: 267-276.

Jarvis A, Mulligan M. 2011. The climate of cloud forests. *Hydrological Processes* **25**: 327-343.

Johansen DA. 1940. *Plant microtechnique*. New York, NY, USA: McGraw-Hill Book Co.

Kerstiens G. 1996. Cuticular water permeability and its physiological significance. *Journal of Experimental Botany* **47**:1813-1832.

Kerstiens G. 2006. Water transport in plant cuticles: an update. *Journal of Experimental Botany* **57**: 2493-2499.

Klein T. 2014. The variability of stomatal sensitivity to leaf water potential across tree species indicates a continuum between isohydric and anisohydric behaviours. *Functional Ecology* **28**: 1313-1320.

Laur J, Hacke UG. 2014. Exploring Picea glauca aquaporins in the context of needle water uptake and xylem refilling. *New Phytologist* **203**: 388–400.

Ledru MP, Salatino MLF, Ceccantini G, Salatino A, Pinheiro F, Pintaud JC. 2007. Regional assessment of the impact of climatic change on the distribution of a tropical conifer in the lowlands of South America. *Diversity and Distributions* **13**: 761–771.

Limm E, Simonin K, Bothman A, Dawson T. 2009. Foliar water uptake: a common water acquisition strategy for plants of the redwood forest. *Oecologia* **161**: 449–459.

Limousin JM, Rambal S, Ourcival JM, Rodríguez-Calcerrada J, Pérez-Ramos I M, Rodríguez-Cortina, Misson L, Joffre R. 2012. Morphological and phenological shoot plasticity in a Mediterranean evergreen oak facing long-term increased drought. *Oecologia* **169**: 565-577.

Martin CE, von Willert DJ. 2000. Leaf epidermal hydathodes and the ecophysiological consequences of foliar water uptake in species of Crassula from the Namib Desert in southern Africa. *Plant Biology* **2**: 229–242.

Martinez-Vilalta J, Cochard H, Mencuccini M, Sterck F, Herrero A, Korhonen JFJ, Llorens P, Nikinmaa E, Nole` A, Poyatos R, Ripullone F, Sass-Klaassen U, Zweifel R. 2009. Hydraulic adjustment of Scots pine across Europe. *New Phytologist* **184**: 353–364.

Martínez-Vilalta J, Poyatos R, Aguadé D, Retana J, Mencuccini M. 2014. A new look at water transport regulation in plants. *New Phytologist* **204**: 105-115.

Mastroberti AA, Mariath JEA. 2008. Development of mucilage cells of *Araucaria angustifolia* (Araucariaceae). *Protoplasma* **232**: 222–245.

Mayr S, Schmid P, Laur J, Rosner S, Charra-Vaskou K, Dämon B, Hacke UG. 2014. Uptake of water via branches helps timberline conifers refill embolized xylem in late winter. *Plant Physiology* **164**: 1731-1740.

McDowell NG, Pockman WT, Allen CD, Breshears DD, Cobb N, Kolb T, Plaut J, Sperry J, West A, Willians DG, Yepez EA. 2008. Mechanisms of plant survival and mortality during drought: why do some plants survive while others succumb to drought? *New Phytologist* **178**: 719-739.

McDowell NG, Beerling,DJ, Breshears DD, Fisher RA, Raffa KF, Stitt M. 2011. The interdependence of mechanisms underlying climate-driven vegetation mortality. *Trends in Ecology & Evolution* **26**: 523-532.

McManus JFA. 1948. Histological and histochemical uses of period acid. *Stain Technology* **23**: 99–108.

Meireles LD, Kinoshita LS, Shepherd GJ. 2014. Floristic composition of high-montane vegetation in the district of Monte Verde (Camanducaia, Minas Gerais), Serra da Mantiqueira Meridional, Southeast Brasil. *Rodriguésia* **65**: 831-859.

Mencuccini M, Grace J. 1994. Climate influences the leaf area/sapwood area ratio in Scots pine. *Tree Physiology* **15**: 1-10.

Mitchell PJ, O'Grady AP, Tissue DT, White DA, Ottenschlaeger ML, Pinkard EA. 2013. Drought response strategies define the relative contributions of hydraulic dysfunction and carbohydrate depletion during tree mortality. *New Phytologist* **197**:862–872.

Morgan JM. 1984. Osmoregulation and water stress in higher plants. *Annual Reviews of Plant Physiology* **35**: 299–319.

Nair US, Asefi S, Welch RM, Ray DK, Lawton RO, Manoharan VS, Mulligan M, Sever TL, Irwin D, Pounds JA. 2008. Biogeography of tropical montane cloud forests. Part II: Mapping of orographic cloud immersion. *Journal of Applied Meteorology and Climatology* **47**: 2183-2197.

Nadezhdina N, David TS, David JS, Ferreira MI, Dohnal M, Tesar M, Gartner K, Leitgeb E, Nadezhdin V, Čermak J et al. 2010. Trees never rest: the multiple facets of hydraulic redistribution. *Ecohydrology* **3**: 431-444.

Oliveira RS, Dawson TE, Burgess SSO. 2005. Evidence for direct water absorption by the shoot of the desiccation-tolerant plant *Vellozia flavicans* in the savannas of central Brazil. *Journal of Tropical Ecology* **21**: 585-588.

Oliveira RS. 2013. Can hydraulic traits be used to predict sensitivity of drought-prone forests to crown decline and tree mortality? *Plant and Soil* **364**: 1-3.

Oliveira RS, Eller CB, Bittencourt P, Mulligan M. 2014. The hydroclimatic and ecophysiological basis of cloud forests distributions under current and projected climates. *Annals of Botany* **113**: 909-920.

Oliveira RS, Christoffersen BO, Barros FV, Teodoro GS, Bittencourt P, Brum-Jr M, Viani RAG. 2014. Changing precipitation regimes and the water and carbon economies of trees. *Theoretical and Experimental Plant Physiology* **26**: 65-82.

Oparka KJ, Read ED. 1994. The use of fluorescent probes for studies of living plant cells. In: Harris N, Oparka KJ eds. *Plant Cell Biology: a practical approach*. Oxford: Oxford University Press, 27–50.

Pinheiro J, Bates D, DebRoy S, Sarkar D, R Core Team. 2015. *nlme: linear and nonlinear mixed effects models*. R package version 3.1-122.

Klein T. 2014. The variability of stomatal sensitivity to leaf water potential across tree species indicates a continuum between isohydric and anisohydric behaviours. *Functional Ecology* **28**: 1313-1320.

Lenth R. 2015. *Lsmeans: least-squares means*. R Package version 2.20-23.

R Core Team. 2015. *R: a language and environment for statistical computing.* Vienna, Austria: R Foundation for Statistical Computing.

Riederer M, Schreiber L. 2001. Protecting against water loss: analysis of the barrier properties of plant cuticles. *Journal of experimental botany* **52**: 2023-2032.

Rowland L, Da Costa AC, Galbraith DR, Oliveira RS, Binks OJ, Oliveira AA, Pullen AM, Doughty CE, Metcalfe DB, Vasconcelos SS, Ferreira LV. 2015. Death from drought in tropical forests is triggered by hydraulics not carbon starvation. *Nature* **528**:119-22.

Ruggiero PGC, Batalha MA, Pivello VR, Meirelles ST. 2002. Soil-vegetation relationships in cerrado (Brazilian savanna) and semideciduous forest, Southeastern Brazil. *Plant Ecology* **160**: 1-16.

Sack L, Pasquet-Kok J, PrometheusWiki contributors. 2011. *Leaf pressure-volume curve parameters.* PrometheusWiki. [WWW document] URL http://www.publish.csiro.au/prometheuswiki/tiki-pagehistory.php?page=Leaf pressure-volume curve parameters&preview=16 [accessed June 22, 2015].

Safford HD. 1999. Brazilian Paramos I. An introduction to the physical environment and vegetation of the campos de altitude. *Journal of Biogeography* **26**: 693–712.

Schönherr J. 2006. Characterization of aqueous pores in plant cuticles and permeation of ionic solutes. *Journal of Experimental Botany* **57**: 2471-2491.

Sheffield J, Wood EF. 2008. Global trends and variability in soil moisture and drought characteristics, 1950–2000, from observation-driven simulations of the terrestrial hydrologic cycle. *Journal of Climate* **21**: 432–458.

Simonin KA, Santiago LS, Dawson TE. 2009. Fog interception by *Sequoia sempervirens* (D. Don) crowns decouples physiology from soil water deficit. *Plant, Cell & Environment* **32**: 882–892.

Skelton RP, West AG, Dawson TE. 2015. Predicting plant vulnerability to drought in biodiverse regions using functional traits. *Proceedings of the National Academy of Sciences* **112**: 5744-5749.

Still CJ, Foster PN, Schneider SH. 1999. Simulating the effects of climate change on tropical montane cloud forests. *Nature* **398**: 608–610.

Tyree MT, Hammel HT. 1972. The measurement of the turgor pressure and the water relations of plants by the pressure-bomb technique. *Journal of Experimental Botany* **23**: 267–282.

Venables WN, Ripley BD. 2002. *Modern Applied Statistics with S.* Fourth Edition. Springer, New York. ISBN 0-387-95457-0.

Williams JW, Jackson ST, Kutzbach JE. 2007. Projected distributions of novel and disappearing climates by 2100 AD. *Proceedings of the National Academy of Sciences* **104**: 5738-5742.

Wright SJ, Machado JL, Mulkey SS, Smith AP. 1992. Drought acclimation among tropical forest shrubs (Psychotria, Rubiaceae). *Oecologia* **89**: 457–463.

Zuur AF, Ieno EN, Walker NJ, Saveliev AA, Smith GM. 2009. *Mixed effect models and extensions in ecology in R.* Berlin, Germany: Springer.

Supporting information

Notes S1. Detailed description of the statistical analysis conducted on the glasshouse experiment data and on the field meteorological data.

Glasshouse data analysis

Preliminary data analysis of the glasshouse experiment data indicated that the $MD\Psi_l$ data for all species had an approximately linear response to drought length after we controlled for the VPD effect on $MD\Psi_l$. The VPD effect on $MD\Psi_l$ could be linearized with a natural logarithmic transformation. Therefore, we used one linear mixed effects model for each species with $MD\Psi_l$ as response variable, and drought length, fog treatment and log-transformed VPD as fixed effects:

$$MD\Psi_{l_{ij}} = \alpha_j + (\beta_1 + b_i)Drougth\ length_i + \beta_2 Treatment_j + \beta_3\ Drougth\ length_i{:}\ Treatment_j + \beta_4 \log(VPD)_i + \varepsilon_{ij} \quad \text{(Eqn S1)}$$

, where the $MD\Psi_{l_{ij}}$ of plant *i* at treatment *j* changes as a function of the intercept (α_j), which is the mean $MD\Psi_l$ at treatment *j* at the beginning of the experiment (drought length = 0) and VPD = 1; and β_n, which is the effect size estimated for each fixed effect. We included the interaction between drought length and fog treatment in the model, as we expected the fog treatment response would change as the drought progressed. The model random slope structure (b_i) allowed each plant $MD\Psi_l$ to vary through the experiment time (i.e. drought length) and was selected using Akaike Information Criterion (AIC) comparison and likelihood-ratio tests following Zuur *et al* (2009). The term ε_{ij} is the residual error of the model.

For the leaf area change data from the glasshouse experiment, we used a linear generalized least squares model to compare leaf area change among species. We used a variance structure in the model that allows each species to have a different spread (Zuur *et al.*, 2009). We conducted comparisons among species using the least square means and 95% confidence intervals from the generalized least squares model.

We described the relationship between g_{s_i} of each plant *i* and its Ψ_{l_i} using the logistic function (Klein, 2014; Guyot *et al.,* 2011):

$$g_{s_i} = \frac{g_{smax}}{\left[1+\left(\frac{\Psi_{l_i}}{\Psi_{g50}}\right)^s\right]} \quad \text{(Eqn S2)}$$

, where g_{smax} is the maximum g_s reached by the species, Ψ_{g50} is the Ψ_l value when g_s drops to half of g_{smax}, and *s* is a parameter related with the slope of the linear portion of the model. We constrained the parameter g_{smax} to the maximum values observed during the experiment for each species to facilitate

model convergence. As we conducted gas exchange and Ψ_l measurements in different plants, we assumed that the Ψ_{l_i}would be similar to the mean Ψ_l of its treatment in a given time.

Field meteorological data analysis

We used the mixed effects models fitted to the glasshouse data and the field meteorological data to predict how many days it would take for each species to reach its π_{TLP} under TMCF field conditions. In order to do that, first we selected the longest periods without rain from each year from 32 years of rain data at the site. We disregarded very weak rain events (<0.5 mm) when selecting the drought periods (the maximum amount of summed weak rain events we detected on our selected periods was 2 mm). We fitted a log-normal probability density distribution on the field drought length data, as it had the lowest AIC value among the probability distributions tested on the data (Log-normal, Normal, Weibull and Gamma). Then, we used this probability distribution to estimate the probabilities for each species losing turgor under three different scenarios. The scenarios we tested were: 1 - *fog*: we used the predictions of the model fitted to the greenhouse data for the fog treatment group and we set the VPD constant at the mean value observed in the field during the dry periods from our dataset (0.9 kPa). 2 – *no fog*: we used the predictions of the model for the control (without fog) treatment and also set the VPD at 0.9kPa. 3 – *no fog and high VPD*: we used the predictions of the model for the control treatment and set the VPD constant at 1.94 kPa; which is the mean of the more extreme VPD values in our dataset (values higher than the 95-percentile). We considered that the plant would lose turgor when the predicted lower boundary of its 95% confidence interval (approximated by 2xSE) reached the species π_{TLP}.

References

Zuur AF, Ieno EN, Walker NJ, Saveliev AA, Smith GM. 2009. *Mixed effect models and extensions in ecology in R.* Berlin, Germany: Springer.

Guyot G, Scoffoni C, Sack L. 2011. Combined impacts of irradiance and dehydration on leaf hydraulic conductance: insights into vulnerability and stomatal control. *Plant, Cell & Environment* **35**: 857–871.

Klein T. 2014. The variability of stomatal sensitivity to leaf water potential across tree species indicates a continuum between isohydric and anisohydric behaviours. *Functional Ecology* **28**: 1313-1320.

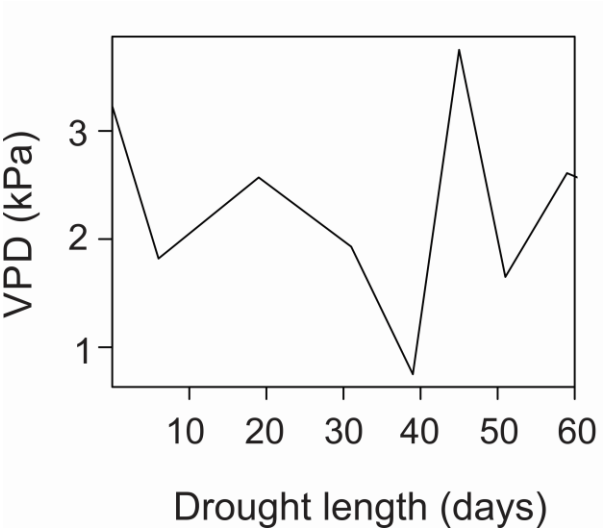

Figure S1. Vapor-pressure deficit (VPD) variation at the glasshouse during the experiment.

CHAPTER 2

Fast growing cloud forest trees grow in a wider range of environmental conditions and are more prone to hydraulic failure than slow growing trees

(Eller CB, Barros FV, Mencuccini M, Oliveira RS)

Fast growing cloud forest trees grow in a wider range of environmental conditions and are more prone to hydraulic failure than slow growing trees

Summary

- Tree growth is an important but poorly understood process, especially in short time scales. We used two distinct techniques to estimate daily stem growth of tropical montane cloud forests (TMCF) trees, and investigate how the growth of trees with different functional traits responds to changes in environmental conditions.
- We estimated stem radial growth (*g*) directly from bark diameter changes (dD_b), and also using a combination of dD_b and sap velocity measurements to exclude the bark capacitance effect from dD_b. We measured tree functional traits such as hydraulic safety margins, stomatal behavior and wood density.
- Both methods to estimate *g* showed a medium to high agreement (R^2=0.46-0.81) in fast-growing trees, but poor agreement in slow growing trees. Fast growing trees were able to grow in a wider range of temperature, irradiance, soil water availability and leaf-wetting conditions than slow growing trees. However, fast growing trees had a narrower hydraulic safety margins and less dense wood. Most trees increased *g* during hotter and cloudy wet season conditions.
- We show that environmental conditions in TMCF are rarely optimal for tree growth; but fast-growing trees can sustain *g* in a wider range of conditions at the cost of hydraulic safety.

Keywords: Tree growth; cloud forests; fog; climate change; stem diameter variations; xylem safety margin; plant models; carbon.

Introduction

Tree growth is a widely studied process in plant ecology due to its enormous importance to forest function and carbon cycle (Luyssaert *et al.*, 2008; Beer *et al.*, 2010). Despite its importance, there are many gaps in our current knowledge of the physiological mechanisms behind tree growth and how it responds to changes in environmental conditions (Steppe *et al.*, 2015; Zuidema *et al.*, 2013; Zweifel, 2016). Tree growth is often studied by monitoring increments in stem diameter (or perimeter) through time, however, much of the changes in tree stem diameter are caused by radial water fluxes between bark and xylem, instead of actually cambium cells multiplication and expansion (Steppe *et al.*, 2015; Zweifel, 2016). This precludes the use of raw stem diameter changes as an accurate measurement of tree growth, especially in short time scales. Recently, some methods have been proposed to separate the cambial growth signal (*g*) from stem changes induced by radial water fluxes (Mencuccini *et al.*, 2013; Zweifel *et al.*, 2016). These methods allows us to investigate how microclimate controls tree growth in a daily temporal scale (Chan *et al.*, 2016), and improve our understanding of the physiological mechanisms controlling tree growth and how they might respond to climate change.

Tropical montane cloud forests (TMCF) are ecosystems very vulnerable to climate change (Hamilton, 1995; Loope & Giambelluca, 1998; Foster, 2001; Oliveira *et al.*, 2014; Hu & Riveros-Iregui, 2016). The high degree of endemism of these ecosystems (Gentry, 1992; Foster, 2001) suggests that many species are only able to thrive in the particular environmental conditions found in TMCF. Climatic changes threaten to change several aspects of the TMCF climate, such as temperature and cloud immersion frequency (Still *et al.*, 1999; Lawton *et al.*, 2001; Karmalkar *et al.*, 2008). Several studies have already shown that cloud immersion events are an important component of the water relations of TMCF trees (Eller *et al.*, 2013; 2015; 2016; Goldsmith *et al.*, 2013; Gotsch *et al.*, 2014). However, carbon relations of TMCF trees and how they interact with climate are a less studied topic (Bruijnzeel & Veneklaas, 1998).

Tree growth in TMCF is often lower than in lowland tropical forests (Bruijnzeel & Veneklaas, 1998; Wilcke *et al.*, 2008; Moser *et al.*, 2008; Girardin *et al.*, 2010). Low irradiance and wet leaves caused by the frequent fog events have been proposed as possible causes for the TMCF low growth rates (Bruijnzeel & Veneklaas, 1998; Letts & Mulligan, 2005). Other studies have suggested that the low availability of soil nutrients, particularly nitrogen, also might limit TMCF growth (Wilcke *et al.*, 2008; Moser *et al.*, 2010; Fisher *et al.*, 2013). There

are limited data supporting both of these views, and a deeper understanding of what controls TMCF tree growth is of utmost importance to predict how these important ecosystems might respond to climate change.

In our study, we used the recently proposed techniques of Mencuccini *et al* (2013) and Zweifel *et al* (2016) to obtain daily scale *g* estimates for TMCF trees, and use it to answer the following questions: 1 - How environmental conditions control TMCF tree growth? 2 - How ecological and physiological traits affect tree growth responses to microclimatic changes? We monitored bark diameter changes (dD_b), sap velocity (v_s) and measured several plant traits of 9 trees, which represent some of the more abundant species in a TMCF fragment located in southeast Brazil. The traits we measured were related with stomatal regulation, xylem hydraulic safety, size-related traits and growing rates (that were derived from the *g* data). We also compared the two methods we used to estimate *g* (Mencuccini *et al.,* 2013 and Zweifel *et al.,* 2016) of the different TMCF tree species.

Material and Methods

Study area and species

We conducted our research in a TMCF fragment located *c.* 2000 m above sea level in the Mantiqueira mountain range, SP, Brazil (22°41'50"S 45°25'17"W). The climate at the site is characterized by a dry and cold winter and a hotter and rainy summer. Fog events are common during the entire year (Eller *et al.,* 2015). The site climate data from 2015 (when our research was conducted) can be found on Fig. S1 and additional details on the site climate can be found in Safford (1999) and Eller *et al* (2015; 2016).

We measured stem radial growth and ecophysiological traits in 9 of the most abundant tree species at the site. The studied species were: *Croton piptocalyx* M. Arg, *Drimys brasiliensis* Miers, *Macropeplus dentatus* Perkins, *Myrceugenia cucullata* D. Legrant, *Myrceugenia ovalifolia* O. Berg, *Myrceugenia ovata* Legrand, *Psychotria vellosiana* Benth, *Symplocos falcata* Brand, *Weinmannia organensis* Gardner (Table 1). The total basal area percentage of each species in Table 1 was based on a floristic survey and DBH measurements we conducted in 15 plots of 225 m^2 in the study area.

Bark diameter measurements

We dD_b with automated high-precision point dendrometers (model ZN12-T-2IP, Natkon, Oetwil am See, ZH, Switzerland) mounted *c.* 1.5 m on the stem. In trees with a very loose or

thick outer bark, we removed the dead outer bark and installed the dendrometer on the inner bark. Most of the studied trees were located on a subtle northwest-southeast slope, so we placed the dendrometer either on the northeast or the southwest side of the stem, to avoid compression/tension wood regions. The dendrometers measured bark diameter every 5 min and these values were averaged every 30 min. The dendrometer data were corrected for temperature induced changes based on temperature changes in the steel rods that attach the dendrometer frame to the tree and the steel linear thermal expansion coefficient (details in Notes S1 and Fig. S2).

Table 1. Diameter at breast height (DBH), height, crown exposition (following Clark & Clark 1992) and the total basal area of each study species.

Species	*Family*	*DBH(cm)*	*Height (m)*	*Crown exposition*	*Species total basal area (%)*
Myrceugenia cucullata	Myrtaceae	49.65	14.5	4	11.98
Myrceugenia ovalifolia	Myrtaceae	41.92	17.5	5	10.86
Weinmannia organensis	Cunoniaceae	51.56	22	5	7.07
Drimys brasiliensis	Winteraceae	22.44	9	3	6.84
Psychothria vellosiana	Rubiaceae	21.07	11.5	5	6.28
Macropeplus dentatus	Monimiaceae	25.68	10	4	6.18
Cróton piptocalyx	Euphorbiaceae	18.46	12	4	4.57
Symplocos falcata	Symplocaceae	14.48	11.7	5	2.07
Myrceugenia ovata	Myrtaceae	8.75	5.1	2	1.39

Extracting the growth component from bark diameter changes

We used two distinct methods to extract *g* from the bark diameter data: the zero-growth method (ZG; Zweifel *et al.,* 2016), which extracts *g* directly from the bark diameter data; and a modification of the method created by Mencuccini *et al* (2013), in which we exclude the bark capacitance effect of the dD_b before extracting *g*. We will call the modified Mencuccini *et al* (2013) method of bark capacitance method (BC) in this paper.

Zero-growth method

In the ZG method we assume that *g* ceases completely when bark diameter starts to decrease (Zweifel *et al.,* 2016). Based on this concept, cambial growth predicted by the ZG method (g_{ZG}) can be written as:

$$g_{ZG}(t) = \begin{cases} D_b(t) - \max[D_b(<t)], & D_b(t) \geq \max[D_b(<t)] \\ 0 \quad , & D_b(t) < \max[D_b(<t)] \end{cases} \quad (1)$$

where $D_b(t)$ is bark diameter at time t, and max[$D_b(< t)$] refers to the maximum bark diameter value measured before t. The remaining variation observed in dD_b can be attributed to radial water fluxes between xylem and bark (mostly related to bark capacitance). This variation is called Tree Water Deficit (TWD) by Zweifel *et al* (2016) and can be calculated as:

$$\frac{dTWD}{dt} = \left(\frac{dD_b - dg_{ZG}}{dt} \right) \quad (2)$$

where dt is the time interval when the changes in TWD (dTWD), D_b (dD_b) and g_{ZG} (dg_{ZG}) are happening.

Bark-capacitance method

In the BC method we first treat the bark as an water reservoir for the xylem with constant osmotic potential, and model bark diameter changes induced by capacitance-related radial water fluxes using xylem water potential (Mencuccini *et al.,* 2013). Once we extract the bark signal without capacitance induced changes, we can separate the osmotic induced diameter changes from g (Chan *et al.*, 2015).

Initially we tried to obtain an estimate of xylem water potential (Ψ_x) by mounting an additional linear displacement differential transformer on the frame of each dendrometer to monitor xylem diameter changes (dD_x) simultaneously with dD_b. We intended to use dD_x as a proxy for Ψ_x, based on Hooke's law (Irvine & Grace, 1997; Perämäki *et al.,* 2001):

$$\frac{dD_x}{dt} = \frac{D_x^*}{E_{r,x}} \frac{d\Psi_x}{dt} \quad (3)$$

where dD_x/dt refers to the xylem diameter changes (dD_x) over a time interval t; D_x^* is the initial xylem diameter (at reference pressure); $E_{r,x}$ is the radial elastic modulus of the xylem tissue and $d\Psi_x/dt$ refers to the xylem water pressure changes ($d\Psi_x$) over a time interval t. However the dD_x we observed in most trees were too small (less than 2-3μm), probably due to a small D_x^* (i.e. small active xylem cross sectional area) or large $E_{r,x}$, which prevented us from using it reliably as a $d\Psi_x$ proxy. This limitation led us to derive a new method to model bark capacitance using v_s,, that we had readily available for all study trees, based on the same principles of the method created by Mencuccini *et al* (2013), but we also incorporate concepts from the ZG method (Zweifel *et al* 2016). We begin by applying the same Hooke's law principle to dD_b:

$$\frac{dD_b}{dt} = \frac{D_b^*}{E_{r,b}} \frac{dP_b}{dt} \tag{4}$$

where dD_b/dt refers to the bark diameter changes (dD_b) over a time interval t; D_b^* is the initial bark diameter (at reference pressure); $E_{r,b}$ is the radial elastic modulus of the bark tissue and dP_b/dt refers to the bark tissue-averaged turgor pressure over a time interval t. Note that equation (4) does not include cambial growth and represents only dD_b caused by pressure changes.

The change in the inner bark pressure due to the water potential difference between the xylem and the inner bark can be written as:

$$\frac{dP_b}{dt} = \frac{E_{r,b} J}{V_b^*} = \frac{E_{r,b}}{V_b^*} L\, A\left(\Psi_x - \left(P_b - \Pi_b\right)\right) \tag{5}$$

where V_b^* (m^3) is the inner bark volume at a reference pressure; J is the water flux ($m^3\ s^{-1}$) between bark and xylem; L ($m\ MPa^{-1}\ s^{-1}$) is the hydraulic conductance of the cross-sectional area A (m^2) of contact between bark and xylem; Π (MPa) is the osmotic pressure of the inner bark. Substituting equation (5) into (4) we have:

$$\frac{dD_b}{dt} = \frac{D_b^*}{V_b^*} L\, A\left(\Psi_x - \left(P_b - \Pi_b\right)\right) \tag{6}$$

We now express the pressure terms at the same reference time when D_b^* and V_b^* are also calculated:

$$\frac{dD_b^*}{dt} = \frac{D_b^*}{V_b^*} L\, A\left(\Psi_x^* - \left(P_b^* - \Pi_b^*\right)\right) \tag{7}$$

where all variables labelled with the * symbol are determined at this reference time. In our study we used the first midnight of the data as reference time. Subtracting (7) from (6) side by side and re-arranging, yields:

$$\frac{dD_b}{dt} = \frac{D_b^*}{V_b^*} L\, A\left(\Delta\Psi_x - (\Delta P_b) + \left(\Delta\Pi_b\right)\right) + \frac{dD_b^*}{dt} \tag{8}$$

where

$$\Delta\Psi_x = \Psi_x - \Psi_x^* \tag{8a}$$

$$\Delta P_b = P_b - P_b^* \tag{8b}$$

$$\Delta\Pi = \Pi_b - \Pi_b^* \tag{8c}$$

We now express the bark pressure term as a function of the measured diameter differences from the reference state:

$$\Delta P_b = \frac{E_{r,b}}{D_b^*}\Delta D_b \tag{9}$$

where

$$\Delta D_b = dD_b - dD_b^* \tag{9a}$$

As explained at the beginning, we assume for the moment that changes in osmotic pressure do not occur. Therefore, the term $\Delta\Pi$ vanishes. Substituting equation (9) into (8), rearranging and simplifying, one obtains:

$$\frac{dD_b}{dt} = \frac{D_b^*}{V_b^*} L\, A\left(\Delta\Psi_x - \frac{E_{r,b}}{D_b^*}\Delta D_b\right) + \frac{dD_b^*}{dt}$$

$$\frac{dD_b}{dt} = \frac{L\, A}{V_b^*}\left(D_b^*\,\Delta\Psi_x - E_{r,b}\Delta D_b\right) + \frac{dD_b^*}{dt} \tag{10}$$

$$\frac{dD_b}{dt} = \frac{L\, A\, E_{r,b}}{V_b^*}\left(\frac{D_b^*}{E_{r,b}}\Delta\Psi_x - \Delta D_b\right) + \frac{dD_b^*}{dt}$$

Let's assume now that estimates of xylem water potential Ψ_x can be obtained using an Ohm's law analogy, i.e.

$$\Psi_x = \Psi_s - \frac{v_s}{K_{pl}} \tag{11}$$

where v_s is the measured sap velocity, and Ψ_s and K_{pl} are soil water potential and plant hydraulic conductance, respectively. Expressing the quantities at a reference time using the usual * symbol and substituting (11) into (10) yields:

$$\Delta\Psi_x = \Psi_s - \frac{v_s}{K_{pl}} - \left(\Psi_s^* - \frac{v_s^*}{K_{pl}^*}\right) = \Delta\Psi_s - \frac{v_s}{K_{pl}} + \frac{v_s^*}{K_{pl}^*} \tag{12}$$

$$\frac{dD_b}{dt} = \frac{L\, A\, E_{r,b}}{V_b^*}\left(-\frac{D_b^*}{K_{pl}\, E_{r,b}}v_s - \Delta D_b\right) + \left(\frac{dD_b^*}{dt} + L\frac{v_s^*}{K_{pl}^*} + L\,\Delta\Psi_s\right)$$

where the K_{pl} and $\Delta\Psi_{\mathrm{s}}$ indicate parameters for the coefficient for sap velocity and for the intercept which are not constant but can vary from day to day to reflect dynamic changes in soil water potential and plant hydraulic conductance. Equation (12) equates to:

$$\frac{dD_b}{dt} = \alpha\left(\beta\, v_s - \Delta D_b\right) + \gamma \tag{13}$$

where:

$$\alpha = \frac{1}{\tau} = \frac{L\, A}{V_b^*}E_{r,b} = \frac{L}{D_b^*}E_{r,b} \tag{13a}$$

$$\beta = -\frac{D_b^*}{K_{pl}\, E_{r,b}} \tag{13b}$$

$$\gamma = \frac{dD_b^*}{dt} + L\frac{v_s^*}{K_{pl}^*} + L\,\Delta\Psi_s \tag{13c}$$

Equation (13) describes changes in dD_b caused only by bark capacitance. Therefore, we cannot estimate the parameters α, β and γ directly from the dD_b, as a large portion of the changes in dD_b are actually being caused by cambium growth (g). If we include an estimate of cambium growth in equation (4), and follow the same derivation process we did to achieve (13), we have (complete derivation in Notes S2):

$$\frac{dTWD}{dt} = \alpha\left(\beta\, v_s - \Delta TWD\right) + \gamma \tag{14}$$

We can now use equation (14) to estimate the parameters α, β and γ from dTWD, without most of the cambium growth influence. In this approach, the BC and ZG are not fully independent; instead, we use BC as a follow-up technique to detect any residual growth signal that was not detected by the ZG method (i.e. growth when stem cells are not completely saturated). Effectively, we are assuming that the portion of TWD changes that are not related with v_s and ΔTWD are actually growth or osmotic related changes that were not detected by the ZG method. We used mixed effects models (Bates *et al.*, 2015) to fit equation (14), which allowed us to represent the parameters α, β and γ with unique values for each day. Therefore our model accounts for daily changes in plant radial hydraulic conductance between bark and xylem, plant axial hydraulic conductance and soil water potential. The parameter estimates from equation (14) are then used in equation (13) to simulate bark thickness changes caused only by bark capacitance ($\hat{\Delta}D_b$):

$$\hat{\Delta}D_b(t+dt) = \hat{\Delta}D_b(t) + \bar{\alpha}\left(\bar{\beta}\, v_s(t) - \hat{\Delta}D_b(t)\right) + \bar{\gamma} \tag{15}$$

where $\hat{\Delta}D_b$ is the bark thickness change from time t to dt, which is estimated from the previous bark thickness value at time t. We use the *vinculum* notation in the parameters $\bar{\alpha}$, $\bar{\beta}$ and $\bar{\gamma}$ to denote the time-dependent nature of these parameters on the equation. The difference between the measured ΔD_b and the predicted $\hat{\Delta}D_b$ reveals a signal ($\hat{\Delta}G_m$) that contains the growth signal of the BC method (g_{BC}) and osmotic induced changes:

$$\hat{\Delta}G_m = \Delta D_b - \hat{\Delta}D_b \tag{16}$$

Finally, g_{BC} can be extracted from $\hat{\Delta}G_m$ by excluding the osmotic induced changes of this signal. This can be done by calculating g_{BC} as the difference between consecutive minimum

values of $\hat{\Delta}G_m$ (Chan *et al.*, 2015), which can be written similarly to equation (1) for the ZG method:

$$g_{BC}(t) = \begin{cases} \hat{\Delta}G_m(t) - \min[\hat{\Delta}G_m(<t)], & \hat{\Delta}G_m(t) \geq \min[\hat{\Delta}G_m(<t)] \\ 0 \quad , & \hat{\Delta}G_m(t) < \min[\hat{\Delta}G_m(<t)] \end{cases} \quad (17)$$

where $\hat{\Delta}G_m(t)$ is the $\hat{\Delta}G_m$ value at time *t*, and min[$\hat{\Delta}G_m$ (< *t*)] refers to the minimum $\hat{\Delta}G_m$ value measured before *t*.

Sap velocity measurements

We used the heat-ratio method (HRM; Burgess *et al*., 2001) to measure v_s. We installed HRM sensors (model SFM1, ICT International Pty Ltd., Armidale, NSW, Australia) at the tree stem *c*. 10 cm from the point dendrometers. The sensors emitted 15 J heat pulses and measured the heat pulse velocity (v_h; cm hr^{-1}) each 30 minutes as:

$$v_h = \frac{k}{x}\ln\left(\frac{v_1}{v_2}\right)3600 \quad (18)$$

where *k* is the sapwood thermal wood diffusivity using the method proposed by Vandegehuchte and Steppe (2012); v_1 and v_2 are the temperature increment after the heat pulse in the probes located *x* cm (*x* equals to 0.5 in our case) above and below the heater. After correcting v_h for wound effects and needle misalignment following Burgess *et al* (2001) we calculated v_s as:

$$v_s = \frac{v_h \rho_b (c_w + m_c c_s)}{\rho_s c_s} \quad (19)$$

where ρ_b is the basic density of dry wood; c_w is the specific heat capacity of dry wood; c_s the specific heat capacity of water; m_c is the moisture content of fresh wood and ρ_s is the water density. All these properties were measured from wood samples collected with an increment borer at breast height, and using the standard protocol to measure wood density (Osazuwa-Peters & Zanne, 2011).

Environmental conditions measurements

We mounted an air temperature (T; °C) sensor (model HOBO U-23 Pro v2, Onset Computer Corp., Pocasset, MA, USA) and a leaf wetness (%) sensor (model LWS, Libelium Comunicaciones Distribuidas S.L., Zaragoza, Spain) at the top of a 15 m tower located in front of the forest fragment with the study trees (less than 150 m from the farthest study tree). We had an automated rainfall gauge (model TB4MM-L, Hydrological Services America, Lake

Worth, FL, USA) and a photosynthetic active radiation (PAR; μmol m^{-2} s^{-1}) sensor (model SQ-110, Apogee instruments, Inc., Logan, UT, USA) located *c.* 500m from the study site. For the more understory study trees (*M. ovata* and *D. brasiliensis*, see Table 1) we also had PAR and T sensors located in the forest understory *c.* 10 m from the trees. All these sensors collected data at 30 minutes intervals. The data from the leaf wetness sensors were transformed in daily leaf wetness time (LW_t) which we defined as the daily sum of the 30-minutes intervals in which more than 90% of the sensor surface was wet.

We used frequency domain reflectometry soil moisture probes (model 5TM, Decagon Devices Inc, Pullman, WA, USA) to measure soil volumetric water content (VWC; cm^3 water cm^{-3} soil) at three different depths (10, 50 and 100 cm). Probes were installed at c. 10 m from each study tree and collected data each 30 minutes. We used the averaged soil VWC of all depths to calculate relative soil water deficit (SWD; %) as:

$$SWD = \frac{VWC_f}{VWC} 100 \quad (20)$$

where VWC_f is soil VWC at soil field capacity. We estimated soil field capacity as the mean soil VWC three days after rain events during the wet season (March-April). When SWD values are higher than 100%, it indicates periods when the soil is oversaturated with water due to recent water input, while values smaller than 100% indicates water deficit in relation to the soil field capacity.

Tree physiological traits measurements

To identify the stomatal behavior of the study species we used the relationship between midday leaf water potential ($MD\Psi_l$) and pre-dawn leaf water potential ($PD\Psi_l$), following Martinez-Vilalta *et al* (2014):

$$MD\Psi_l = \Lambda + \sigma PD\Psi_l \quad (21)$$

where the intercept (Λ) represents the tree maximum transpiration rate per unit of hydraulic conductance; and the slope (σ) the stomatal sensitivity to Ψ_s (represented by $PD\Psi_l$ in the model). On this approach a high σ indicates a more anisohydric plant, while a smaller σ indicates a more isohydric plant (Martinez-Vilalta *et al.,* 2014). The leaf water potential measurements were conducted in 3-6 trees for each species using a Scholander pressure chamber (model 500D, PMS Instrument Co., Corvallis, OR, USA).

We measured xylem vulnerability to cavitation in detached branches of all the studied species using bench dehydration (n=4-5 trees per species; Sperry *et al.*, 1988). Xylem percentage of conductance loss (PLC) was assessed with the traditional hydraulic method (Sperry *et al.*, 1988) for *C. piptocalyx, D. brasiliensis, M. cucullata, M. ovalifolia, M. ovata, S. falcata, W. organensis*. For *M. dentatus* we used the pneumatic method (Pereira *et al.*, 2016). We could not measure the PLC in *P. vellosiana* with any of the methods. The curve fitting was done with the Pammenter & Vander Willigen (1998) model:

$$PLC = \frac{100}{(1+\exp(s(\Psi_x - P50)))} \tag{22}$$

where *s* is related with the slope of the linear portion of the curve, and P50 is the Ψ_x value when PLC reaches 50%. We used the P50 parameter of the model and the Ψ_x value when PLC reaches 88% (P88) to calculate the hydraulic safety margin ($SM_{50/88}$) of each species:

$$\begin{aligned} SM_{50} &= \Psi_{min} - P50 \\ SM_{88} &= \Psi_{min} - P88 \end{aligned} \tag{23}$$

where Ψ_{min} is the minimum water potential reached by the plant during our observations.

Data analysis

Implementing and comparing growth models

Both growth models and all the subsequent analyses were implemented on the software R version 3.2.2 (R Core Team, 2015). The equations (1) and (2) were implemented to calculate g_{ZG} and TWD, respectively. We fitted equation (14) to the *d*TWD data of each study tree using mixed effects models with the lmer library (Bates *et al.*, 2015), and then we implemented equations (15), (16) and (17) to calculate g_{BC}. To compare g_{BC} with g_{ZG} we used ordinary least square regressions, and used the R^2 and the slope of the regressions to indicate the agreement between methods and the departure from a 1:1 linear relationship. We used nonlinear least-squares (NLS) to describe the R^2 and slopes of the regressions between g_{BC} with g_{ZG} as a Michaelis-Menten function of the daily maximum growth rates ($g_{bas\ max}$) of each species:

$$R^2 \ methods \ \ or \ slopes \ \ methods \ = \frac{Vg_{basmax}}{K + g_{basmax}} \tag{24}$$

where V is the asymptote of the model and K the $g_{bas\ max}$ value when the response variable (R^2 or slopes) is $V/2$. We used Efron's pseudo-R^2 (Efron, 1978) as an indicative of the variance explained by the NLS models used in this study.

Growth rates

For the subsequent growth rates and environmental drivers analysis we used only g_{BC}, as it should produce more accurate growth estimates than g_{ZG} in most cases (an in depth explanation for this can found at the discussion). The g_{BC} represents tree linear growth (μm), and this measurement might lead to misleading conclusions when comparing trees with very different DBH, as the same linear growth means a much smaller carbon investment for a small tree than for a large tree. Therefore, we assumed growth was homogenous throughout the stem and transformed g_{BC} in basal area growth (g_{bas}; μm^2) using the initial DBH of the trees:

$$g_{bas} = \left(\frac{DBH}{2} + g_{BC} \right)^2 \pi \tag{25}$$

where we approximated π to 3.14. We still used the linear growth data (g_{BC}) to compare our results with other results found in literature. We used g_{bas} to calculate $g_{bas\ \max}$ and daily middle growth rates ($g_{bas\ \mathrm{mid}}$) for each species. We defined $g_{bas\ \max}$ as the mean of the values higher than the 95 percentile of the daily g_{bas} data; and it represents the maximum possible growth rates reached by the tree during our observations. While $g_{bas\ \mathrm{mid}}$ is the mean of the values between 25 and 75 percentiles of the daily g_{bas} data; and represents the growth rates that were frequently reached by the tree. The $g_{bas\ \mathrm{mid}}$ value is influenced by the period which the daily g_{bas} data covers; if we restrict the g_{bas} data to a period of unfavorable growth conditions the estimated $g_{bas\ \mathrm{mid}}$ value would be lower than if we select a larger period which includes favorable and unfavorable growth conditions. This is relevant for our dataset as our study trees have different temporal intervals of data (see in Fig. 1 and Table 2). To avoid this bias, we restricted our $g_{bas\ \mathrm{mid}}$ calculations to a period where all trees had data during most of it (from 01/September to 30/November). The $g_{bas\ \max}$ value is less influenced by the period selection; as long as you have data during favorable growth conditions, including less favorable growth periods in the dataset only have a small effect on $g_{bas\ \max}$. So we did not subset our dataset for the $g_{bas\ \max}$ calculations.

Plant physiological traits

To estimate the parameters from equation (21) we used mixed-effects models (lmer; Bates *et al.,* 2015) with random slopes and intercepts for each individual tree. We used NLS regressions to fit PLC data to equation (22) and estimate P50/P88. To measure the effect of plant physiological traits on growth rates we used generalized linear models (GLM) with a Gamma error distribution and a log link function; we used this kind of model because the $g_{bas\ max}$ data was always positive and had a heavily right skewed distribution. We use the deviance explained by the models (D^2), calculated following Guisan & Zimmerman (2000), as an indicative of the goodness-of-fit for the GLMs used in this study.

Environmental drivers

The g_{bas} data for all study trees contained many days when growth was zero, which makes difficult to use traditional statistical tools to model g_{bas} in function of environmental conditions. We dealt with this by adopting a two-step modelling approach: 1- We first treat the g_{bas} data as a binary variable: growth days (when g_{bas}>0) *versus* no growth days (when g_{bas}=0). We use the growth|no growth data to estimate the effects of environmental conditions on the probability of the tree growing or not using logistic regressions. 2 – Then, we used GLMs with Gamma or Gaussian error distribution and a log link function on the non-zero *gbas* data to estimate the effects of environmental conditions on the tree growth magnitude. We choose the error distribution for the GLM based on the analysis of the model residuals.

We estimated the effect of the following environmental conditions on g_{bas}: mean daily T, mean daily PAR (only data from 06:00 to 18:00), mean daily SWD and LW_t. The structure of the models we fitted to the tree growth data (both for the logistic regressions and for the GLMs) can be written generically as:

$$\text{logit}\left(growth|no\ growth\right) or\ \ln(g_{bas}>0) = a + bT + cPAR + dSWD + eLW_t + fSWD{:}LW_t \quad (26)$$

where logit(*growth*|*no growth*) is the logit transformation (i.e. log of the odds) of the growth|no growth data (for the logistic regression) and ln(g_{bas} > 0) are the log transformed means of the positive g_{bas} data (for the GLM). On the right side, *a* is the intercept and *b* to *f* are the coefficients of each parameter. We included the interaction SWD:LW_t in the model because we expect a different g_{bas} response to LW_t depending on SWD levels: if SWD is high, too much LW_t might impair tree gas exchange and compromise growth, but if SWD is low the water input and turgor improvements caused by longer LW_t might favor growth.

Results

Growth signal comparison

The ZG and the BC methods predicted different *g* from the bark diameter data, but the magnitude of this difference varied among species (Fig. 1). In most species both methods had a medium to high agreement (R^2 = 0.46-0.81; slopes=0.8-1; Table 2; Fig. S3), but in species such as *M. ovata* and *M. dentatus*, g_{ZG} and g_{BC} showed very different patterns (R^2 = 0.04-0.16; slopes=0.22-0.5; Table 2; Fig. S3). We have found that the agreement between methods was asymptotically related with the species $g_{bas\ max}$ (Fig. 2). The R^2 from the linear regressions fitted between methods starts reaching its estimated asymptote (V=0.85) when $g_{bas\ max}$ is *c.* 5000 $\mu m^2\ day^{-1}$ (Fig. 2a). The slope of the linear regressions fitted between methods has an asymptote value very close to 1 (V=0.96) and starts reaching it when $g_{bas\ max}$ is *c.* 850 $\mu m^2\ day^{-1}$ (Fig. 2b).

Growth rates and physiological traits

The studied species showed a variety of $g_{bas\ max}$ (Fig. 3a-b), ranging from very fast growing species like *C. piptocalyx* to slow growing species like *M. ovata* and *M. ovalifolia*. The average middle linear growth rate of all study trees, weighted by their respective basal area percentages, was 4.88 $\mu m\ day^{-1}$ (Fig. 3a). The species with higher $g_{bas\ max}$ generally also showed higher $g_{bas\ mid}$ (Fig. 3c). There were some exceptions to this trend though, like *D. brasiliensis* which had a higher $g_{bas\ mid}$ than what it would be expected from its $g_{bas\ max}$.

The $g_{bas\ max}$ was not related with plant stomatal behavior, as indicated by the slope (σ; Fig. 4a) or the intercept (Λ; Fig. 4b) of the relationship between $MD\Psi_l$ and $PD\Psi_l$. We also found no relationship between $g_{bas\ max}$ and size related traits, such as DBH (Fig. 4c) and tree height (Fig. 4d). However, we have found that trees with higher $g_{bas\ max}$ tended to have narrower xylem safety margins, but only when the safety margins are calculated using the P88 (SM_{88}; Fig. 4e). Wood density was also strongly negatively related with $g_{bas\ max}$ (Fig. 4f).

Growth environmental drivers

Our analysis indicates that fast growing species were more likely to grow in a wider range of environmental conditions than slow growing species (Table 3; Fig. 5). In fig. 5a we can see that most of the slower growing species were unlikely to grow in the colder temperatures from the dry season. Slow growing species were more likely to grow during the hotter wet season, with the exception of *M. ovata* which prefers colder temperatures. Slow growing species are also more likely to grow in conditions of PAR, SWD and LW_t found during the wet season (Fig. 5b-d), with the exception of *M. ovalifolia* and *M. ovata.* The *M. ovalifolia*

tree was more likely to grow in a wider range of PAR, SWD and LW_t than the other slow growing species, however its growth probabilities were always lower than 0.5. The *M. ovata* tree always had very low growth probabilities (< 0.3), regardless of environmental conditions, but it was more likely to grow in T, SWD and LW_t conditions that are more common in the dry season (Fig. 5b-d).

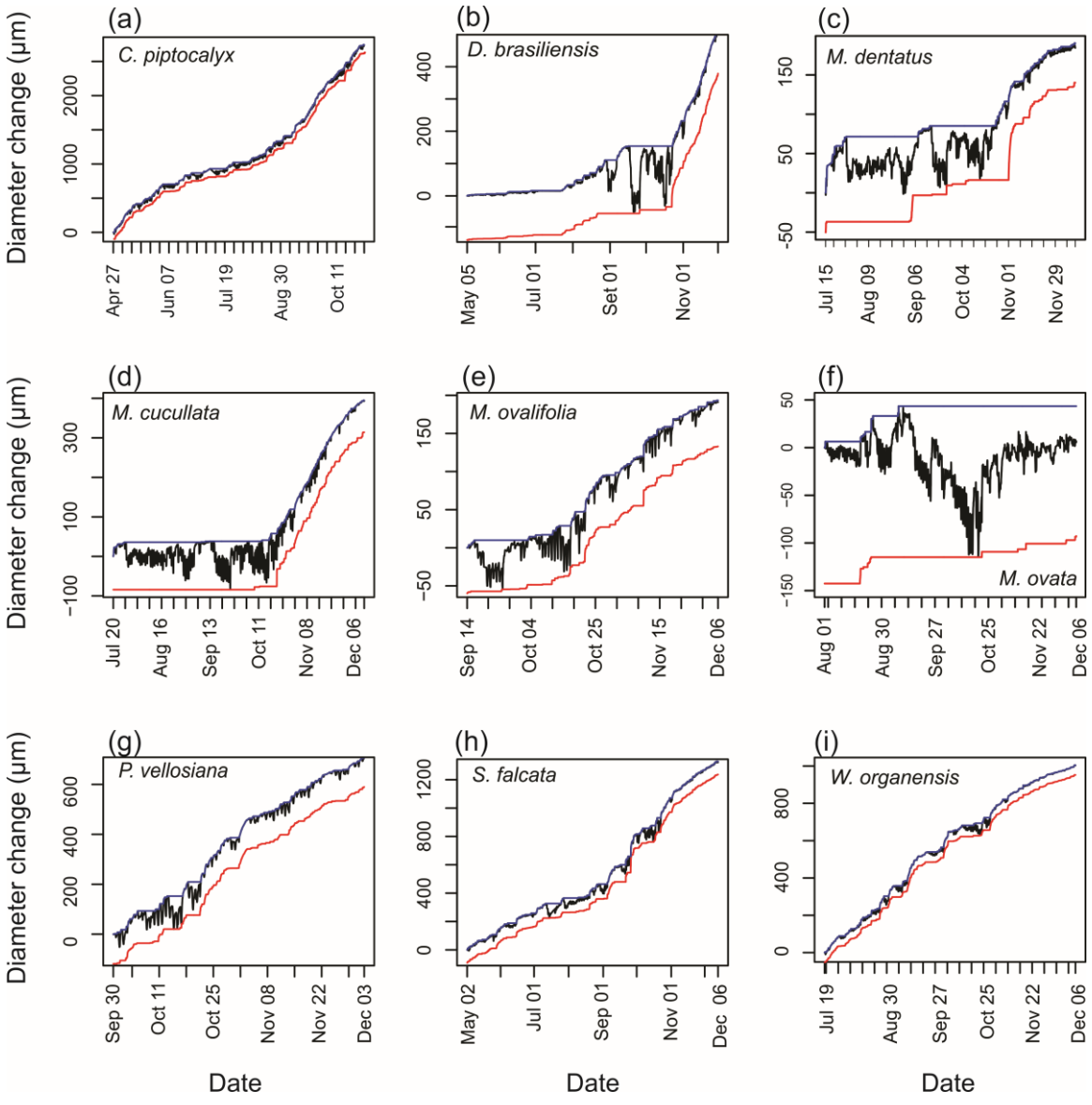

Figure 1. Growth patterns of the study trees. The black line is the bark diameter change data, the blue line is the cambial growth signal predicted by the zero-growth method (g_{ZG}), and the red line is the signal predicted by the bark-capacitance method (g_{BC}).

Table 2. Number of growth days predicted using the zero-growth method (ZG) and the bark-capacitance method (BC).

Species	*Total days*	*Growth days ZG*	*Growth days BC*	R^2	*Common growth days*
C. piptocalyx	189	132 (69%)	142 (75%)	0.81	119
D. brasiliensis	209	85 (40%)	84 (40%)	0.72	58
M. dentatus	150	51(34%)	33 (22%)	0.16	20
M .cucullata	145	52 (36%)	50 (34%)	0.46	41
M. ovalifolia	82	62 (76%)	44 (53%)	0.59	41
M. ovata	132	8 (6%)	10 (7%)	0.04	3
P. vellosiana	65	55 (84%)	50 (77%)	0.65	49
S. falcata	225	134 (59%)	149 (66%)	0.69	112
W. organensis	145	118 (81%)	121 (83%)	0.72	107

Obs. Values inside brackets are the percentage of growth days in relation to the total number of days. The R^2 refers to the linear relationship between the growth signals predicted by both methods. Common growth days are the number of days when both methods predict growth.

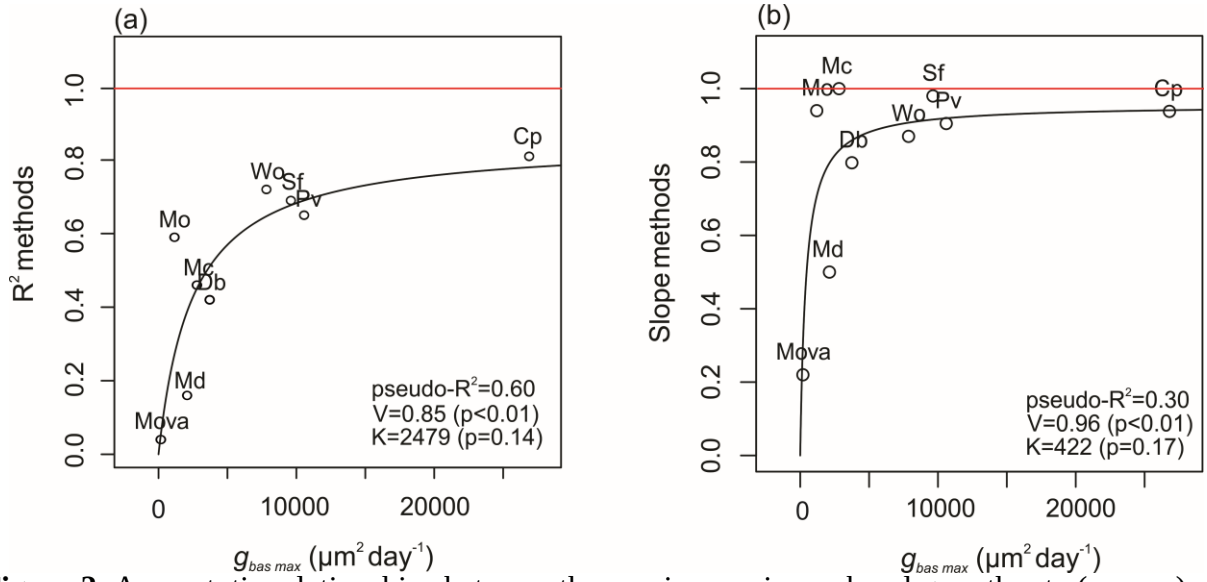

Figure 2. Asymptotic relationships between the species maximum basal growth rate ($g_{bas\ max}$) and the R^2 (a) and slope (b) of the linear regressions fitted to the growth signal predicted by the zero-growth method and the bark-capacitance method. The black lines are the predicted values by the Michaelis-Menten models fitted to the data, and V and K are the model parameters estimated by nonlinear least squares. The red line indicates complete agreement between methods (i.e. 1). The abbreviations used for the species are: Cp: *Croton piptocalyx*, Db: *Drimys brasiliensis*, Md: *Macropeplus dentatus*, Mc: *Myrceugenia cucullata*, Mo: *Myrceugenia ovalifolia*, Mova: *Myrceugenia ovata*, Pv: *Psychotria vellosiana*, Sf: *Symplocos falcata*, Wo: *Weinmannia organensis*.

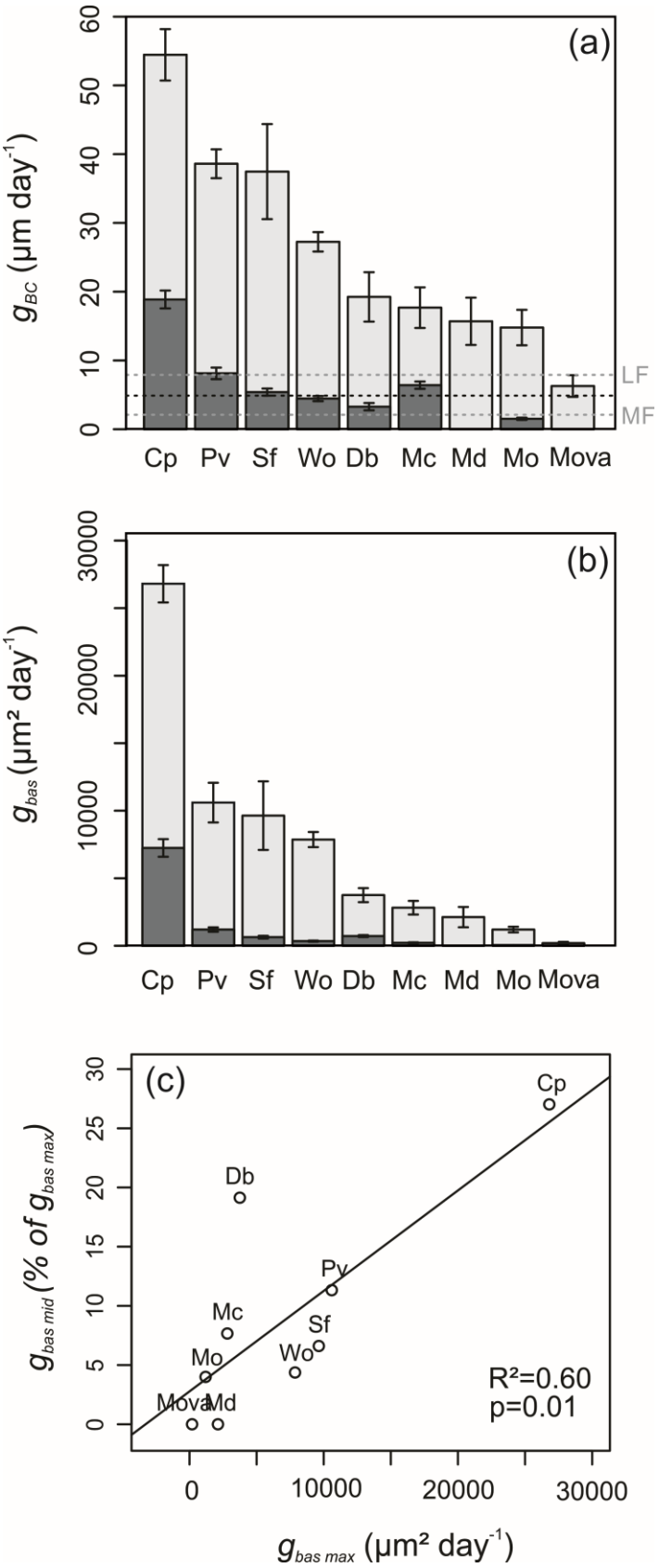

Figure 3. Growth rates of the study trees. (a) Linear growth calculated by the bark capacitance method (g_{BC}). The lighter gray bars are the maximum linear growth rates, estimated as the mean of the values above the 95 percentile of the g_{BC} data. The darker gray bars are the middle linear growth rates, estimated as the mean of the values between 25 and 75 percentile of the g_{BC} data from September to December/2015. The gray dashed lines are the mean stem increment from Amazon lowland tropical forests (LF; Vieira *et al.*, 2004) and Jamaican montane tropical forests (MF; Bellingham & Tanner, 2000). The black dashed line is the average of the middle growth rates of our data weighted by the basal area percentage of each species. (b) Basal growth rates (g_{bas}) calculated using equation 25 (see text). The lighter gray bars are the maximum basal growth rates ($g_{bas\ max}$) and the darker bars are middle basal growth rates ($g_{bas\ mid}$). The error bars in (a) and (b) are the standard error. (c) Linear relationship between $g_{bas\ mid}$ and $g_{bas\ max}$. The abbreviations used for the species are: Cp: *Croton piptocalyx*, Db: *Drimys brasiliensis*, Md: *Macropeplus dentatus*, Mc: *Myrceugenia cucullata*, Mo: *Myrceugenia ovalifolia*, Mova: *Myrceugenia ovata*, Pv: *Psychotria vellosiana*, Sf: *Symplocos falcata*, Wo: *Weinmannia organensis*.

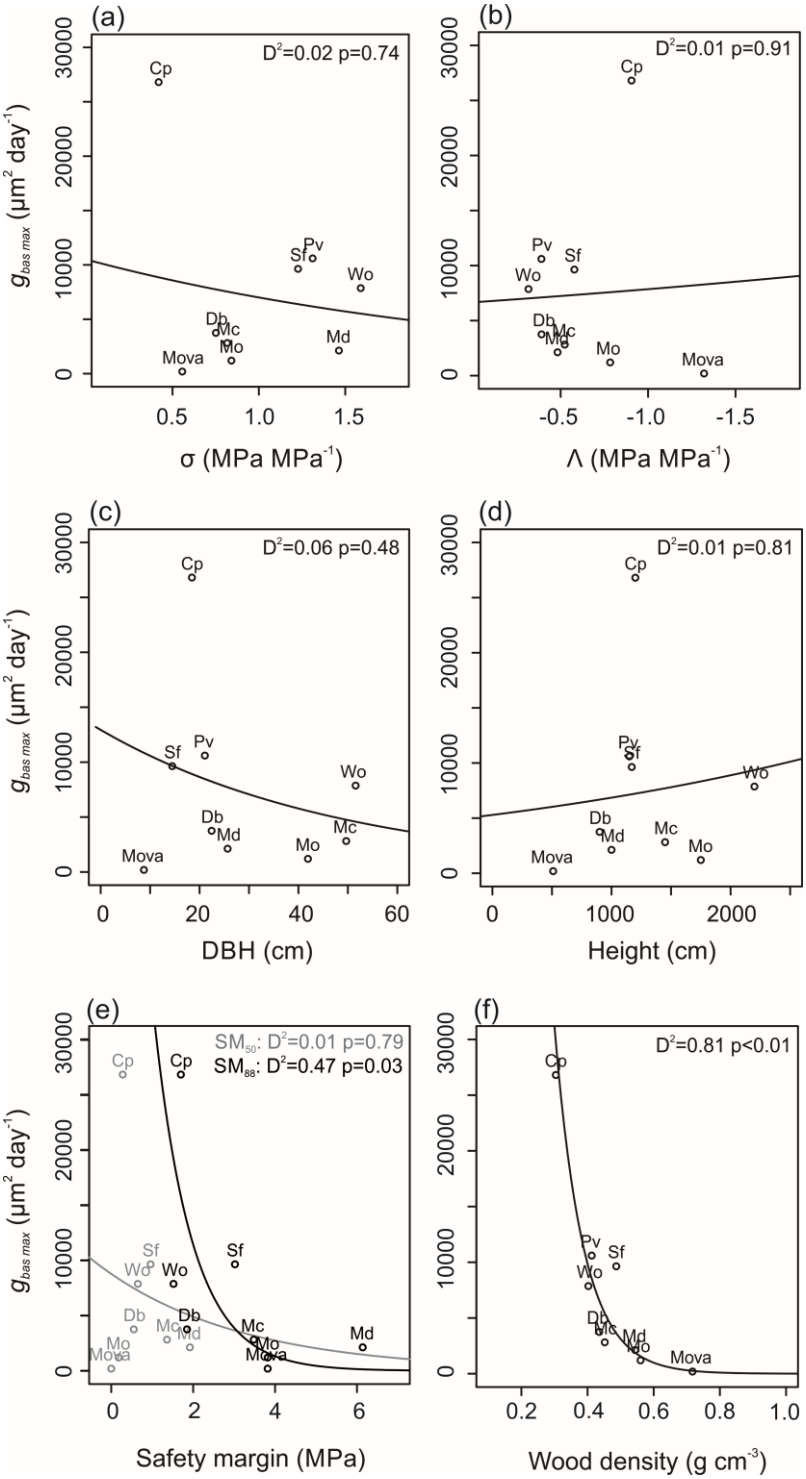

Figure 4. Relationships between maximum basal growth rates ($g_{bas\ max}$) and stomatal behavior (σ; a); maximum transpiration rate per unit of hydraulic conductivity (Λ; b); stem diameter at breast height (DBH; c); tree height (d); xylem safety margin based on the loss of 50% of xylem conductivity (SM_{50}; gray) and 88% of xylem conductivity (SM_{88}; black; c); and wood density (d). The lines are the predicted values by the generalized linear model fitted to the data, and the p-values refer to the significance of the coefficient estimated for the independent variable. The abbreviations used for the species are: Cp: *Croton piptocalyx*, Db: *Drimys brasiliensis*, Md: *Macropeplus dentatus*, Mc: *Myrceugenia cucullata*, Mo: *Myrceugenia ovalifolia*, Mova: *Myrceugenia ovata*, Pv: *Psychotria vellosiana*, Sf: *Symplocos falcata*, Wo: *Weinmannia organensis*.

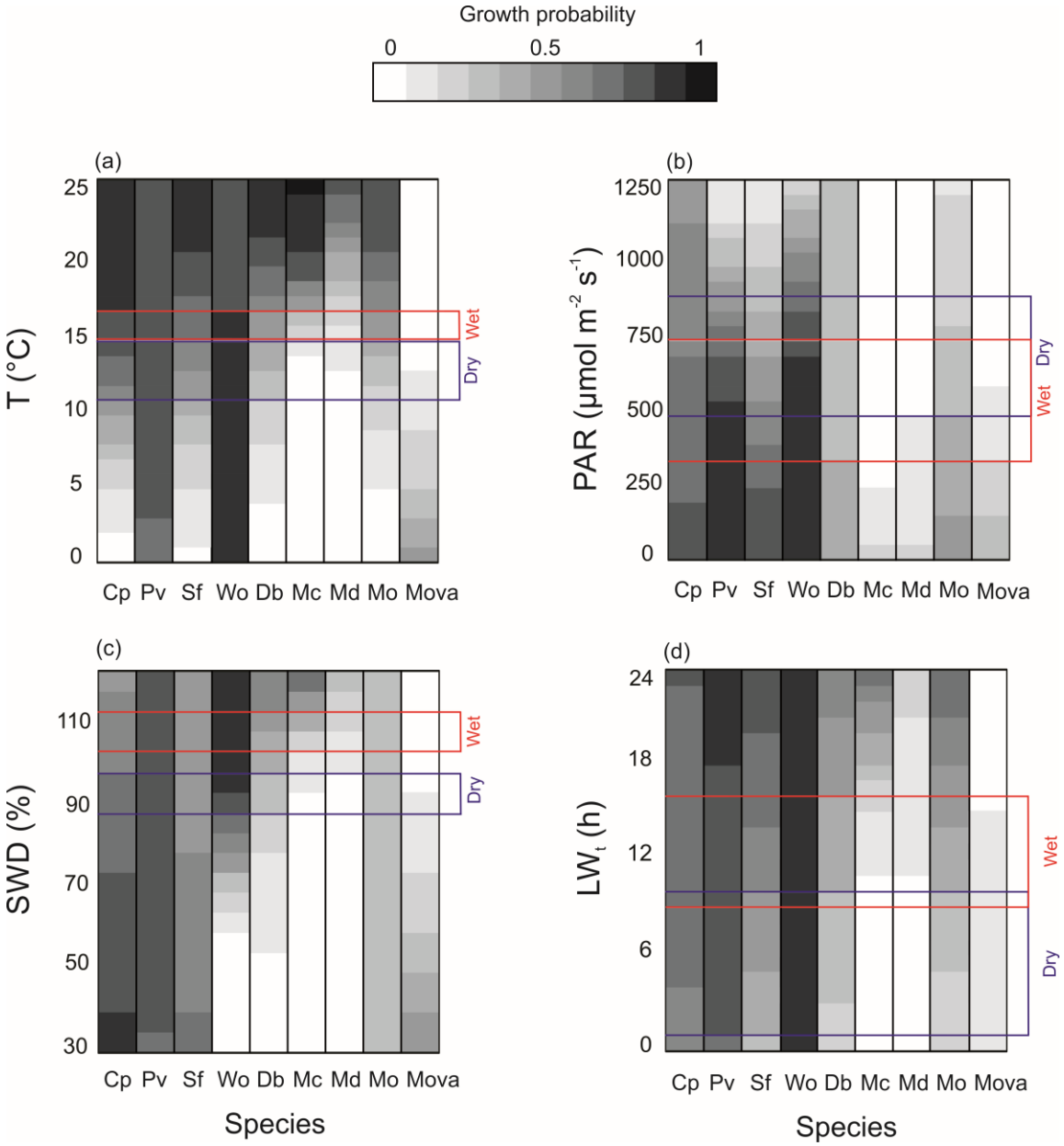

Figure 5. Predicted growth probability of the study trees in a range of environmental conditions. The species are sorted from the faster growing (to the left) to the slower growing (to the right). The red and blue regions represent the conditions during the wet (November-December) and dry season (August-September), respectively, and they comprise the values between the 25 and 75 percentile of the data. (a) Air temperature (T), (b) Photosynthetic active radiation (PAR), (c) Soil water deficit (SWD), (d) Leaf wetness time (LW_t). The abbreviations used for the species are: Cp: *Croton piptocalyx*, Db: *Drimys brasiliensis*, Md: *Macropeplus dentatus*, Mc: *Myrceugenia cucullata*, Mo: *Myrceugenia ovalifolia*, Mova: *Myrceugenia ovata*, Pv: *Psychotria vellosiana*, Sf: *Symplocos falcata*, Wo: *Weinmannia organensis*.

Table 3. Parameter estimates for the logistic regressions and generalized linear models fitted to the daily basal growth data.

Logistic regressions															
Species	***T***			***PAR***			***SWD***			***LW_t***			***SWD:LW_t***		
	Coef	***z-val***	***p***	***Coef***	***z-val***	***p***	***Coef***	***z-val***	***p***	***Coef***	***z-val***	***p***	***Coef***	***z-val***	***p***
C. piptocalyx	0.29	2.81	**<0.01**	-0.01	-1.21	0.23	0.02	0.15	0.88	0.54	0.75	0.88	-0.01	-0.72	0.47
P. vellosiana	-0.01	-0.03	0.97	-0.01	-3.04	**<0.01**	0.03	0.61	0.54	0.32	0.78	0.43	-0.01	-0.76	0.45
S. falcata	0.22	3.38	**<0.01**	-0.01	-3.89	**<0.01**	-0.01	-0.28	0.77	0.12	0.47	0.63	-0.01	-0.09	0.92
W. organensis	-0.09	-0.87	0.38	-0.01	-3.41	**<0.01**	0.12	1.59	0.53	-0.06	-0.09	0.92	0.01	0.08	0.93
D. brasiliensis	0.17	3.48	**<0.01**	-0.01	-0.70	0.48	0.05	2.24	**0.02**	0.30	1.42	0.15	-0.01	-1.18	0.48
M .cucullata	0.66	3.04	**<0.01**	-0.01	-1.58	0.11	0.30	3.05	**<0.01**	2.26	3.13	**<0.01**	-0.02	-2.90	**<0.01**
M. dentatus	0.30	2.74	**<0.01**	-0.01	-1.36	0.17	0.06	0.93	0.35	-0.07	-0.12	0.90	0.01	0.24	0.81
M. ovalifolia	0.23	1.04	0.30	-0.01	-1.18	0.24	-0.02	-0.51	0.61	-0.14	-0.34	0.73	0.02	0.61	0.54
M. ovata	-0.17	-0.88	0.37	-0.01	-1.90	0.06	-0.03	-0.25	0.80	0.03	0.03	0.97	-0.01	-0.04	0.96
Generalized linear models															
Species	***T***			***PAR***			***SWD***			***LW_t***			***SWD:LW_t***		
	Coef	***t-val***	***p***	***Coef***	***t-val***	***p***	***Coef***	***t-val***	***p***	***Coef***	***t-val***	***p***	***Coef***	***t-val***	***p***
C. piptocalyx	0.32	6.31	**<0.01**	-0.01	-4.33	**<0.01**	-0.03	-0.58	0.56	0.01	0.01	0.98	0.01	0.17	0.86
P. vellosiana	0.13	1.12	0.26	-0.01	-2.52	**0.01**	-0.02	-0.92	0.36	0.22	1.51	0.14	-0.01	-1.39	0.17
S. falcata	0.32	7.17	**<0.01**	-0.01	-3.70	**<0.01**	-0.01	-0.37	0.71	0.51	3.02	**<0.01**	-0.01	-3.01	**<0.01**
W. organensis	-0.01	-0.35	0.72	-0.01	-7.11	**<0.01**	0.02	0.83	0.41	1.10	0.83	0.41	-0.01	-3.94	**<0.01**
D. brasiliensis	0.46	4.64	**<0.01**	-0.01	-3.15	**<0.01**	0.07	2.41	**0.02**	1.30	4.50	**<0.01**	-0.01	-4.25	**<0.01**
M .cucullata	0.28	2.43	**0.02**	-0.01	-3.22	**<0.01**	-0.01	-0.08	0.93	0.31	0.61	0.54	-0.01	-0.62	0.53
M. dentatus	0.26	0.56	0.58	-0.01	-1.27	0.21	-0.41	-1.33	0.19	-1.98	-0.69	0.49	0.02	0.72	0.47
M. ovalifolia	0.62	4.68	**<0.01**	-0.01	-3.99	**<0.01**	0.06	2.25	**0.03**	1.30	4.95	**<0.01**	-0.01	-4.45	**<0.01**
M. ovata	0.07	1.17	0.33	-0.01	-0.30	0.78	1.24	3.51	**0.04**	7.82	3.27	0.04	-0.08	-3.39	**0.04**

Obs. T = Air temperature; PAR = Photosynthetic active radiation; SWD = Soil water deficit; LW_t = Leaf wetness time. P-values lower than 0.05 marked in bold.

We calculated the ratio of the probability of growth with and without leaf wetting events (i.e. setting the LW_t constant at zero in the logistic regression models) during the dry and the wet season (Fig. 6). Removing leaf wetting events during the wet season clearly decreases the probability of growth in some species (*S. falcata*, *D. brasiliensis*, *M. dentatus* and *M. ovalifolia*), while other species are not affected (*C. piptocalyx*, *P. vellosiana* and *W. organensis*) or are favored by it (*M. ovata* and *M. cucullata*). The average probability ratio weighted by each species basal area is 0.94, which indicates that the removal of leaf wetting events during the wet season have only a small negative effect on TMCF growth (Fig. 6a). The removal of leaf wetting events during the dry season has a stronger negative effect on the growth probability of most species (Fig. 6b), and consequently, the weighted average growth

probability ratio during the dry season winter is 0.88. This indicates leaf-wetting events are more important for the growth of TMCF trees during drier conditions.

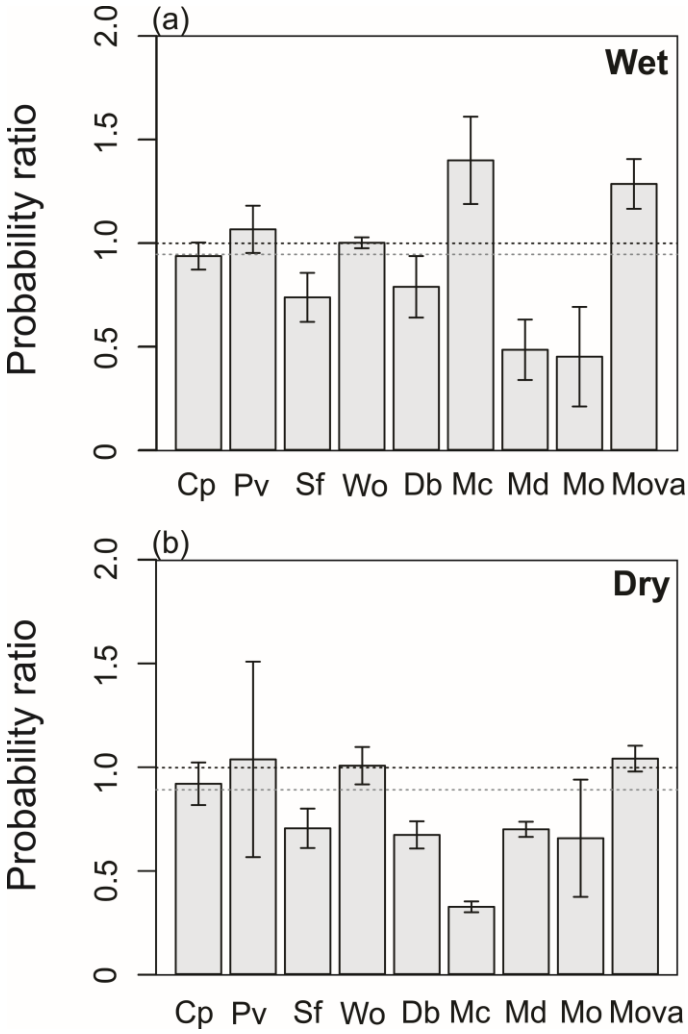

Figure 6. Probability ratio between the probability of the trees growing with and without leaf wetting events, during the wet (a) and the dry (b) seasons. The black dashed line indicates the ratio of 1 (absence of leaf-wetting does not affect tree growth probability), values above 1 indicate that the probability of tree growth increases with the absence of leaf wetting events, and values below 1 indicate that absence of leaf wetting events decreases the probability of tree growth. The gray dashed line is the weighted average probability ratio for all the study species, calculated using their total basal area percentage. The species are sorted from the faster growing (to the left) to the slower growing (to the right). The bars represent the standard errors. The abbreviations used for the species are: Cp: *Croton piptocalyx*, Db: *Drimys brasiliensis*, Md: *Macropeplus dentatus*, Mc: *Myrceugenia cucullata*, Mo: *Myrceugenia ovalifolia*, Mova: *Myrceugenia ovata*, Pv: *Psychotria vellosiana*, Sf: *Symplocos falcata*, Wo: *Weinmannia organensis*.

Regarding the magnitude of tree growth, we found that most of the study trees are able to grow more at higher temperatures (T weighted t-value for all species = 2.9±0.9; Fig. 7a-b), and have their growth inhibited by high radiation (PAR weighted t-value for all species = -3.6±0.6; Fig. 7c). The interaction between SWD and LW_t was generally more important at regulating the growth magnitude than it was at regulating growth probability (SWD:LW_t weighted t-value for all species = -2.2±0.6; Table 3, Fig. 7d). As we can see in Fig. 7 and Table 3, many species had their growth enhanced by LW_t during low SWD conditions, and inhibited during high SWD conditions.

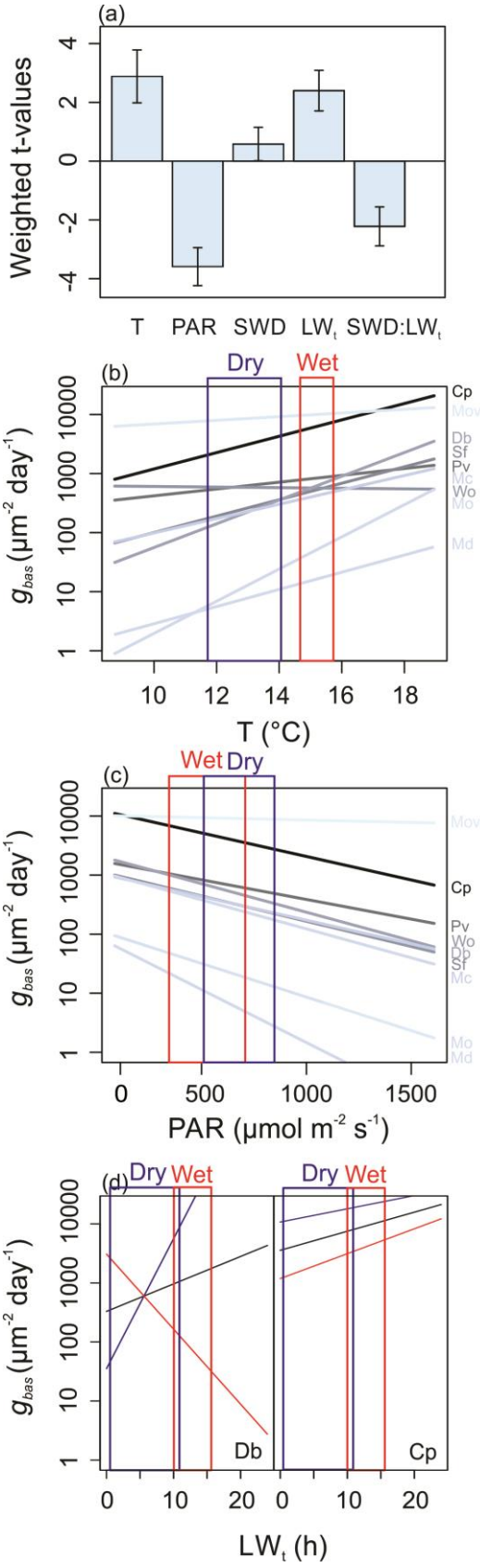

Figure 7. Environmental drivers of the study trees growth magnitude. (a) Weighted average of the t-values estimated by the generalized linear model fitted to the data for all the species. The t-values were weighted based on the total basal area percentage of each species. Response of tree growth magnitude to air temperature (T; b), photosynthetic active radiation (PAR; c), and the soil water deficit (SWD) and leaf wetness time (LW_t) interaction (d). On the panels (b) and (c) we show the predicted growth response of each species to T and PAR, if we hold all the other variables constant at their median values. The color of the line that represents each species is proportional to the growth speed of the species, so that darker colors represent faster growing species. In (d) we show the predicted growth response to LW_t at medium SWD (SWD= 90%; black line), low SWD (SWD=60%; blue line), and high SWD (SWD=120%; red line). On the left panel of (d) we show a species with a strong response (Db) and on the right, we show a species with a weak response (Cp). The red and blue regions represent the conditions during the wet (November-December) and dry season (August-September), respectively, and they comprise the values between the 25 and 75 percentile of the data. The abbreviations used for the species are: Cp: *Croton piptocalyx*, Db: *Drimys brasiliensis*, Md: *Macropeplus dentatus*, Mc: *Myrceugenia cucullata*, Mo: *Myrceugenia ovalifolia*, Mova: *Myrceugenia ovata*, Pv: *Psychotria vellosiana*, Sf: *Symplocos falcata*, Wo: *Weinmannia organensis*.

Discussion

Our results show that the hotter, more humid and lower irradiance environmental conditions of the wet season are more favorable to TMCF tree growth than the dry season conditions (Fig. 5, 7). However, fast growing trees, such as *C. pyptocalyx*, *P. velloziana*, *S. falcata* and *W. organensis*, are able to grow even during the dry season. Growing during the dry season appears to be a more hydraulically risky strategy, as faster growing trees operate under narrower xylem safety margins than slower growing trees (Fig. 4e). During the dry season leaf wetting events become particularly important for most trees to enhance or sustain growth (Fig. 6, 7). We also show that the BC method (Mencuccini *et al.,* 2013) for extracting *g* derived from bark diameter measurements and sap velocity data produces similar results to the ZG method (Zweifel *et al.,* 2016) in fast growing species (Fig. 2). The greater differences between methods in slow growing species might be related to the principles behind each method and will be discussed below.

Methods for extracting the growth signal

The methods proposed by Mencuccini *et al.,* (2013) and Zweifel *et al.,* (2016) are both based on theoretical assumptions about tree physiology, and we do not have enough data to test these assumptions and judge which method is more accurate. This is why in this study we tried to combine and take advantage of both methods. Both methods agree that bark capacitance is an important component of dD_b data (Zweifel *et al.,* 2016; Mencuccini *et al.,* 2013), but they differ at the point where bark capacitance is calculated. In the ZG method, bark capacitance related changes (TWD) are calculated after g_{ZG} is extracted from dD_b, as the difference between the raw dD_b and the estimated g_{ZG} (equation 2). In other words, it assumes that cambial growth only happens when the tree tissues are completely saturated, consequently, capacitance-related changes cannot directly influence g_{ZG}. As stated in Zweifel *et al* (2016), this premise might be too rigorous, since some growth is still possible under non-saturated conditions (Lockhart, 1965; Ruts *et al.,* 2012). In the form we implemented the BC method, it uses the theoretical relationship that bark diameter changes induced by capacitance should have with xylem water potential (Mencuccini *et al.,* 2013), to separate the residual growth and osmotic related changes, left in the TWD data by the ZG method, from the actual bark capacitance signal. After that, we exclude the "pure" bark capacitance signal from dD_b before extracting g_{BC}. The high agreement between methods on fast-growing trees suggests that the TWD data of these trees have a smaller proportion of residual growth and osmotic changes (i.e. TWD is close to actual

bark capacitance). This might be caused by the difference in the relative importance of *g* and the capacitance signal in the dD_b data between fast and slow-growing trees. We believe that in fast growing trees, *g* comprises a large portion of the dD_b data in relation to bark capacitance and osmotic related processes. Therefore, the ZG method can detect most of the *g* in the dD_b data, without needing to account for bark capacitance.

The ZG method have the practical advantage of needing only dD_b data for providing estimates of tree growth, especially accurate for faster growing trees with low bark capacitance. The BC method can be used as a complement to the ZG method, to estimate tree growth in trees with lower *g* (i.e. slow growing and/or high bark capacitance). In addition, the BC also provides coefficient estimates that have a potentially useful physiological meaning (see equation 13 and Mencuccini *et al.,* 2013) and an estimate of the osmotic component of dD_b (Mencuccini *et al.,* 2013; Chan *et al.,* 2016). The main disadvantage of BC is needing either direct xylem water potential measurements or data to be used as a proxy for it, such as xylem diameter variation (Mencuccini *et al.,* 2013; Chan *et al.,* 2016), or sap velocity as we used in this study.

Growth rates and tree hydraulic risk

The BC method allowed us to estimate for the first time the growth of TMCF trees at a daily time scale. While cloud forests are usually considered low productivity environments with slow growing trees (Weaver *et al.,* 1986; Bruijnzeel & Veneklaas, 1998; Bellingham & Tanner, 2000; Wilcke *et al.,* 2008; Moser *et al.,* 2010), we have found some trees with very fast growth rates, such as *C. pyptocalyx* and *P. vellosiana* (Fig. 3). However, the slower growing species, like *M. cucullata* and *M. ovalifolia*, comprised a bigger fraction of the study site basal area (Table 1). Therefore, the weighted average of all study species was relatively low, in comparison for example with the average stem increment commonly found in lowland Atlantic tropical forests (Fig. 3; Vieira *et al.,* 2004). Our daily scale measurements also allowed us to show that TMCF trees were capable of high daily growth rates, but they rarely reach their maximum growth potential; especially the slower growing trees (Fig. 3c). Even the faster growing trees like, *C. pyptocalyx* usually only reach *c.* 27% of their maximum observed growth rates in the field (Fig. 3). This might indicate that during most of the time the climatic conditions in TMCF are not optimal for tree growth.

The relationship between maximum growth rates and xylem safety margin we observed (Fig. 4e) suggests that faster growing species are more likely to keep growing even under non-

optimal climatic conditions and, consequently, subject their hydraulic system to more risk than slow growing species. This relationship was only significant when using the xylem P88, which provides further evidence that the xylem hydraulic safety margin estimated using the P88 (SM_{88}) possess a greater ecological significance for angiosperms than SM_{50} (Choat, 2013; Urli *et al.,* 2013; Delzon & Cochard, 2014). The narrower SM_{88} in fast growing trees implies that these trees favor carbon gain over cavitation avoidance (Tyree & Sperry, 1989; Choat *et al.,* 2012). Considering that fast growing trees also have lower wood density (Fig. 4f), which is cheaper for the plant (i.e. lower energetic investment), these trees could compensate for the high percentage of embolized vessels by frequently producing newer vessels (Brodribb, 2010; Delzon & Cochard, 2014). If we consider the P88 as an indicative of the threshold for hydraulic failure induced mortality in angiosperms (McDowell, 2011; Choat, 2013; Urli *et al.,* 2013; Delzon & Cochard, 2014), this fast growing-narrow safety margin strategy is riskier than a slow growing-wide safety margin strategy. Therefore, our results suggests that plant hydraulics could be one of the mechanisms subjacent to the classical trade-off between growth and mortality risk often observed in tropical forest trees (Lawton, 1984; King *et al.,* 2006; Wright *et al.,* 2010). The negative relationship between growth rates and wood density (Fig. 4f) also supports the idea that fast growing TMCF trees are subjected to higher mortality risks; as trees with less dense wood are more prone to suffer wind damage (Lawton, 1984; King *et al.,* 2006).

Environmental drivers of growth

Temperature had an important role on the growth of our study trees; higher temperatures had a positive effect in the growth of almost all trees (Fig. 5, 7). We believe this effect might be attributed to the influence that temperature might have on net photosynthesis and on phloem transport of photoassimilates. The radial conductivity between phloem and xylem increases at higher temperatures due to aquaporin activity (Steppe *et al.,* 2012; Mencuccini *et al.,* 2013), which might facilitate phloem loading. Lower temperatures also decrease phloem viscosity and difficult long-distance transport of carbohydrates (Cavender-Bares, 2005). The response of net photosynthesis to temperature follows a parabolic trajectory (Berry & Björkman, 1980). Higher temperatures increase photorespiration and respiration, which leads to reductions in net photosynthesis (Berry & Björkman, 1980). On the other hand, lower temperatures decrease the efficiency of the photosynthetic reactions (Berry & Björkman, 1980); even artic species adapted to extreme cold only reach their optimum photosynthetic levels at *c.* 15°C (Billings *et al.,* 1971). Our results suggest that TMCF trees are on the lower end of their optimum temperature for growth and, contrary to lowland tropical forests (Clark,

2004; Doughty & Goulden, 2008; Way & Oren, 2010); increments in temperature could possibly favor growth in these ecosystems.

The inhibitory effect that PAR had on tree growth was an unexpected result, as irradiance is often considered a strong factor limiting TMCF productivity due the persistence of clouds (Bruijnzeel & Veneklaas, 1998; Letts & Mulligan, 2005). We propose two possible explanations for this result. The first is that the frequent cloudiness of these environments could have acclimated TMCF trees to low irradiance conditions. Plants acclimated to low irradiance conditions are more vulnerable to light induced damage on the photosystem II (PSII) reaction center, a process often called photoinhibition (Powles, 1984; Aro *et al.*, 1994). Trees can also adapt to low irradiance conditions by increasing leaf area in relation to root area (Poorter & Nagel, 2000), so they can maintain an optimum amount of transpiration rate per unit of root mass (Sims & Pearcy, 1994). When a low irradiance adapted plant is exposed to high irradiance it has to either close its stomata, or sustain a higher transpiration demand that could damage the plant hydraulic system (i.e. cavitation). As we observed that faster growing species are more likely to grow during high PAR (Fig. 5), it is possible that these species often experience higher transpiration rates than they are optimized to sustain, and because of this they are more prone to hydraulic damage (Fig. 4e). While this explanation appears plausible based on our data, other studies suggests that some TMCF have a higher belowground/aboveground biomass ratio than lowland forests (Moser *et al.*, 2010; Girardin *et al.*, 2010). This implies that in some TMCF nutrient limitation might play a more important role than adaptations for low irradiance conditions.

The second possible explanation is that there was a temporal decoupling between assimilation and growth on TMCF trees. The TMCF trees could favor carbon assimilation during the relatively rare periods of high PAR, and only transport and use the photoassimilates for cambial growth during low PAR periods (i.e. cloudy or rainy periods). This temporal decoupling is thought to be important in a diel scale (Steppe *et al.*, 2015), but it could also play a role between sunny and cloudy or rainy days. In a sunny day, the plant would spend a large fraction of the day assimilating carbon, but due to cell turgor limitation (Steppe *et al.*, 2015; Hsiao, 1973); its growth would be restricted to nocturnal periods. In contrast, in a cloudy or rainy day, the plant could use its carbon reserves to grow during a large fraction of the day. That explanation gives a mechanistic basis for the effect that LW_t had on tree growth (Fig. 6, 7).

Soil water availability only had a small direct effect on tree growth, but its interaction with LW_t was important for many trees (Fig. 6, 7). The LW_t data we used included both fog and rain events, but much of the LW_t during the dry season is caused by fog, as rainfall is low during this period (Fig. S1). The increase in tree growth observed during leaf wetting events, especially at low SWD, can be attributed to cell turgor improvements caused by tree rehydration (Steppe *et al.*, 2015; Hsiao, 1973). We postulate that this rehydration could be induced by three non-exclusive processes: 1- direct foliar water uptake (FWU; Eller *et al.*, 2013; 2016; Goldsmith *et al.*, 2013); 2- the transpiration reduction caused by low atmospheric vapor pressure deficit and wet leaves (Smith & McClean, 1989; Letts & Mulligan, 2005); 3- the increase in soil moisture caused by throughfall of either fog or rain. Considering that many trees responded differently to LW_t (Fig. 6, 7), we believe that these differences are more likely to be caused by differences in FWU between trees. Trees in TMCF are known to possess different FWU capabilities, which affects the rate which leaves can rehydrate when they are wet and also have consequences for plant turgor maintenance during drought (Eller *et al.*, 2016). Some study trees had almost no response or even a negative response to leaf-wetting events (Table 3; Fig. 6, 7). We postulate that these trees have very low FWU capability and their growth could be impaired by the reduction in gas exchange caused by wet leaves (Smith & McClean, 1989; Letts & Mulligan, 2005; Oliveira *et al.*, 2014).

Conclusion

The methods proposed by Mencuccini *et al* (2013) and Zweifel *et al* (2016) to extract the growth signal from dD_b data are very promising tools that allow us to investigate factors controlling tree growth at a time scale that was not possible before (Zweifel, 2016). Using the BC method, we could observe that the microclimatic conditions of TMCF might present several difficulties for tree growth, such as low temperatures and high irradiance. Fast growing TMCF trees can grow in wide range of environmental conditions by maintaining a narrow xylem hydraulic safety margin. Slow growing TMCF trees generally maintain their xylem hydraulic safety, growing only when environmental conditions are favorable. Some climate change scenarios predict that TMCF might experience higher temperatures in the future (Still *et al.*, 1999; Karmalkar *et al.*, 2008). While this could favor TMCF tree growth, it could also favor the upward migration of lowland tropical species populations that would become more competitive at these new temperatures (Hillyer & Silman, 2010; Feeley *et al.*, 2011; Corllet & Wetcott, 2013). In addition, earth surface temperature increments are associated with increases in the height of clouds formation in tropical mountains (Still *et al.*, 1999), and consequently,

the decrease of leaf-wetting events in TMCF. As leaf-wetting events favor the growth of most TMCF trees, especially during the dry season, the overall effect of temperature increments might threaten TMCF trees more than benefit them.

Acknowledgements

We thank Roman Zweifel, Reinhard Bischoff, Leonardo Dias Meireles and Fazenda Lavrinhas. This research was funded by FAPESP/Microsoft research (grant 11/52072-0) awarded to R.S.O., and the Higher Education Co-ordination Agency (CAPES/Brazil) and FAPESP (grant 13/19555-2) awarded scholarships to C.B.E.

References

Aro EM, McCaffery S, Anderson JM. 1994. Recovery from photoinhibition in peas (*Pisum sativum* L.) acclimated to varying growth irradiances (role of D1 protein turnover). *Plant Physiology* **104**:1033-1041.

Beer C, Reichstein M, Tomelleri E, Ciais P, Jung M, Carvalhais N, Rödenbeck C, Arain MA, Baldocchi D, Bonan GB, Bondeau A. 2010. Terrestrial gross carbon dioxide uptake: global distribution and covariation with climate. S*cience* **329**: 834-838.

Bellingham PJ, Tanner EV. 2000. The Influence of Topography on Tree Growth, Mortality, and Recruitment in a Tropical Montane Forest. *Biotropica* **32**: 378-84.

Billings WD, Godfrey PJ, Chabot BF, Bourque DP. 1971. Metabolic acclimation to temperature in arctic and alpine ecotypes of *Oxyria digyna*. *Artic and Alpine Research* **3**: 277-89.

Burgess SSO, Adams MA, Turner NC, Ong CK, Khan AAH, Beverly CR, Bleby TM. 2001. An improved heat pulse method to measure low and reverse rates of sap flow in woody plants. *Tree Physiology* **21**:589–598.

Brodribb TJ, Bowman D, Nichols S, Delzon S, Burlett R. 2010. Xylem function and growth rate interact to determine recovery rates after exposure to extreme water deficit. *New Phytologist* **188**: 533–542.

Bruijnzeel LA, Veneklaas EJ. 1998. Climatic conditions and tropical montane forest productivity: the fog has not lifted yet. *Ecology* **79**: 3-9.

Cavender-Bares J. 2005. Impacts of freezing on long distance transport in woody plants. In: Holbrook NM, Zweiniecki MA, eds. *Vascular transport in plants.* Boston, USA. Elsevier, 401-424.

Chan T, Hölttä T, Berninger F, Mäkinen H, Nöjd P, Mencuccini M, Nikinmaa E. 2016. Separating water-potential induced swelling and shrinking from measured radial stem variations reveals a cambial growth and osmotic concentration signal. *Plant, cell and environment* **39**: 233-244.

Choat B, Jansen S, Brodribb TJ, Cochard H, Delzon S, Bhaskar R, Bucci SJ, Feild TS, Gleason SM, Hacke UG, Jacobsen AL. 2012. Global convergence in the vulnerability of forests to drought. *Nature* **491**: 752-755.

Choat B. 2013. Predicting thresholds of drought-induced mortality in woody plant species. *Tree Physiology* **33**: 669–671.

Clark DA. 2004. Sources or sinks? The responses of tropical forests to current and future climate and atmospheric composition. *Philosophical Transactions of the Royal Society of London B: Biological Sciences* **359**: 477-491.

Clark DA, Clark DB. 1992. Life history diversity of canopy and emergent trees in a neotropical rain forest. *Ecological monographs* **62**: 315-344.

Corlett RT, Westcott DA. 2013. Will plant movements keep up with climate change? *Trends in ecology & evolution* **28**: 482-488.

Delzon S, Cochard H. 2014. Recent advances in tree hydraulics highlight the ecological significance of the hydraulic safety margin. *New Phytologist* **203**: 355-358.

Douglas Bates, Martin Maechler, Ben Bolker, Steve Walker. 2015. Fitting Linear Mixed-Effects Models Using lme4. *Journal of Statistical Software* **67**: 1-48.

Doughty CE, Goulden ML. 2008. Are tropical forests near a high temperature threshold*? Journal of Geophysical Research – Biogeoscience:* 113.

Efron B. 1978. Regression and ANOVA with Zero-One Data: Measures of Residual Variation. *Journal of the American Statistical Association* **73**: 113-121.

Eller CB, Lima AL, Oliveira RS. 2013. Foliar uptake of fog water and transport belowground alleviates drought effects in the cloud forest tree species, *Drimys brasiliensis* (Winteraceae). *New Phytologist* 199: 151-162.

Eller CB, Burgess SSO, Oliveira RS. 2015. Environmental controls in the water use patterns of a tropical cloud forest tree species, *Drimys brasiliensis* (Winteraceae). *Tree physiology* **35**: 387-399.

Eller CB, Lima AL, Oliveira RS. 2016. Cloud forest trees with higher foliar water uptake capacity and anisohydric behavior are more vulnerable to drought and climate change. *New Phytologist* 10.1111/nph.13952.

Feeley KJ, Silman MR, Bush MB, Farfan W, Cabrera KG, Malhi Y, Meir P, Revilla NS, Quisiyupanqui MN, Saatchi S. 2011. Upslope migration of Andean trees. *Journal of Biogeography* **38**: 783-791.

Fisher JB, Malhi Y, Torres IC, Metcalfe DB, van de Weg MJ, Meir P, Silva-Espejo JE, Huasco WH. 2013. Nutrient limitation in rainforests and cloud forests along a 3,000-m elevation gradient in the Peruvian Andes. *Oecologia* 172:889-902.

Foster P. 2001. The potential negative impacts of global climate change on tropical montane cloud forests. *Earth-Science Reviews* **55**: 73-106.

Gentry AH. 1992. Tropical forest biodiversity: distributional patterns and their conservational significance. *Oikos* **63**: 19–28.

Girardin CA, Malhi Y, Aragao LE, Mamani M, Huaraca Huasco W, Durand L, Feeley KJ, Rapp J, Silva-Espejo JE, Silman M, Salinas N. 2010. Net primary productivity allocation and cycling of carbon along a tropical forest elevational transect in the Peruvian Andes. *Global Change Biology* **16**:3176-3192.

Goldsmith GR, Matzke NJ, Dawson TE. 2013. The incidence and implications of clouds for cloud forest plant water relations. *Ecology letters* **16**: 307-314.

Gotsch SG, Asbjornsen H, Holwerda F, Goldsmith GR, Weintraub AE, Dawson TE. 2014. Foggy days and dry nights determine crown-level water balance in a seasonal tropical montane cloud forest. *Plant, cell and environment* **37**: 261-272.

Guisan A, Zimmermann NE. 2000. Predictive habitat distribution models in ecology. *Ecological modelling* **135**: 147-186.

Hamilton LS. 1995. Mountain cloud forest conservation and research: a synopsis. *Mountain Research and Development* **1**: 259-266.

Hargreaves GL, Samani ZA. 1982. Estimating potential evapotranspiration. *Journal of Irrigation and Drainage Engineering (ASCE)* **108**: 225–230.

Hillyer R, Silman MR. 2010. Changes in species interactions across a 2.5 km elevation gradient: effects on plant migration in response to climate change. *Global Change Biology* **16**: 3205-3214.

Hsiao TC. 1973. Plant responses to water stress. *Annual Review of Plant Physiology* **24**: 519–570.

Hu J, Riveros-Iregui DA. 2016. Life in the clouds: are tropical montane cloud forests responding to changes in climate? *Oecologia* 6:1-3.

Irvine J, Grace J. 1997. Continuous measurements of water tensions in the xylem of trees based on the elastic properties of wood. *Planta* **202**: 455–461.

Karmalkar AV, Bradley RS, Diaz HF. 2008. Climate change scenario for Costa Rican montane forests. *Geophysical Research Letters* 35 (11).

King DA, Davies SJ, Tan S, Noor NS. 2006. The role of wood density and stem support costs in the growth and mortality of tropical trees. *Journal of Ecology* **94**: 670-680.

Lawton RO. 1984. Ecological constraints on wood density in a tropical montane rain forest. *American Journal of Botany* **1**: 261-267.

Lawton RO, Nair US, Pielke RA, Welch RM. 2001. Climatic impact of tropical lowland deforestation on nearby montane cloud forests. *Science* **294(5542)**:584-587.

Letts MG, Mulligan M. 2005. The impact of light quality and leaf wetness on photosynthesis in north-west Andean tropical montane cloud forest. *Journal of Tropical Ecology* **21**: 549-557.

Lockhart JA. 1965. An analysis of irreversible plant cell elongation. *Journal of Theoretical Biology* **8**: 264-275.

Loope LL, Giambelluca TW. 1998. Vulnerability of island tropical montane cloud forests to climate change, with special reference to East Maui, Hawaii. *Climatic Change* **39**: 503-517.

Luyssaert S, Schulze ED, Börner A, Knohl A, Hessenmöller D, Law BE, Ciais P, Grace J. 2008. Old-growth forests as global carbon sinks. *Nature* **455**: 213-215.

Martínez-Vilalta J, Poyatos R, Aguadé D, Retana J, Mencuccini M. 2014. A new look at water transport regulation in plants. *New Phytologist* **204**:105-15.

McDowell NG. 2011. Mechanisms linking drought, hydraulics, carbon metabolism, and vegetation mortality. *Plant Physiology* **155**: 1051–1059.

Mencuccini M, Hölttä T, Sevanto S, Nikinmaa E. 2013. Concurrent measurements of change in the bark and xylem diameters of trees reveal a phloem-generated turgor signal. *New Phytologist* **198**:1143-1154.

Moser G, Leuschner C, Hertel D, Graefe S, Soethe N, Iost S. 2011. Elevation effects on the carbon budget of tropical mountain forests (S Ecuador): the role of the belowground compartment. *Global Change Biology* **17**: 2211-2226.

Oliveira RS, Eller CB, Bittencourt PR, Mulligan M. 2014. The hydroclimatic and ecophysiological basis of cloud forest distributions under current and projected climates. *Annals of botany* **113**: 909-920.

Osazuwa-Peters O, Zanne AE, PrometheusWiki contributors. 2011. Wood density protocol. PrometheusWiki. [WWW document] URL http://prometheuswiki.publish.csiro.au/tiki-index.php?page=Wood+density+protocol [accessed 26 May 2016].

Pammenter NW, Vander Willigen C. 1998. A mathematical and statistical analysis of the curves illustrating vulnerability of xylem to cavitation. *Tree physiology* **18**: 589-593.

Perämäki M, Nikinmaa E, Sevanto S, Ilvesniemi H, Siivola E, Hari P, Vesala T. 2001. Tree stem diameter variations and transpiration in Scots pine: an analysis using a dynamic sap flow model. *Tree Physiology* **21**: 889–897.

Pereira L, Bittencourt PR, Oliveira RS, Junior M, Barros FV, Ribeiro RV, Mazzafera P. 2016. Plant pneumatics: stem air flow is related to embolism–new perspectives on methods in plant hydraulics. *New Phytologist* 10.1111/nph.13905

Poorter H, Nagel OW. 2000. The role of biomass allocation in the growth response of plants to different levels of light, CO2, nutrients and water: a quantitative review. *Australian Journal of Plant Physiology* **27:** 595–607.

Powles SB. 1984. Photoinhibition of photosynthesis induced by visible light. *Annual Review of Plant Physiology* **35**:15-44.

R Development Core Team. 2015. R: a language and environment for statistical computing. R Foundation for Statistical Computing, Vienna, Austria.

Ruts T, Matsubara S, Wiese-Klinkenberg A, Walter A. 2012. Diel patterns of leaf and root growth: endogenous rhythmicity or environmental response? *Journal of Experimental Botany* **63:** 3339-3351.

Safford HD. 1999. Brazilian Paramos I. An introduction to the physical environment and vegetation of the campos de altitude. *Journal of Biogeography* **26**: 693–712.

Sims DA, Pearcy RW. 1994. Scaling sun and shade photosynthetic acclimation of *Alocasia macrorrhiza* to whole-plant performance – I. Carbon balance and allocation at different daily photon flux densities. *Plant, Cell and Environment* **17**: 881–887.

Smith WK, McClean TM. 1989. Adaptive relationship between leaf water repellency, stomatal distribution, and gas exchange. *American Journal of Botany* **76**: 465-469.

Sperry JS, Donnelly JR, Tyree MT. 1988. A Method for Measuring Hydraulic Conductivity and Embolism in Xylem. *Plant, Cell and Environment* **11**: 35-40.

Steppe K, Cochard H, Lacointe A, Ameglio T. 2011. Could rapid diameter changes be facilitated by a variable hydraulic conductance. *Plant, Cell and Environment* **35**: 150–157.

Steppe K, Sterck F, Deslauriers A. 2015. Diel growth dynamics in tree stems: linking anatomy and ecophysiology. *Trends in plant science* **20**: 335-343.

Still CJ, Foster PN, Schneider SH. 1999. Simulating the effects of climate change on tropical montane cloud forests. *Nature* **398**: 608-610.

Urli M, Porté AJ, Cochard H, Guengant Y, Burlett R, Delzon S. 2013. Xylem embolism threshold for catastrophic hydraulic failure in angiosperm trees. *Tree Physiology* **33**: 672–683.

Vandegehuchte MW, Steppe K. 2012. Improving sap flux density measurements by correctly determining thermal diffusivity, differentiating between bound and unbound water. *Tree Physiology* **32**: 930–942.

Vieira S, de Camargo PB, Selhorst D, Da Silva R, Hutyra L, Chambers JQ, Brown IF, Higuchi N, Dos Santos J, Wofsy SC, Trumbore SE. 2004. Forest structure and carbon dynamics in Amazonian tropical rain forests. *Oecologia* **140**: 468-79.

Way DA, Oren R. 2010. Differential responses to changes in growth temperature between trees from different functional groups and biomes: a review and synthesis of data. *Tree physiology* **30**: 669-688.

Weaver PI, Medina E, Pool D, Dugger K, Gonzales-Liboy J, Cuevas E. 1986. Ecological observations in the dwarf cloud forest of the Luquillo Mountains of Puerto Rico. *Biotropica* **18:** 79–85.

Wilcke W, Oelmann Y, Schmitt A, Valarezo C, Zech W, Homeier J. 2008. Soil properties and tree growth along an altitudinal transect in Ecuadorian tropical montane forest. *Journal of plant nutrition and soil science* **171**: 220-230.

Wright SJ, Kitajima K, Kraft NJ, Reich PB, Wright IJ, Bunker DE, Condit R, Dalling JW, Davies SJ, Díaz S, Engelbrecht BM. 2010. Functional traits and the growth-mortality trade-off in tropical trees. *Ecology* **91**:3664-3674.

Zuidema PA, Baker PJ, Groenendijk P, Schippers P, van der Sleen P, Vlam M, Sterck F. 2013. Tropical forests and global change: filling knowledge gaps. *Trends in Plant Science* 18:413-419.

Zweifel R. 2016. Radial stem variations – a source of tree physiological information not fully exploited yet. *Plant, Cell and Environment* **39**: 231-232.

Zweifel R, Haeni M, Buchmann N, Eugster W. 2016. Are trees able to grow in periods of stem shrinkage? *New Phytologist* **211**: 839-849.

Supporting information

Notes S1. *Temperature correction procedures:* We measured the temperature of 3 stainless steel rods that attach the point dendrometer to the tree with a thermistor (precision of ±0.25°C; model 3950 NTC Epoxy thermistor, adafruit.com, NY, USA). Then, we fitted a linear ordinary least squares regression between the stainless steel rods temperature (T_{sr}) and the air temperature measured (T) by a sensor located on the forest understory *c.* 10 m to the dendrometers. We used this relationship ($R^2 = 0.76$; $T_{sr}=2.25+0.87T$) to predict the T_{sr} for the dendrometers of the other trees. Based on the predicted T_{sr} we calculated the linear thermal expansion of the steel rods (ΔL) as:

$$\Delta L = T_{sr} \alpha L \tag{S1}$$

where α is the linear thermal expansion coefficient for steel (0.00001 m m^{-1} °C^{-1}) and L is the initial length of the steel rod. We considered L the distance from the tip of the steel rod inside the wood to the point where the frame was fastened with screws (see Fig. S2). We subtracted ΔL from the raw dD_b to remove the temperature effects from our data.

Notes S2. *Derivation of bark diameter changes including cambium growth:* We use the same Hooke's law principle to dD_b, but now we also add the changes in D_b caused by cambium growth (g):

$$\frac{dD_b}{dt} = \frac{D_b^*}{E_{r,b}} \frac{dP_b}{dt} + \frac{dg_{ZG}}{dt} \tag{S2}$$

where dD_b/dt refers to the bark diameter changes (dD_b) over a time interval t; D_b^* is the initial bark diameter (at reference pressure); $E_{r,b}$ is the radial elastic modulus of the bark tissue and dP_b/dt refers to the bark tissue-averaged turgor pressure over a time interval t. We now are using g_{ZG} as a first approximation of g.

The change in the inner bark pressure due to the water potential difference between the xylem and the inner bark can be written as:

$$\frac{dP_b}{dt} = \frac{E_{r,b} J}{V_b^*} = \frac{E_{r,b}}{V_b^*} L\, A\left(\Psi_x - \left(P_b - \Pi_b\right)\right) \tag{S3}$$

where V_b^* (m^3) is the inner bark volume at a reference pressure; J is the water flux (m^3 s^{-1}) between bark and xylem; L (m MPa^{-1} s^{-1}) is the hydraulic conductance of the cross-sectional area A (m^2) of contact between bark and xylem; Π (MPa) is the osmotic pressure of the inner bark. Substituting equations (S3) and equation (2; from the main text) into (S2) we have:

$$\frac{dTWD}{dt} = \frac{D_b^*}{V_b^*} L\ A\left(\Psi_x - \left(P_b - \Pi_b\right)\right) \tag{S4}$$

whereas now we will be deriving a model for tree water deficit changes over time (dTWD/dt) instead of total bark diameter changes over time (dD_b/dt).

We now express the pressure terms at the same reference time when D_b^* and V_b^* are also calculated:

$$\frac{dTWD^*}{dt} = \frac{D_b^*}{V_b^*} L\ A\left(\Psi_x^* - \left(P_b^* - \Pi_b^*\right)\right) \tag{S5}$$

where all variables labelled with the * symbol are determined at this reference time. Subtracting (S5) from (S4) side by side and re-arranging, yields:

$$\frac{dTWD}{dt} = \frac{D_b^*}{V_b^*} L\ A\left(\Delta\Psi_x - (\Delta P_b) + \left(\Delta\Pi_b\right)\right) + \frac{dTWD^*}{dt} \tag{S6}$$

where

$$\Delta\Psi_x = \Psi_x - \Psi_x^* \tag{S6a}$$

$$\Delta P_b = P_b - P_b^* \tag{S6b}$$

$$\Delta\Pi = \Pi_b - \Pi_b^* \tag{S6c}$$

We now express the bark pressure term as a function of the TWD differences from the reference state:

$$\Delta P_b = \frac{E_{r,b}}{D_b^*} \Delta TWD \tag{S7}$$

where

$$\Delta TWD = dTWD - dTWD^* \tag{S7a}$$

As explained at the beginning, we assume for the moment that changes in osmotic pressure do not occur. Therefore, the term $\Delta\Pi$ vanishes. Substituting equation (S7) into (S6), rearranging and simplifying, one obtains:

$$\frac{dTWD}{dt} = \frac{D_b^*}{V_b^*} L\ A\left(\Delta\Psi_x - \frac{E_{r,b}}{D_b^*}\Delta TWD\right) + \frac{dTWD^*}{dt}$$

$$\frac{dTWD}{dt} = \frac{L\ A}{V_b^*}\left(D_b^*\ \Delta\Psi_x - E_{r,b}\Delta TWD\right) + \frac{dTWD^*}{dt} \tag{S8}$$

$$\frac{dTWD}{dt} = \frac{L\ A\ E_{r,b}}{V_b^*}\left(\frac{D_b^*}{E_{r,b}}\Delta\Psi_x - \Delta TWD\right) + \frac{dTWD^*}{dt}$$

Let's assume now that estimates of xylem water potential Ψ_x can be obtained using an

Ohm's law analogy, i.e.

$$\Psi_x = \Psi_s - \frac{v_s}{K_{pl}} \tag{S9}$$

where v_s is the measured sap velocity, and Ψ_s and K_{pl} are soil water potential and plant hydraulic conductance, respectively. Expressing the quantities at a reference time using the usual * symbol and substituting (S9) into (S8) yields:

$$\Delta\Psi_x = \Psi_s - \frac{v_s}{K_{pl}} - \left(\Psi_s^* - \frac{v_s^*}{K_{pl}^*}\right) = \Delta\Psi_s - \frac{v_s}{K_{pl}} + \frac{v_s^*}{K_{pl}^*} \tag{S10}$$

$$\frac{dTWD}{dt} = \frac{L\,A\,E_{r,b}}{V_b^*}\left(-\frac{D_b^*}{K_{pl}\,E_{r,b}}v_s - \Delta TWD\right) + \left(\frac{dTWD^*}{dt} + L\frac{v_s^*}{K_{pl}^*} + L\,\Delta\Psi_s\right)$$

where the K_{pl} and $\Delta\Psi_s$ indicate parameters for the coefficient for sap velocity and for the intercept which are not constant but can vary from day to day to reflect dynamic changes in soil water potential and plant hydraulic conductance. Equation (S10) equates to:

$$\frac{dTWD}{dt} = \alpha\left(\beta\, v_s - \Delta TWD\right) + \gamma \tag{S11 or Eqn. 14 in the main text}$$

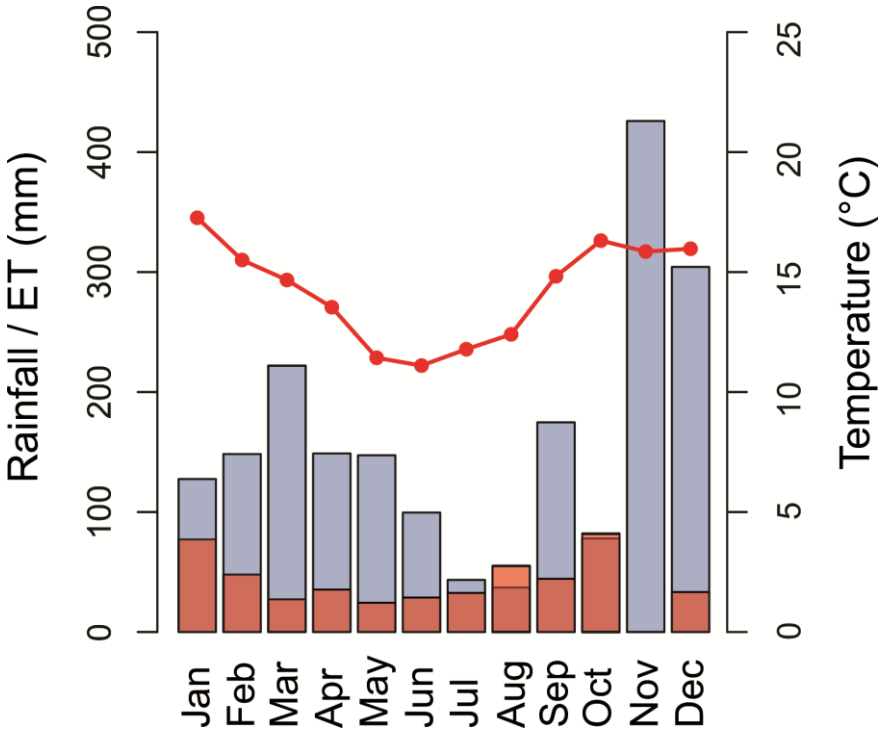

Figure S1. Climate data from the study site at Mantiqueira mountain range during 2015. The gray bars are total monthly rainfall, the red bars are the potential evapotranspiration calculated using Hargreaves equations (Hargreaves & Samani, 1982) and the red line is the mean monthly temperature.

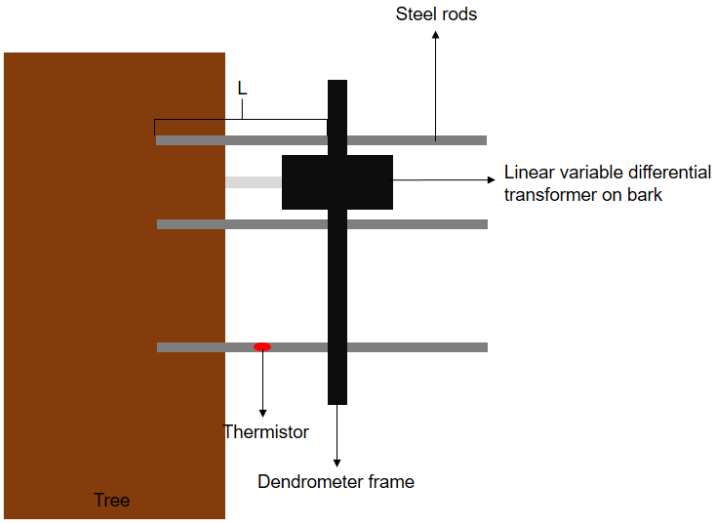

Figure S2. Schematic representation of the point dendrometers used in our study. The additional linear variable differential transformer installed on xylem is not represented in the figure.

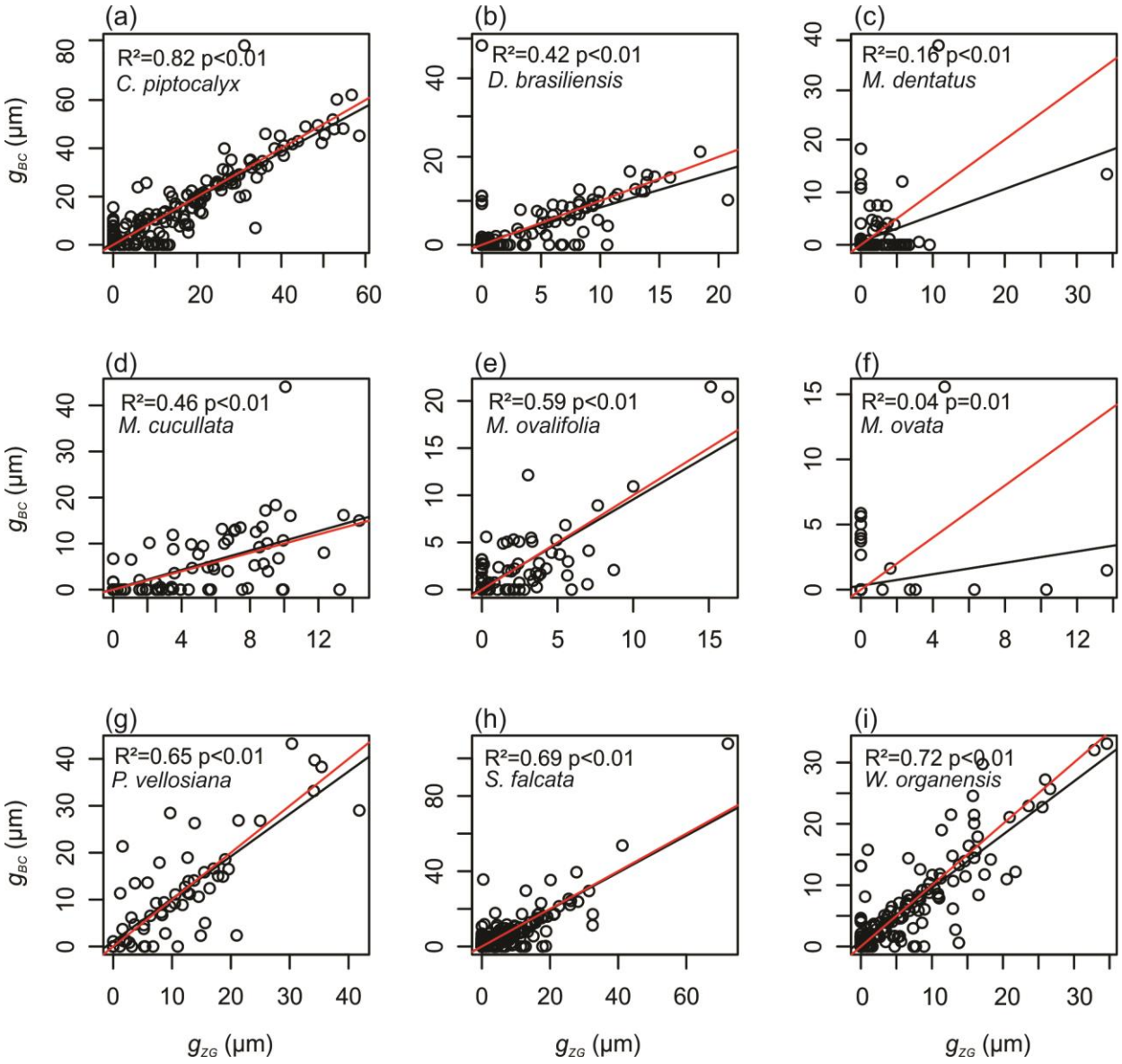

Figure S3. Linear relationships between the growth signal predicted by the zero-growth (g_{ZG}) method and bark-capacitance method (g_{BC}). The black line is the line predicted by the linear regression and the red line is a 1:1 reference line.

Table S1. List of the abbreviations and symbols used in this study

Abbreviation	*Definition*
A	Cross-sectional area between bark and xylem
BC	Bark capacitance method
c_w	Specific heat capacity of dry wood
c_s	Specific heat capacity of water
dD_b	Bark diameter changes
dD_x	Xylem diameter changes
dP_b	Bark pressure changes
dt	Time interval
$d\Psi_x$	Xylem water potential changes
$dTWD$	Tree water deficit changes
D_b	Bark diameter
D_x	Xylem diameter
DBH	Diameter at breast height
$E_{r,b}$	Radial elastic modulus of the bark
$E_{r,x}$	Radial elastic modulus of the xylem tissue
FWU	Foliar Water Uptake
g	Cambial growth
g_{bas}	Radial cambial growth
$g_{bas\ max}$	Daily maximum radial cambial growth
$g_{bas\ mid}$	Daily middle radial cambial growth
g_{BC}	Linear growth predicted by the Bark capacitance method
g_{ZG}	Linear growth predicted by the Zero-growth method
GLM	Generalized linear model
HRM	Heat-ration method
J	Water flux between bark and xylem
k	Sapwood thermal diffusivity
K	x value when the y variable reaches 50% of the asymptote in the Michaelis-Menten function
K_{pl}	Plant hydraulic conductance
L	Hydraulic conductance between bark and xylem
LW_t	Leaf wetness time
m_c	Moisture content of fresh wood
$MD\Psi_l$	Mid-day leaf water potential
NLS	Nonlinear least squares
P50	Water potential value when the xylem loses 50% of its conductance
P88	Water potential value when the xylem loses 88% of its conductance
PAR	Photosynthetic active radiation
$PD\Psi_l$	Pre-dawn leaf water potential
PLC	Xylem percentage of conductance loss
s	Parameter related with the slope of the xylem vulnerability curve
SM_{50}	Minimum xylem water potential minus P50
SM_{88}	Minimum xylem water potential minus P88
SWD	Soil water deficit
t	Time
T	Air temperature
TMCF	Tropical Montane Cloud Forest
TWD	Tree water deficit
v_1	Temperature increment in the sap flow probe above the heater
v_2	Temperature increment in the sap flow probe below the heater
v_h	Heat pulse velocity
v_s	Sap velocity
V	Asymptote of the Michaelis-Menten function

V_b^*	Bark volume at reference pressure
VWC	Volumetric water content
$\mathbf{VWC_f}$	Volumetric water content at soil field capacity
x	Distance between heater and sap flow temperature probes
ZG	Zero-growth method
α	Parameter related with the radial conductivity between xylem and bark
β	Parameter related with the plant axial hydraulic conductance
γ	Parameter related with the soil water potential
$\widehat{\Delta G}_m$	Signal that contains cambial growth and osmotic induced changes
ΔD_b	Bark diameter change in relation to bark diameter at reference pressure
$\widehat{\Delta D}_b$	Predicted bark diameter change in relation to bark diameter at reference pressure excluding bark capacitance effects
ΔTWD	Tree water deficit change in relation to tree water deficit at reference pressure
Λ	Parameter representing the maximum transpiration rate per unit of hydraulic conductance
Π	Bark osmotic pressure
π	Number pi (approximated to 3.14 in the study)
ρ_b	Basic wood density
ρ_s	Water density
σ	Parameter representing the stomatal sensitivity to soil water availability
Ψ_{min}	Minimum xylem water potential
Ψ_s	Soil water potential
Ψ_x	Xylem water potential

GENERAL CONCLUSION

The climatic conditions of Tropical Montane Cloud Forests (TMCF) houses a large diversity of species, many of which could not to exist elsewhere (Foster, 2001). In this thesis, I investigated how TMCF trees function on this environment, and used this knowledge to predict how they would respond to changes on TMCF environmental conditions that could be caused by climate change. TMCF trees have different strategies to thrive in the particular climatic conditions of TMCF, and many TMCF trees appear to function close to their physiological limits, which suggests that changes on TMCF environmental conditions could threaten water transport, leaf turgor maintenance and growth of these trees. Reduced fog frequency can compromise leaf turgor maintenance in TMCF trees with high foliar water uptake capacity, which rely more on leaf wetting events and foliar water uptake to maintain leaf turgor. The results from chapter 1 indicates that leaves from species with high FWU have a probability ranging from 0.2 to 0.9 of losing leaf turgor if there were no leaf wetting events in TMCF. Species with low FWU can maintain turgor regardless of leaf wetting events, because of their more strict stomatal regulation (i.e. more isohydric). However, this conservative strategy also might have its own drawbacks, as a strong stomatal regulation often results in lower carbon assimilation rates and higher risks of carbon starvation (McDowell *et al.*, 2008).

The drawbacks of a more conservative strategy are illustrated on chapter 2, where I found a clear trade-off between growth rates and xylem hydraulic safety in TMCF trees. Fast growing TMCF trees grow in a wider range of environmental conditions, but to do so their xylem conductivity reaches levels close to the threshold of hydraulic failure (i.e. the water potential value where the xylem loses 88% of its conductivity, see Choat, 2013; Urli *et al.*, 2013; Delzon & Cochard, 2014). Because fast-growing TMCF trees are so close to their hydraulic failure threshold, a drier and hotter TMCF could push these trees over this threshold and induce the mortality of fast-growing TMCF trees. However, most trees in the studied TMCF possessed slower growing rates; over 65% of the basal area among the studied trees were from species that never reached growing rates higher than 5000 μm^2 per day (for comparison, some fast growing species such as *Croton pyptocalyx* could grow more than 25000 μm^2 per day). These slower-growing TMCF trees restricted its growth to periods of very favorable climatic conditions, which were generally days with more humid days, with higher temperature and lower radiation. This more conservative growth strategy allowed these trees to maintain larger xylem safety margins, and might make these species more resistant to a

hotter and drier climate. In fact, as the growth of most TMCF trees appear to be strongly constrained by lower temperatures, increases in TMCF temperatures could, in theory, even increase TMCF tree growth. However, higher temperatures and less fog could turn TMCF into a more suitable environment for lowland tropical species, and favor the upward migration of lowland tropical trees populations (Foster, 2001; Hillyer & Silman, 2010; Feeley *et al.*, 2011; Corlett & Wetcott, 2013). On this scenario, slower growing TMCF trees, despite having higher xylem hydraulic safety margins, could be more easily outcompeted by fast growing lowland species (Roy, 1990).

The results of this thesis provides some novel ecophysiological basis for the vulnerability of TMCF to climate change, which have important implications for management of these important and vulnerable ecosystems. Contrary to many lowland tropical species, TMCF species are not expected to shift to a new location in response to climate change (Colinvaux et al., 1997, 2000; Foster, 2001), instead many TMCF species are likely to go extinct, as they would have no suitable environment to migrate (Walker & Flenley, 1979; Foster 2001). This would cause an irreparable loss of biodiversity due to the high biodiversity and endemism rates of TMCF (Gentry, 1992; Leon & Young, 1996). Changes in TMCF structure and function would also have a direct impact on human populations, as it would compromise the many ecosystem services provided by TMCF, such as maintenance of water supply and quality, and soil stability (Sidle *et al.*, 2006; Tognetti *et al.*, 2010; Bruinzeel *et al.*, 2011). Mountainous tropical regions that depend on TMCF for the maintenance of their water supply, which might include large cities in South America, Africa and Asia (Bruijnzeel, 2004; Bubb *et al*., 2004), will be seriously threatened by loss of TMCF.

The increase in atmospheric carbon dioxide and consequent increments in earth temperature are considered largely irreversible (Solomon *et al.*, 2009). Therefore, the only way to minimize the effects of climate change on many ecosystems and on the services provided by them is to understand *how* and *why* ecosystems will respond to climate change, and use this knowledge to elaborate effective management strategies. The results of this thesis illustrate how some key functional traits, such as foliar water uptake capability, stomatal regulation strategy and growth rates can determine the response of TMCF tree species to climate change. This knowledge can be incorporated in process-based vegetation models, to improve model predictions regarding the vegetation responses to climate. Currently most vegetation models have very simplistic representations of vegetation processes that constrains the predictive power of these models (Powell *et al.*, 2013; Xu *et al.*, 2016). In addition, the results from this

thesis could contribute for building a theoretical basis for TMCF management strategies. These strategies could be based on species key functional traits, such as the traits studied on this thesis, and the specific vulnerabilities associated with each trait.

REFERENCES

Bruijnzeel LA. 2004. Hydrological functions of tropical forests: not seeing the soil for the trees? *Agriculture, ecosystems & environment* **104**:185-228.

Bruijnzeel LA, Mulligan M, Scatena FN. 2011. Hydrometeorology of tropical montane cloud forests: emerging patterns. *Hydrological Processes* **25**: 465-498.

Bubb P, May IA, Miles L, Sayer J. 2004. Cloud forest agenda. *UNEP World Conservation Monitoring Centre*.

Choat B. 2013. Predicting thresholds of drought-induced mortality in woody plant species. *Tree Physiology* **33**: 669–671.

Colinvaux PA, Bush MB, Kannan MS, Miller MC, 1997. Glacial and postglacial pollen records from the Ecuadorian Andes and Amazon. *Quaternary. Research.* **48**: 69–78.

Colinvaux PA, De Oliveira P, Bush MB. 2000. Amazonian and neotropical plant communities on glacial time-scales: the failure of the aridity and refuge hypotheses. *Quaternary Science Reviews* **19**: 141–169.

Corlett RT, Westcott DA. 2013. Will plant movements keep up with climate change? *Trends in ecology & evolution* **28**: 482-488.

Delzon S, Cochard H. 2014. Recent advances in tree hydraulics highlight the ecological significance of the hydraulic safety margin. *New Phytologist* **203**: 355-358.

Feeley KJ, Silman MR, Bush MB, Farfan W, Cabrera KG, Malhi Y, Meir P, Revilla NS, Quisiyupanqui MN, Saatchi S. 2011. Upslope migration of Andean trees. *Journal of Biogeography* **38**: 783-791.

Foster P. 2001. The potential negative impacts of global climate change on tropical montane cloud forests. *Earth-Science Reviews* **55**: 73-106.

Gentry AH. 1992. Tropical forest biodiversity: distributional patterns and their conservational significance. *Oikos* **63**: 19–28.

Hillyer R, Silman MR. 2010. Changes in species interactions across a 2.5 km elevation gradient: effects on plant migration in response to climate change. *Global Change Biology* **16**: 3205-3214.

Karmalkar AV, Bradley RS, Diaz HF. 2008. Climate change scenario for Costa Rican montane forests. *Geophysical Research Letters* 35 (11).

Leon, B., Young, K.R., 1996. Distribution of pteridophyte diversity and endemism in Peru. In: Camus JM, Gibby M, Johns RJ, eds. *Pteridology in Perspective*. Kew, UK. Royal Botanic Gardens, 77–91.

McDowell NG, Pockman WT, Allen CD, Breshears DD, Cobb N, Kolb T, Plaut J, Sperry J, West A, Willians DG, Yepez EA. 2008. Mechanisms of plant survival and mortality during drought: why do some plants survive while others succumb to drought? *New Phytologist* **178**: 719-739.

Powell TL, Galbraith DR, Christoffersen BO, Harper A, Imbuzeiro H, Rowland L, Almeida S, Brando PM, Costa AC, Costa MH, Levine NM. 2013. Confronting model predictions of carbon fluxes with measurements of Amazon forests subjected to experimental drought. *New Phytologist* **200:** 350-65.

Roy J. 1990. In search of the characteristics of plant invaders. In: Di Castri F, Hansen AJ, Debussche M, eds. *Biological invasions in Europe and the Mediterranean basin*. Berlin, Germany. Kluwer Academic Publishers, 333-352.

Sidle RC, Ziegler AD, Negishi JN, Nik AR, Siew R, Turkelboom F. 2006. Erosion processes in steep terrain: truths, myths, and uncertainties related to forest management in Southeast Asia. *Forest Ecology and Management* **224**: 199-225.

Solomon S, Plattner GK, Knutti R, Friedlingstein P. 2009. Irreversible climate change due to carbon dioxide emissions. *Proceedings of the national academy of sciences* **28**: pnas-0812721106.

Still CJ, Foster PN, Schneider SH. 1999. Simulating the effects of climate change on tropical montane cloud forests. *Nature* **398**: 608-610.

Tognetti S, Aylward B, Bruijnzeel LA. 2010. Assessment needs to support the development of arrangements for Payments for Ecosystem Services from tropical montane cloud forests. In:

Bruijnzeel LA, Scatena FN, Hamilton LS, eds. *Tropical Montane Cloud Forests. Science for Conservation and Management.* Cambridge, UK. Cambridge University Press, 671–685.

Urli M, Porté AJ, Cochard H, Guengant Y, Burlett R, Delzon S. 2013. Xylem embolism threshold for catastrophic hydraulic failure in angiosperm trees. *Tree Physiology* **33**: 672–683.

Walker D, Flenley JR. 1979. Late Quaternary vegetational history of the Enga District of upland Papua New Guinea. *Philosophical Transactions of the Royal Sociecty B* **286**: 265–344.

Xu X, Medvigy D, Powers JS, Becknell JM, Guan K. 2016. Diversity in plant hydraulic traits explains seasonal and inter-annual variations of vegetation dynamics in seasonally dry tropical forests. *New Phytologist* DOI: 10.1111/nph.14009.

UNICAMP
COORDENADORIA DE PÓS-GRADUAÇÃO
INSTITUTO DE BIOLOGIA
Universidade Estadual de Campinas
Caixa Postal 6109. 13083-970, Campinas, SP, Brasil
Fone (19) 3521-6378. email: cpgib@unicamp.br
IB

DECLARAÇÃO

Em observância ao **§5º do Artigo 1º da Informação CCPG-UNICAMP/001/15**, referente a Bioética e Biossegurança, declaro que o conteúdo de minha Tese de Doutorado, intitulada "***EFEITO DE MUDANÇAS AMBIENTAIS NAS RELAÇÕES HÍDRICAS E DE CARBONO DE ÁRVORES DE FLORESTAS NEBULARES***", desenvolvida no Programa de Pós-Graduação em Ecologia do Instituto de Biologia da Unicamp, não versa sobre pesquisa envolvendo seres humanos, animais ou temas afetos a Biossegurança.

Assinatura: _____
Nome do(a) aluno(a): Cleiton Breder Eller

Assinatura: _____
Nome do(a) orientador(a): Rafael Silva Oliveira

Data: 12/08/2016

Profa. Dra. Rachel Meneguello
Presidente
Comissão Central de Pós-Graduação
Declaração

As cópias de artigos de minha autoria ou de minha co-autoria, já publicados ou submetidos para publicação em revistas científicas ou anais de congressos sujeitos a arbitragem, que constam da minha Dissertação/Tese de Mestrado/Doutorado, intitulada **EFEITO DE MUDANÇAS AMBIENTAIS NAS RELAÇÕES HÍDRICAS E DE CARBONO DE ÁRVORES DE FLORESTAS NEBULARES**, não infringem os dispositivos da Lei n.° 9.610/98, nem o direito autoral de qualquer editora.

Campinas, 12 de Agosto de 2016.

Assinatura : _____
Nome do(a) autor(a): **Cleiton Breder Eller**
RG n.° 29.992.470-1

Assinatura : _____
Nome do(a) orientador(a): **Rafael Silva Oliveira**
RG n.° 1472069